University of Hamburg

Institute for Hydrobiology and Fisheries Science

Benthic structures in the Namibian Upwelling Region and the Pelago-benthic coupling.

Master Thesis

by

Matthias Mertzen

MN: 6367570

born 17th February 1987

November 2013

1st Supervisor: Prof. Dr. Christian Möllmann

2nd Supervisor: Dr. Rolf Koppelmann

Table of Contents

List of Figures V

List of Tables VII

Abstract VIII

Zusammenfassung IX

1 Introduction 1

2 Materials and Methods 6

2.1 Research area 6

2.2 Satellite Data 8

2.3 Field Sampling 8

2.3.1 Microzooplankton sampling 8

2.3.2 Sampling of biogeochemistry data 9

2.3.3 Benthic sampling 10

2.3.4 Remotely Operated Vehicle (ROV) 10

2.4 Laboratory work and calculations 11

2.4.1 Microzooplankton 11

2.4.2 Mesozooplankton 11

2.4.3 Biochemistry 12

2.4.4 Bacterial mats 12

2.4.5 Benthic macrofauna 13

2.4.6 ROV tracking and idealization 13

2.4.7 Identification and abundance calculation of the benthic megafauna 17

2.4.8 Estimation of species with high abundance 17

2.4.9 Correlation of the main parameters 17

3 Results 19

3.1 Physical parameters at the three transects 19
3.1.1 Hydrography on the Terrace Bay transect (20° S) 19
3.1.2 Hydrography on the Rocky Point transect (19° S) 20
3.1.3 Hydrography on the Kunene transect (17.5° S) 21
3.1.4 Summary of the hydrographical situation in the investigation area 22
3.2 Chlorophyll *a* concentrations 22
3.2.1 Chlorophyll *a* concentrations on the Terrace Bay transect (20° S) 22
3.2.2 Chlorophyll *a* concentrations on the Rocky Point transect (19° S) 23
3.2.3 Chlorophyll a concentrations on the Kunene transect (17.5° S) 24
3.2.4 Summary of the chlorophyll *a* distribution in the investigation area 25
3.3 Microzooplankton abundance and vertical distribution 26
3.3.1 Microzooplankton abundance on the Terrace Bay transect (20° S) 26
3.3.2 Microzooplankton abundance on the Rocky Point transect (19° S) 27
3.3.3 Microzooplankton abundance on the Kunene transect (17.5° S) 30
3.3.4 Summary of the microzooplankton distribution in the investigation area 33
3.4 Mesozooplankton abundance and vertical distribution 35
3.4.1 Mesozooplankton abundance on the Rocky Point transect (19° S) 35
3.4.2 Mesozooplankton abundance on the Kunene transect (17.5° S) 39
3.4.3 Summery of the mesozooplankton abundance in the investigation area 44
3.5 Biomass of mesozooplankton 45
3.5.1 Biomass of mesozooplankton on the Rocky Point transect (19° S) 45
3.5.2 Biomass of mesozooplankton on the Kunene transect (17.5° S) 46
3.5.3 Summary of the mesozooplankton biomass in the investigation area 49
3.6 Biochemistry 49
3.6.1 Summary of the biochemistry 51
3.7 Benthic macrofauna distribution 52
3.7.1 Summary of the benthic macrofauna abundances in the investigated area 57

3.8 ROV video analysis of the benthic megafauna 57
3.8.1 Benthic megafauna abundance on the Terrace Bay transect (20° S) 57
3.8.2 Benthic megafauna abundance on the Rocky Point transect (19° S) 58
3.8.3 Benthic megafauna abundance on the Kunene transect (17.5° S) 58
3.8.4 Summary of the megafauna abundances in the investigation area 59
3.9 Correlation of benthic megafauna abundance with different biotic and abiotic parameters 62
3.9.1 Correlation pattern of benthic megafauna in the investigated area 63
3.9.2 Correlations at the Terrace Bay transect (20° S) 63
3.9.3 Correlations at the Rocky Point transect (19° S) 63
3.9.4 Correlations at the Kunene transect (17.5° S) 64
3.9.5 Sperman' rho correlation 65
3.9.6 Relation of the biological and chemical parameters in the pelago-benthic coupling 66
3.9.7 Corellation of the benthos and pelagial at all stations of the three transects 67
4 Discussion 68
4.1 Hydrography 68
4.2 Plankton abundances 70
4.2.1 Phytoplankton distribution detected by satellite 70
4.2.2 Microzooplankton abundance 71
4.2.3 Mesozooplankton abundance 72
4.3 Sedimentation 73
4.4 The sediment structure 74
4.5 Sediment flux 75
4.6 Bacteria mats 76
4.7 Benthic macrofauna abundance 77
4.8 Benthic megafauna abundances 79
5 Conclusion 84

6 Acknowledgement 86

7 References 87

7.1 Image sources 102

7 Appendix 103

List of Figures

Figure 1: Currents of the Benguela Upwelling System 1
Figure 2: Research area with the sampled stations 6
Figure 3: Transformation of raw track data onto idealized linear track route..... 14
Figure 4: Raw data points of the ROV position and reference points which are connected for the idealized track route for all ROV stations 16
Figure 5: Distribution of salinity [PSU], temperature [°C] and oxygen [µmol/l] on the Terrace Bay transect (12.-13.02.2011). 19
Figure 6: Distribution of salinity [PSU], temperature [°C] and oxygen [µmol/l] on the Rocky Point transect (14.-17.02.2011). 20
Figure 7: Distribution of salinity [PSU], temperature [°C] and oxygen [µmol/l] on the Kunene transect (19.-22.02.2011). 21
Figure 8: Chlorophyll a surface distribution detected via satellite..... 23
Figure 9: Microzooplankton abundance [ind. m^{-3}] in depth intervals and relative composition [%] at the Terrace Bay outer shelf station (st. 276) during daytime. 26
Figure 10: Microzooplankton abundance [ind. m^{-3}] in depth intervals and related composition [%] at the Rocky Point inner shelf station (st. 282) during night time..... 27
Figure 11: Microzooplankton abundance [ind. m^{-3}] in depth intervals and relative composition [%] at the Rocky Point outer shelf station (st. 285) during daytime. 28
Figure 12: Microzooplankton abundance [ind. m^{-3}] in depth intervals and relative composition [%] at the Kunene shelf station (st. 305) during daytime..... 30
Figure 13: Microzooplankton abundance [ind. m^{-3}] in depth intervals and relative composition [%] at the Kunene upper slope station (st. 306) during daytime. 31
Figure 14: The abundance [ind. m^{-3}] and the relative composition [%] were displayed at two microzooplankton hauls with different depth intervals at the Kunene lower slope station 307 during daytime..... 32
Figure 15: Mesozooplankton abundance [ind. m-3] in depth intervals and relative composition [%] at the Rocky Point outer shelf station (st. 285) at daytime. 35
Figure 16: Mesozooplankton abundance [ind. m^{-3}] in depth intervals and relative composition [%] at the Rocky Point outer shelf station (st. 285) at night time. 37

Figure 17: Mesozooplankton abundance [ind. m^{-3}] in depth intervals and relative composition [%] at the Kunene shelf station (st.305) during daytime..... 39
Figure 18: Mesozooplankton abundance [ind. m^{-3}] in depth intervals and relative composition [%] at the Kunene upper slope station (st. 306) at night time. 41
Figure 19: Mesozooplankton abundance [ind. m^{-3}] in depth intervals and relative composition [%] at the Kunene lower slope station (st. 307) at daytime. 43
Figure 20: Mesozooplankton biomass [g 1000 m^{-3}] for all depth intervals at the Rocky Point outer shelf station (st. 285) at daytime and at night time. 45
Figure 21: Mesozooplankton biomass [g 1000 m^{-3}] for all depth intervals at the Kunene shelf station (st. 305) at daytime. 46
Figure 22: Mesozooplankton biomass [g 1000 m^{-3}] for all depth intervals at the Kunene upper slope station (st. 306) at night time 47
Figure 23: Mesozooplankton biomass [g 1000 m^{-3}] for all depth intervals at the Kunene lower slope station (st. 307) at daytime and night time..... 48
Figure 24: Benthic macrofauna taxa of the three transects.. 53
Figure 25: Benthic macrofauna abundance [ind. $^{m-2}$] and relative composition [%] at the Kunene shelf station (st.305)..... 54
Figure 26: Benthos abundance and relative composition at the Kunene shelf station (st. 305) in nine different cores..... 56
Figure 27: Overview of the benthic megafauna on the northern Namibian shelf. 60
Figure 28: Overview of the benthic megafauna on the Kunene slope. 61
Figure 29: A: Megafauna values related to physical and chemical parameters and the values of benthic macrofauna, mesozooplankton and microzooplankton at all stations of the three transects. B: magnification of the relations of the three stations with the lowest benthic megafauna abundances..... 62
Figure 30: Relation of the different biological and chemical parameters in the pelagial and benthos. 66
Figure 31: The correlation of the sum of all benthic abundances and the sum of all pelagic concentrations and abundances at all stations of the three transects..... 67
Figure 32: Main taxa composition on the tree transects..... 83
Figure 33: Main taxa composition on the Kunene transect..... 83

List of Tables

Table 1: Overview of sample types taken at the different stations 7
Table 2: Availability of benthic data from the sediment cores, water samples and mooring. . 12
Table 3: Categories of bacterial mats covering 13
Table 4: Bottom concentrations [µmol l-1] of the different elements: 49
Table 5: Percentage of total nitrogen (N_{tot}) and organic carbon (C_{org}) in the sediment (molar ratio of both elements). Oxygen concentration compared to oxygen consumption 50
Table 6: Fluxes and production of nitrogen, ammonium and phosphate (µmol m^{-2} d^{-1})..... 50
Table 7: Two sided Spearman's rho correlation test for all standardized abundance and concentration values of the pelagical and benthos with the associated p-values ($p < 0.05$). 65

Appendix tables

Table 8: Raw data of each benthic megafauna, taxa captured by a Remotely Operated Vehicle (ROV) at the different stations. 103
Table 9: Individual numbers per 100 m [ind. $100m^{-1}$] of each benthic megafauna taxa captured by a Remotely Operated Vehicle (ROV). at the different stations. 104

Abstract

The benthic megafauna has been observed on the shelf of the northern Benguela Upwelling System (BUS) using a Remotely Operated Vehicle (ROV). The structures of the sediment and the benthic megafauna composition was very heterogeneous at the different sites and depths in small areas, which rose the question for the regional factors influencing this structural differences. Patterns in the structure are controlled by physical, chemical and biological factors in the overlaying water column. Four different benthic community structures were detected on the three transects. The southern Terrace Bay shelf (20° S) station was dominated by Medusa, whereas mainly bacteria mats with a high individual number of *Sufflogobius bibarbatus* (Bearded Gobies) were found at the Rocky Point shelf (19° S) stations. At the northern Kunene shelf and upper slope station (17.5° S) Pennatulacea and Gastropoda were the main taxa, but fishes dominated at the lower slope. Oxygen minimum zones (OMZ) were detected on the shelf on the two southern transects which influenced the distribution of benthic and pelagic organisms. Chlorophyll *a* concentrations, microzooplankton and mesozooplankton abundances were higher inshore than offshore and positively correlated with the benthic macrofauna and megafauna abundances. However, these correlations were not significant. The benthic macrofauna and megafauna communities are probably affected by the differences in particle flux and the OMZ. The sediment structure and chemical processes at the sediment-water-interface, the width of the shelf and the Kunene River outflow are further factors which influence the benthic community structures. Overall, along the Namibian coast the different benthic megafauna structures are allocated by depth and also by the location on the continental shelf.

Zusammenfassung

Die benthische Megafauna wurde auf dem Schelf und Kontinentalhang des Benguela Auftriebs Systems unter Nutzung eines Remotely Operated Vehicle (ROV; Tauchroboters) erfasst. An den verschiedenen Untersuchungsorten und in unterschiedlichen Tiefen waren die Sedimentstruktur und die Zusammensetzung der Megafauna in eng begrenzten Gebieten sehr heterogen, was zu der Frage führte, wie sich die regionalen Faktoren auf diese unterschiedliche Strukturierung auswirken. Das strukturelle Muster wird durch physikalische, chemische und biologische Faktoren in der darüber liegenden Wassersäule beeinflusst. Vier verschiedene Benthos Gemeinschaften wurden auf drei untersuchten Transekten nachgewiesen. Die südliche Terrace Bay Schelfstation (20° S) wurde von Medusa dominiert, wohingegen an den Rocky Point Schelfstationen (19° S), hauptsächlich Bakterienmatten mit einer hohen Individuen Zahl von *Sufflogobius bibarbatus* (Meergrundel) gefunden wurden. An der nördlichen Kunene Schelf- und der oberen Hangstation (17.5° S) waren Pennatulacea und Gastropoda die häufigsten Taxa, jedoch dominierten Fische am unteren Hang. Auf dem Schelf der beiden südlichen Transekten wurden Sauerstoffminimumzonen festgestellt, welche die Verbreitung der benthischen und pelagischen Organismen beeinflussen. Chlorophyll *a* Konzentrationen, Mikrozooplankton- und Mesozooplanktonabundanzen zeigten küstennah höhere Werte als ablandig und korrelierten positiv mit den benthischen Makro- und Megafaunaabundanzen. Allerdings waren diese Korrelationen nicht signifikant. Die benthischen Makrofauna- und Megafaunagemeinschaften sind wahrscheinlich hauptsächlich durch unterschiedliche Sedimentationsraten und durch Sauerstoffminimumzonen beeinflusst. Die Benthosgemeinschaftsstrukturen werden durch weitere Faktoren wie die Sedimentstruktur, chemische Prozesse an der Sediment-Wasser-Grenze, die Breite des Schelfs und den Ausstrom des Kunene Flusses beeinflusst. Die benthische Makrofauna entlang der Küste Namibias ist sowohl durch die Tiefe als auch durch die Lage am Kontinentalschelf strukturiert.

1 Introduction

Oceanic upwelling systems are very productive regions of the ocean. The Benguela Upwelling System (BUS) is one of the five largest eastern boundary current systems on earth and is located at the southwestern coast of Africa between 15–37° S and 0–20° E (Figure 1). An upwelling system is driven by along-shore winds (Nelson and Hutchings, 1983) and affected by the Coriolis force caused by the earth's rotation. This results in a drift of the surface water from inshore to offshore. The surface water near the coast is replaced by nutrient-rich deep water (Ekman, 1905).

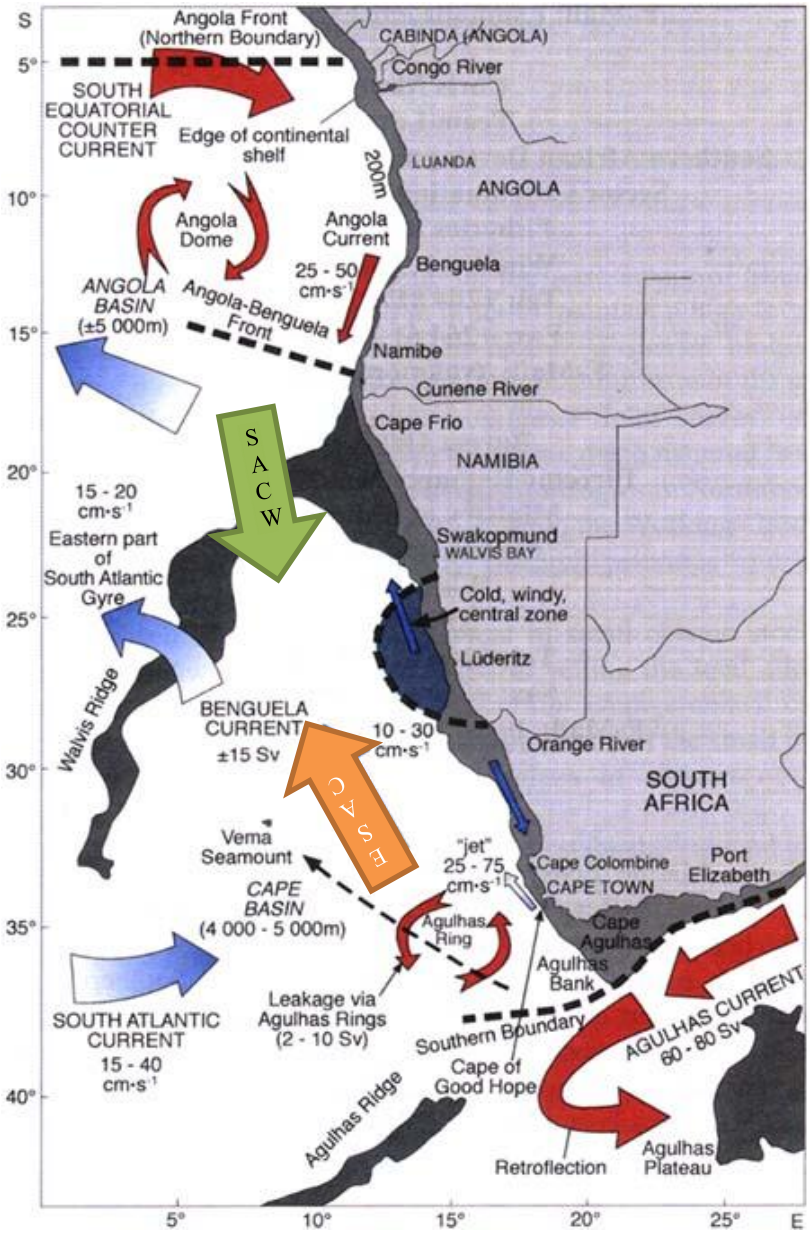

Figure 1: Currents of the Benguela Upwelling System (modified according to Shannon and O'Toole, 2003)

The dominant surface current along the Namibian coast is named Benguela Current and is the eastern part of the South Atlantic subtropical gyre (Peterson and Stramma, 1991). The northern boundary is formed by the Angola-Benguela Frontal Zone (ABFZ) with spatial fluctuations between 14-16° S (Meeuwis and Lutjeharms, 1990; Stramma and England, 1999). The main upwelling center is off Lüderitz (26.6° S; Lass et al., 2000; Shannon, 1985). The BUS is influenced by southern and northern currents. From the South Atlantic Current mixed cold, oxygen-deficient and nutrient rich water masses flow into the BUS. Moreover, from the south east warm, mostly ring-shaped surface water from the Agulhas Current (32-37° S), which has its origin in the Indo-Pacific, recharges the BUS. These two water masses create the fresh and oxygenated Eastern South Atlantic Central Water (ESACW; Mohrholz et al., 2001). This water body is transported from the Cape of Good Hope across the South African coast to the equator (Shannon and O'Toole, 2003). Further north (27° S) the Benguela Current splits into two water bodies. The larger one becomes part of the South Equatorial Current. The smaller one near the coast line and the northern Angola Current constitutes the (ABFZ; Stramma and England, 1999; Meeuwis and Lutjeharms, 1990).

The northern BUS is influenced by the southern part of the Angola Current. This water mass has a higher nutrient concentration and a higher temperature and salinity than the water masses from the north and is named South Atlantic Central Water (SACW; Poole and Tomczak, 1999; Mohrholz et al., 2001). The water streams southwards along the shelf. Due to the higher salinity and therefore higher density of the SACW, the slightly lighter ESACW flows above it. The oxygen and nutrient allocation is depending on the mixing ratio of SACW and ESACW (Mohrholz et al., 2007).

Upwelling in northern Namibia has its maximum between August and October (southern winter) and its minimum between January and March (southern summer; Hart and Currie, 1960). The upwelling water originates from 100-200 m depth (Shannon, 1985), is rich in nutrients (10-30 mmol m^{-3} nitrite, 2-3 mmol m^{-3} phosphate, 20-50 mmol m^{-3} silicate; Wasmund et al., 2010) and generally well oxygenated (> 200 µM O_2; Chapmann and Shannon, 1985). As a result there is a very high primary production in the BUS. This production is higher than in other eastern boundary current regions such as Peru-Humboldt Current, California Current, and Canary Current (Carr, 2002; Gruber and Sarmiento, 1997). However, phytoplankton production is highly variable in the BUS due to varying

meteorological, hydrographical, chemical and biological factors. Several studies were obtained to measure the spatial distribution of phytoplankton biomass by in-situ experiments (Brown et al., 1991) and satellite data of chlorophyll *a* (Chl *a*) as an indicator of phytoplankton biomass (Shannon, 1985; Weeks and Shillington, 1995; de Villiers, 1998; Demarcq et al., 2003). The analysis of the data in these studies indicated that the inshore Chl *a* concentrations were usually larger than 10 mg m^{-3}. Offshore, the Chl *a* concentrations decreased and altered seasonally (Huggett et al., 1998). The average primary production is 1.2 g C m^{-2} d^{-1} in the northern BUS and 2.0 g C m^{-2} d^{-1} in the southern BUS (Brown et al., 1991). 60-70 % of the phytoplankton is consumed by microzooplankton (Calbet and Landry, 2004). Mesozooplankton, in particular copepods, generally consume 10-40 % of the phytoplankton (Calbet, 2001). Microzooplankton itself is an important diet in mesozooplankton feeding (Rollwagen Bollens and Penry, 2003; Calbet and Saiz, 2005). However, the contribution of microzooplankton to mesozooplankton carbon consumption is very variable (Calbet and Saiz, 2005). These processes are obtained in a thin surface layer, but also influence the ocean region below the euphotic zone. Organic material enters the deeper ocean by mixing, advection, diffusion, passive sinking and active transport. In particular, sedimentation of sinking particles like living and dead phytoplankton cells, dead animals, faeces and marine snow is the link between the primary production at the eutrophic zone and the benthic community (Koppelmann and Frost, 2008).

Important contributors to the vertical particle flux are mesozooplankton organisms like Salpida and Euphausiacea that feed on phytoplankton, microzooplankton, other mesozooplankton and detritus in the surface water (Al-Mutairi and Landry, 2001). The vertical migration of zooplankton which is caused by biological factors like prey and predators and physical factors such as salinity, temperatures and oxygen (Pearre, 1979; Forward, 1988) transports organic material into deeper water layers. Therefore, physical barriers like thermoclines (Pillar et al., 1989; Kiorboe et al., 1990) and haloclines (Sprintall and Tomczak, 1992) have an impact on the distribution of plankton. At depth, the mesoplankton excrete rapidly sinking faecal pellets, but heterotrophic consumption leads to a reduced flux of organic material (Nival et al., 1988; Buitenhuis et al., 2006). Particulate organic carbon (POC) concentrations decrease in the depth interval from 100 to 1000 m by a factor of 10 (Suess, 1980).

The vertical and horizontal distribution of the mesozooplankton has an influence on the partial flux (Martin et al., 1987; Burd and Jackson, 2009; Burd and Jackson, 2009). When estimating the carbon supplied by POC and heterotrophic activity in field studies, the heterotrophic activity was found to be two to three times higher (Boyd et al., 1999; Reinthaler et al., 2006; Steinberg et al., 2008; Baltar et al., 2009) and is partly transformed into dissolved organic carbon (DOC) by metabolic activity (Koppelmann et al., 2000).The particulate material flux in the BUS is highest in southern fall and spring (Wefer and Fischer, 1993).

A further characteristic of the BUS are frequently occurring oxygen minimum zones (OMZ; Hamukuaya et al., 1998) which are located on the shelf between 50 m and 150 m water depth and down to 300 m at the shelf break (Hart and Currie, 1960). The OMZ may cover 50 % of the shelf (Brüchert, 2006) and have an oxygen concentration of < 10 µM O_2 due to the consumption of O_2 during the decomposition of settling organic matter (Chapmann and Shannon, 1985). The extensions of the OMZ are limited by physical barriers such as fronts and seasonal changes (Monteiro and van der Plas, 2006). OMZ are also caused by biochemical processes like a strong N-deficit in the bottom waters due to denitrification (Perry et al., 1993; Shannon and Weaver, 1949). Another factor causing the reduced O_2-concentration is the oxygen-deficient South Atlantic Central Water (SACW) (Poole and Tomczak, 1999; Mohrholz et al., 2001) which is entering the BUS from the north (Steffani, 2012; Hutchings et al., 2009).

Besides the impact of the OMZ, the seafloor conditions in this habitat are influenced by other important processes as transformations of oxygen, nitrate and sulphate into carbon dioxide, dinitrogen, hydrogen sulphide and methane at the sediment-water interface (Emeis et al., 2004).

These sediment-water processes on the shelf cause a high sulphide concentration, which is created by the decomposition of organic material. This decomposition occurs either by the use of oxygen or under anaerobic conditions in up to 7000 km² of 9000 km^2 of the OMZ (Brüchert, 2006). These processes favor the development of chemolithoautotrophic and sulphide oxidizing bacterial mats on the seafloor (Schulz et al., 1999). High seasonal productions and growing of bacterial mats are also caused by the relatively warm bottom water, which furthermore increases the rates of nutrient turnover. Anaerobic bacterial mats reduce the sulphide and produce hydrogen sulphide gas (H_2S). This toxic gas in association

with hypoxia may cause the absence of fish in these regions (Steffani, 2012). If the concentrations of gaseous products exceed solubility, the gas is saved in the sediment. An abrupt elusion into the water column may cause mass extinctions (Emeis et al., 2004).

The mass extinction caused by toxic gas, the OMZ and the availability of food via organic material input influence the structure and the appearance of benthic animals in, on and above the seafloor (Ricklefs, 1987; Roughgarden, 2006). Another source of food could be provided by the lateral advection and river discharge (Parsons et al., 1984). Benthic communities are formed by several species of the same or different trophic levels and essentially different niches are defined by their requirements and resource usage (Leibold, 1995). In the northern BUS, the benthic fauna shows a heterogeneous distribution and structure in different regions and at different depths. This can be obtained and recorded by the usage of Remotely Operated Vehicle (ROV) operating on the shelf and at the continental slope (Werner, 2012). It is presumed that these differences in the habitat structure of the benthos are caused by physical, chemical and biological processes (Narvarrete et al., 2005; Siegel et al., 2008).

Different factors causing the heterogeneity in benthic structures will be analyzed in this study.

(1) ROV observation of the benthic megafauna and bacterial mats will be re-evaluated.
(2) The benthos of the top 5 cm of the sediment will be analyzed using sediment cores.
(3) This data will be supplemented and linked to physical water parameters and Chl *a* satellite observations (primary production).
(4) The biomass, the vertical and horizontal distribution of microzooplankton and mesozooplankton will be analyzed and correlated with the observations of benthic structures.
(5) Finally, the data of the chemical parameters of the seafloor sediment-water interface will be linked to the observed data.
The correlation of the abiotic and biotic data will provide a better understanding of the factors forming the benthic community.

2 Materials and Methods

2.1 Research area

Data used in this study was collected during the expedition 17/3 of the RV MARIA S. MERIAN in February 2011 on a research cruise in the area between Lüderitz (26.6° S) and Kunene (17.5° S) off the Namibian coast. This study is a part of the BMBF (Bundesministerium für Bildung und Forschung) project GENUS (Geochemistry and Ecology of the Namibia Upwelling System). The aim of this project is to identify structures and links between organisms in an upwelling ecosystem and biogeochemical processes for a better understanding of the functional and trophical relationships in this habitat (Lahajnar et al., 2012). Samples for this study were taken at 10 stations on three transects (Terrace Bay, Rocky Pointy and Kunene) from the coast line to open waters (Figure 2).

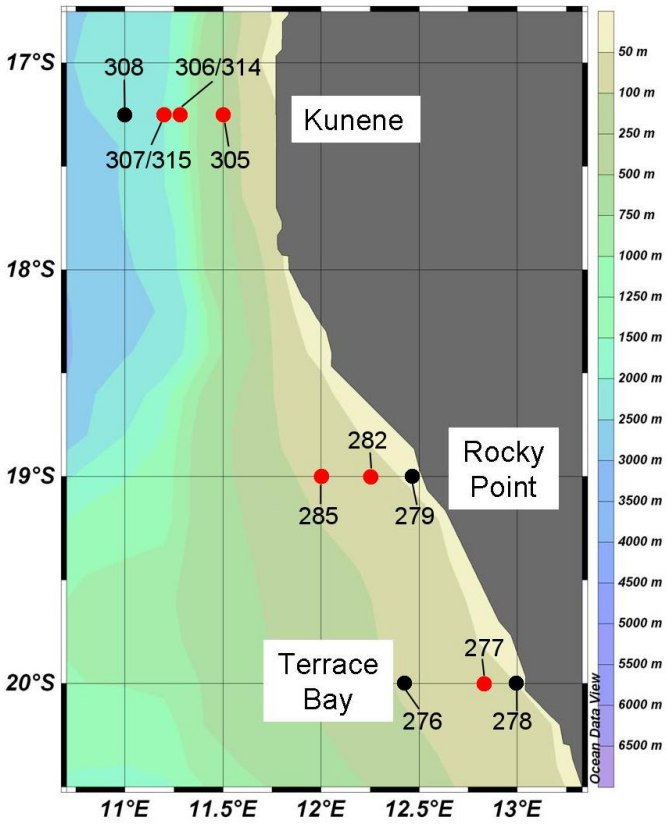

Figure 2: Research area with the sampled stations (red dots illustrate the ROV stations, black dots illustrate the further sampling stations of other gears, mostly Multicore) during the expedition 17/3 of the RV MARIA S. MERIAN in the year 2011. The samples from the three northern transects (Terrace Bay, Rocky Point and Kunene) were used for this study.

On the Terrace Bay transect (20° S) five stations which covered the shelf area with water depths between 50 m and 400 m were sampled. At six stations at water depths between 38 m and 2080 m samples were taken on the shelf and the continental margin of the Rocky Point transect (19° S). Both areas are characterized by a broader shelf zone and a more gradual slope than at the Kunene transect (17.5° S), where 8 stations at depths between 35 m and 4826 m were sampled. This area is characterized by an extremely narrow shelf and a steep slope. For that purpose a pumping CTD system (Conductivity, Temperature and Depth) "SBE 911plus" (SEABIRD-ELECTRONICS, USA), a multinet (HYDRO-BIOS, Kiel, Germany), a 1 m²-Double Multiple Opening/Closing Net and Environmental Sensing Systems (MOCNESS; BESS, North Falmouth Mass, USA), a Remotely Operated Vehicle (ROV) (MOHAWK Sub-Atlantic, Aberdeen, UK) and a multicorer (Oktopus, Kiel) were applied (Table 1).

Table 1: Overview of sample types taken at the different stations

Station	Tran-sect	CTD[1]	Chl *a* Satel-lite[2]	Microzo-opl. abundance	Mesozoopl. abundance	Mesozo-opl. Bio-mass[4]	Bio-chemis-try[5]	Benthos sieve pictures[5]	ROV
276 for 277	Terrace Bay			✓					
277	Terrace Bay	✓	✓				✓		✓
278 for 277	Terrace Bay						✓	✓	
279 for 282	Rocky Point						✓	✓	
282	Rocky Point	✓	✓	✓ (night)					✓
285	Rocky Point	✓	✓	✓ (day)	✓ (day[4]/night)	✓ (day/night)			✓
305	Kunene	✓	✓	✓ (day)[3]	✓ (day)	✓(day)	✓	✓ (9 hauls)	✓
306/314	Kunene	✓	✓	✓ (day)[3]	✓ (night)	✓ (night)	✓		✓
307/315	Kunene	✓	✓	✓ (day)[3]	✓ (day)[4]	✓ (day/night)			✓
308 for 307	Kunene						✓	✓	

inherited by: V. Mohrholz[1], NASA Earth Science EaSUREs DISCOVER Project (MODIS)[2], K. Bohata[3], , B. Martin[4], A. Neumann[5].

2.2 Satellite Data

Near-surface chlorophyll *a* concentrations (Chl *a*; mg m^{-3}) were obtained by the Moderate Resolution Imaging Spectroradiometer (MODIS) level-3 product. These MODIS data are produced by Remote Sensing Systems sponsored by the NASA Earth Science EaSUREs DISCOVER Project (data source: http://oceancolor.gsfc.nasa.gov/; Feldman and McClain, 2012).

The data was integrated as weekly and monthly means from January 1th to February 25th, since high concentrations of clouds in the Benguela Upwelling area disabled a fine temporal resolution. The spatial resolution was set to 4 km. To consider the influence of temporarily changing conditions to the allocation of zooplankton biomass, Chl *a* data was collected 4-6 weeks prior to the actual sampling period (Table 1).

2.3 Field Sampling

A pumping system CTD was used to obtain vertical profiles of the following abiotic parameters: conductivity, temperature, pressure, salinity and oxygen concentration. The data was monitored and stored via the program Seasave (Version 7).

2.3.1 Microzooplankton sampling

Microzooplankton was sampled by vertical hauls with a multinet. The multinet was equipped with four nets with a mesh size of 55 µm, which can be opened and closed at defined water depths, allowing a vertical resolution of the water column. Sampling was done during heaving from the maximum sampling depth at a winch speed of 0.5 m s^{-1}. The multinet was used twice at stations deeper than 200 m. At shallow stations, the intervals were 200-100-50-25-0 m. At deeper stations, the additional intervals were 1000-600-400-200-0 m, depending on the total water depth. The samples were fixed in 4% formaldehyde-seawater solution buffered with sodium-tetraborate.

Mesozooplankton samples were taken with a MOCNESS. The gear was equipped with 2*9 nets parallel to each other with a mesh size of 330 µm (Wiebe et al., 1985). The opening and closing system allowed sequential sampling. Intervals for sampling were 250-200-100-50-25-0 m depth at the shelf stations (0 m to 250 m) and 1000-800-600-400-200-100-50-25-0 m depth at the deeper shelf break (250 m to 500 m) and slope stations (500 m to 1500 m) depending on the total water depth.

The left nets were used for biomass and taxonomical analyses, whereas organisms from the right nets were selected for physiological experiments and biogeochemical analyses. The filtered volume of each net was measured by a flow-meter (HYDROBIOS, Kiel, Germany). Veering and heaving speed of the winch was 0.5 m s^{-1} and was reduced to 0.2-0.3 m s^{-1} in the upper 200 m. This way a MOCNESS-frame angle of 45° and an effective opening of 1 m^2 was maintained. Changes in tilt were measured with an inclinometer and considered in the calculation of the filtered volume (Koppelmann and Weikert, 1992). The towing speed was 2 knots.

2.3.2 Sampling of biogeochemistry data

A multicorer equipped with twelve acrylic glass PMMA-tubes was used for benthic sampling. The tubes had an inner diameter of 10 cm and were 60 cm long. Profiles were obtained by multicorer casts at five stations on the three transects (Terrace Bay, Rocky Point and Kunene; Table 1). Additionally, at five stations of each transect water from the corers above the sediment was taken for further analytical investigation of nutrients. Oxygen profiles in the sediment were measured via microprobes (PRESENS) and an automated micromanipulator (PYRO SCIENCE). Carbon dioxide and nitrogen profiles were simultaneously measured for each profile with a quardrupole mass spectrometer (INPROCESS INSTRUMENTS) equipped with a needle-type membrane inlet and a second micromanipulator (PYRO SCIENCE). To prevent instabilities and to avoid increased reaction rates caused by warming of the sediment, both setups were kept in a temperature controlled laboratory. Furthermore, pore water was sampled with rhizon core solution samplers (Rhizophere Research), using core lines prepared with sealed ports for nutrients and δ^{15} N analysis. Simultaneously, overlying water of the sediment cores was sampled.

The calculated reaction rates of nitrate were evaluated with Isotope-Pairing Incubations (IPI) according to Risgaard-Petersen et al. (2003). We conducted all IPI at 15 °C. Therefore, the stations for IPI were selected based on the temperature of the bottom water. A 4 cm sub core of the multicores was used for sampling. Afterwards, the samples were filled with 98 % ^{15}N-Nitrate and incubated by a constant mix via magnetic stirrers for six hours. The sub cores were homogenized to slurries and the resultant $^{29}N_2$ and $^{30}N_2$ were measured using a quadruple mass spectrometer (INPROCESS INSTRUMENTS) equipped with a flow through membrane inlet, developed at HZG Geesthacht, on board. (For further details see Neumann 2012.)

2.3.3 Benthic sampling

The first 5 cm of the core sample were sieved through a 500 µm sieve (Retsch). Macrozoobenthic organisms were immediately presorted through the sieve. Empty conches were arranged with the concave part (blank) facing up. Living bivalves were deposited with the convex side up. Samples with a lot of seashells were not arranged. From each sieve a complete photo as well as some close-ups were taken via DSLR (Nikon D70; NIKON CORPORATION, Japan).

2.3.4 Remotely Operated Vehicle (ROV)

A modified ROV was used to observe the benthic megafauna. The ROV can reach a depth of 1000 m. The vehicle was equipped with four horizontal and one vertical propeller, which allowed a maximum forward speed of 2 knots. The ROV was linked to a control unit via fiber-optic cable. Power (400 V three phase) was supplied via copper cable. The vehicle was equipped with a color-zoom and a black and white camera. The physical parameters of the water column were measured with a CTD and an oxygen optode. The video link enabled recording and a direct view of the environment from the control room. The depths and distance to the sea bottom were overlaid on the screen and two laser point markers defined a distance of 10 cm on the ground. A positioning system (manufactured by IXSEA) was used to link the position of the ROV and the position of the vessel relative to each other via transmitter and receiver from the ROV as well as from the vessel. The

travel time of the sound enabled a determination of the location of the ROV in relation to the vessel. The Global Positioning System (GPS) of the vessel made it possible to calculate the coordinates of the ROV.

The ROV was used at four shelf stations (100 to 200 m water depths): one on the Terrace Bay transect, two on the Rocky Point transect and one on the Kunene transect. Furthermore, deeper ROV stations were examined on the Kunene transect at 500 and 800 m depth.

2.4 Laboratory work and calculations

2.4.1 Microzooplankton

In the home laboratory the samples were transferred into a sorting solution consisting of 0.5 % propylene phenoxetol, 5 % propylene glycol and 94.5 % tap water. The material was split using Hensen-pipettes. After transferring the subsample into a Bogorov Counting Chamber, the species were identified and the numbers of individuals of each species were determined under a binocular (Leica M165c, Leica Camera AG, Germany)

2.4.2 Mesozooplankton

The fixed samples were separated into five size categories (> 5 mm, 2 to 5 mm, 1 to 2 mm, 0.5 to 1 mm, < 0.5 mm) using a sieve chain. The fractions were placed into 70 % ethanol for 1 min to eliminate adherent water and then transferred onto absorbent paper (Tranter, 1962). The wet mass (WM) was determined on an analytical balance. This method was used instead of the more precise dry mass determination to allow subsequent taxonomical analyses. Wet biomass was standardized to mg m^{-3}. The size fractions were fixed in a sorting solution consisting of 0.5 % propylene phenoxetol, 5 % propylene glycol and 94.5 % tap water for further taxonomical identification. The sample was divided according to density into smaller, more easily countable fractions using a Motodo plankton splitter and transferred into a Bogorov Counting Chamber. The plankton species were then determined and the numbers of individuals were counted using the binoculars Leica M165c and Leica M16 (Leica Camera AG, Germany). Finally, the numbers of species were counted and

standardized to numbers of individuals per m^3. Copepoda were divided into Calanoida and non-Calanoida. The latter group consists of Cyclopoida, Harpactioida etc. (Huggett and Bradford-Grieve, 2007).

2.4.3 Biochemistry

The water samples were analyzed for nutrients and dissolved organic carbon (DOC). The concentration profiles of oxygen and dissolved inorganic nitrogen across the sediment water interface are the basis of flux calculation according to Berg et al. (1998). Measurement and calculations of the elements (N_{tot} (total) % (sediment), C_{org} (organic) % (sediment), C_{org} : N_{tot} (molar ratio), oxygen consumption (µmol/$m^{-2}d^{-1}$), phosphate production (µmol m^{-2} d^{-1}), nutrients (bottom concentration (c.) (PO4), bottom c. (NO_x), bottom c. (NO_2^-), bottom c. (NH_4^-), bottom c. (Din), bottom water oxygen (µM)) and fluxes (nitrate flux, nitrite surface flux, N^2 flux, ammonium flux, phosphate flux) were done by Neumann (Table 2).

Table 2: Availability of benthic data from the sediment cores, water samples and mooring.

Station	Transect	Latitude	Longitude	Depth [m]	Sieve pictures	Elements	Nutrients	Flux
277	Terrace Bay	-20.000	12.833	99			✓	
278	Rocky Point	-20.000	13.000	30	✓	✓	✓	✓
279	Rocky Point	-19.000	12.450	35	✓	✓	✓	✓
305	Kunene	-17.253	11.507	142	✓	✓	✓	✓
308	Kunene	-17.250	11.000	2103	✓	✓	✓	✓

2.4.4 Bacterial mats

Bacterial mats were assessed with the help of a still image taken every 10 m on the idealized straight line. The percentage categories in Table 3 were used in the assessment.

Table 3: Categories of bacterial mats covering

Categories	Covering (%)
Extensive	80-100
Frequently	50-79
Rare	20-49
Infrequent	1-19
Nonexistent	0

The average bacterial mat covering from all still images was calculated for each transect. If a still image did not show the sea floor it was excluded from the calculation.

2.4.5 Benthic macrofauna

The taxa were defined and counted on the sieve photos per station (Table 2). For comparison, the results were standardized on an area of 1 m^2 via the formula:

$$B = C \; co \times 100.$$

B: Benthic macrofauna per m^2
C: counting's of one taxon
co: 78 = cm^2 of each core.

2.4.6 ROV tracking and idealization

The tracks of the ROV surveys were displayed using coordinates from the IXSEA positioning system and the data was recalibrated to calculate an idealized track route. First, the coordinates were converted into travelled distance (in meters) from a starting point by using the following formulas:

Latitude: $dLa = -1 \times La0 - La_1 \times mpNM \times NM.$
Longitude: $dLo = -1 \times Lo_0 - Lo_1 \times mpNM \times NM \times \cos La_1 \times \pi \; 180$.

La_0 and Lo_0: start latitude (La) and longitude (Lo) coordinates
La_1 and Lo_1: actual latitude/ longitude
NM: 60 NM: sea miles per degree
mpNM: 1852 m/NM: meter per nautical mile

Starting latitude (La_0) and longitude (Lo_0) were presented in decimal numbers and were used for all further calculations. Variations in the actual longitude (Lo_1) and latitude (La_1) are caused by the recorded coordinates of the ROV and were indicated by red points. The starting point is 0.0. Deviations to the south and west from the starting point have negative values. To obtain a track route, distinct points (green points) were marked to create an idealized track route (It; blue line, Figure 3) via the following formula:

$$It = \overline{Y_1 - Y_2\ ^2 + X_1 - X_2\ ^2}.$$

X_1 and X_2: starting point coordinates
Y_1 and Y_2: end point coordinates.

All defined sub tracks of the ROV deployment were cumulated to create an idealized total track (Figure 3) and all raw data points were later fitted into the idealized straight sub tracks (blue line) to relate the observations on this line.

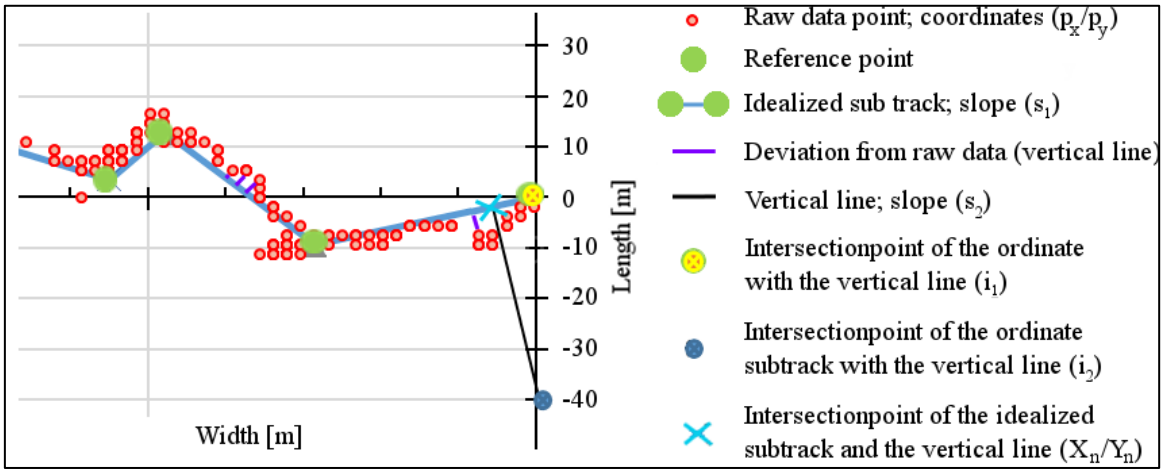

Figure 3: Transformation of raw track data onto idealized linear track route

The idealized sub track slopes (s_1) were calculated. Each vertical line slope (s_2) of the idealized sub track and the raw data point was calculated via the following formula:

$$s_2 = -\ 1\ \ s_1\ .$$

s_1= slope of the idealized sub track

The intersection point of the ordinate of the vertical lines (i_2) was defined by

$$i_2\ = p_y - s_2\ \times p_x.$$

p_y= y-coordinate of the raw data point
p_x= x-coordinate of the raw data point
s_2= vertical line slope between the idealized sub track and the raw data point

The following formula was utilized for the calculation of the new x-coordinates (X_n) on the idealized sub track for the raw data points:

$$X_n = \quad i_2 - i_1 \quad s_2 - s_1 \quad .$$

i_2: intersection point of the ordinate with the vertical line
i_1: intersection point of the ordinate with the idealized sub track
s_2: vertical line slope between the idealized sub track and the raw data point
s_1: slope of the idealized sub track

For definition of the new y-coordinates (Y_n) the following idealized linear equation was used:

$$Y_n = s_1 * X_n + i_1.$$

s_1: slope of the idealized sub track
X_n: new x-coordinate of the idealized sub track
i_1: intersection point between the ordinate and the idealized sub track

All measured points (red points) were transferred with the exact time of observation onto the idealized linear track route (blue line) via the vertical lines (black line). Outliers, inaccurate and distinct points were removed from the idealized track route by using an if-else function. This function displayed all data points where:

- The x-coordinate of the suspended measured point on the line is not ahead of the last x-coordinate of the idealized sub track route in moving direction of the ROV.
- The x-coordinate of the point is not located between the start and the end x-coordinate of the sub linear tracks.

The remaining points were used to calculate the modified track distance, which was similar to the calculated idealized total track route using the distinct points (Figure 3).

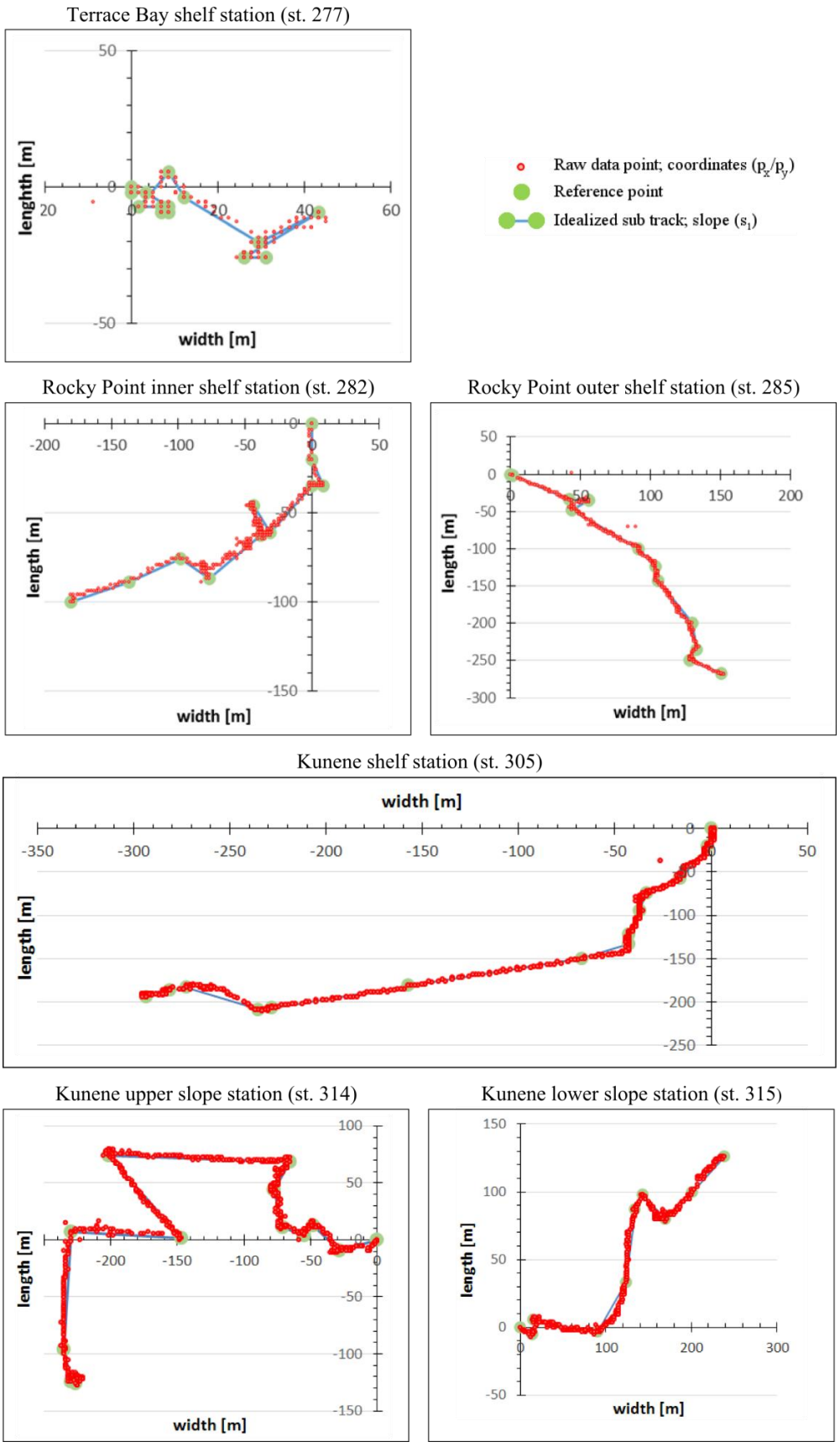

Figure 4: Raw data points of the ROV position and reference points which are connected for the idealized track route for all ROV stations

2.4.7 Identification and abundance calculation of the benthic megafauna

Organisms detected on the ROV videos were identified and counted; the displayed time on the video was used to relate the detected organisms to the modified idealized track. The travel time of the sound waves (ca. 1500 m s^{-1}) of the positioning system and the elimination of outliers are the reason for a slight discrepancy between time and exact position. For comparisons of the numbers of individuals per species between the different stations the counts were standardized to 100 m of the idealized track route via the formula:

$$X = n \times 100 \quad R.$$

n: the number of individuals of one species
R: the length of the idealized track route [m]

2.4.8 Estimation of species with high abundance

At stations with a high abundance of individuals (more than 500 ind. 100 m^{-1}), subsamples were evaluated and individuals were counted every 10 minutes for 30 seconds while the distance traveled during this time was also determined. The results were standardized to one meter and the average was calculated.

2.4.9 Correlation of the main parameters

The mean concentrations of microzooplankton and mesozooplankton were calculated by dividing the standing stock (ind. m^{-2}) of the whole sampled water column by the total sampling depth. The relative contributions (rc) of all main parameters (Chl *a*, microzooplankton, mesozooplankton, benthic megafauna, benthic macrofauna, benthic organic carbon, dissolved inorganic nitrogen and bottom water oxygen) of the stations were calculated using the following formula and plotted against each other:

$$rc = \frac{St_i}{\sum_{i=1}^{n} St_i}.$$

St_i: Single measured values for the different parameters at the different stations
$\sum_{i=1}^{n} St_i$: Sum of measured values for the different parameters

The relationship of variables was correlated by the spearman's rho correlation (Spearman, 1904).

To achieve an overall view of all pelagic and benthic abundances, the sum of all standardized abundances and concentrations of Chl *a*, microzooplankton and mesozooplankton of the pelagial and the sum of all standardized abundances of the benthic macrofauna and megafauna were displayed.

3 Results

3.1 Physical parameters at the three transects

3.1.1 Hydrography on the Terrace Bay transect (20° S)

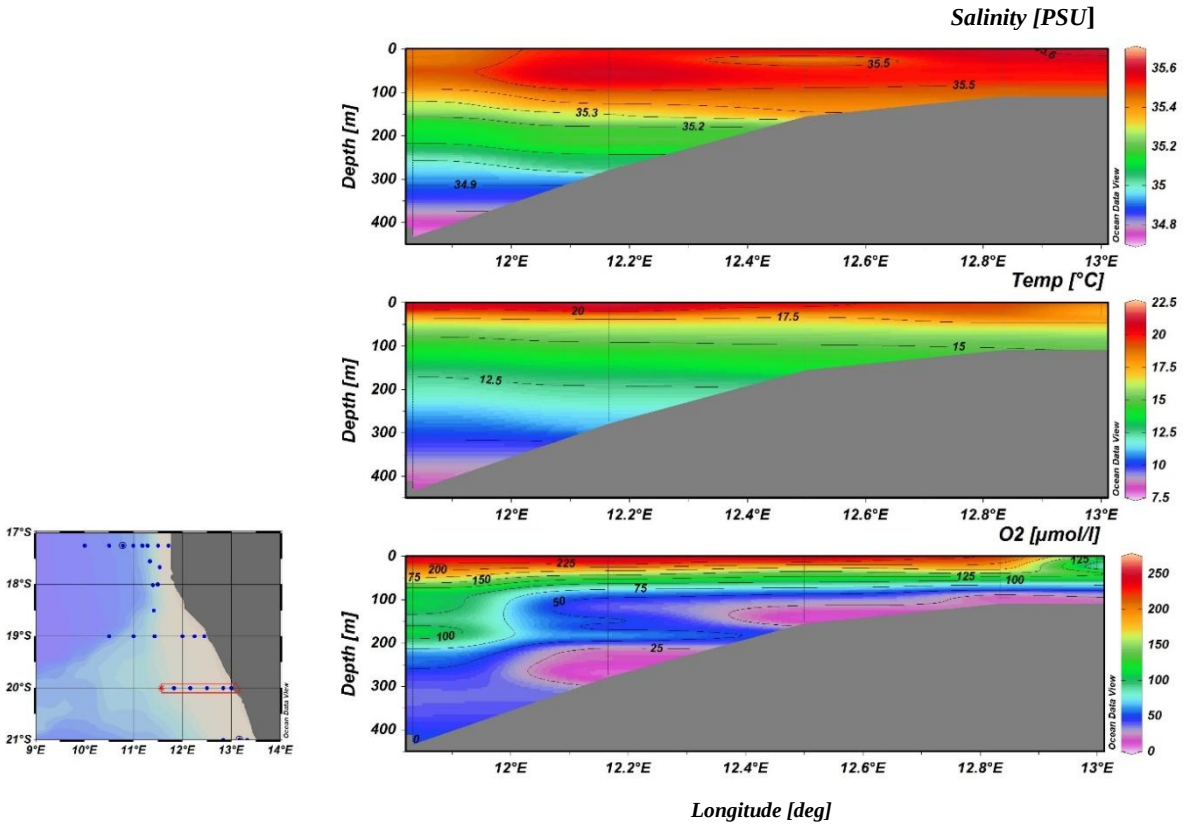

Figure 5: Distribution of salinity [PSU], temperature [°C] and oxygen [µmol/l] on the Terrace Bay transect (12.-13.02.2011).

Salinity was high near the surface layer (35.4 PSU) and decreased with depth to 34.8 PSU near the bottom on the Terrace Bay transect (Figure 5). The temperature near the surface layer had a maximum value of 21.5 °C and decreased down to 7.5 °C at 400 m depth.

Close to the coast in the upper 50 m the oxygen concentrations varied between 100 µml l^{-1} and 125 µml l^{-1}. Below this surface layer, the oxygen levels decreased down to almost 0 µmol l^{-1} (oxygen minimum zone). Offshore, the oxygen concentrations decline with depth from around 200 µmol l^{-1} near the surface to less than 50 µmol l^{-1} at deeper depths. Be-

tween 200 m and 300 m depth on the slope a minimum zone (close to 0 µmol l^{-1}) was localized.

3.1.2 Hydrography on the Rocky Point transect (19° S)

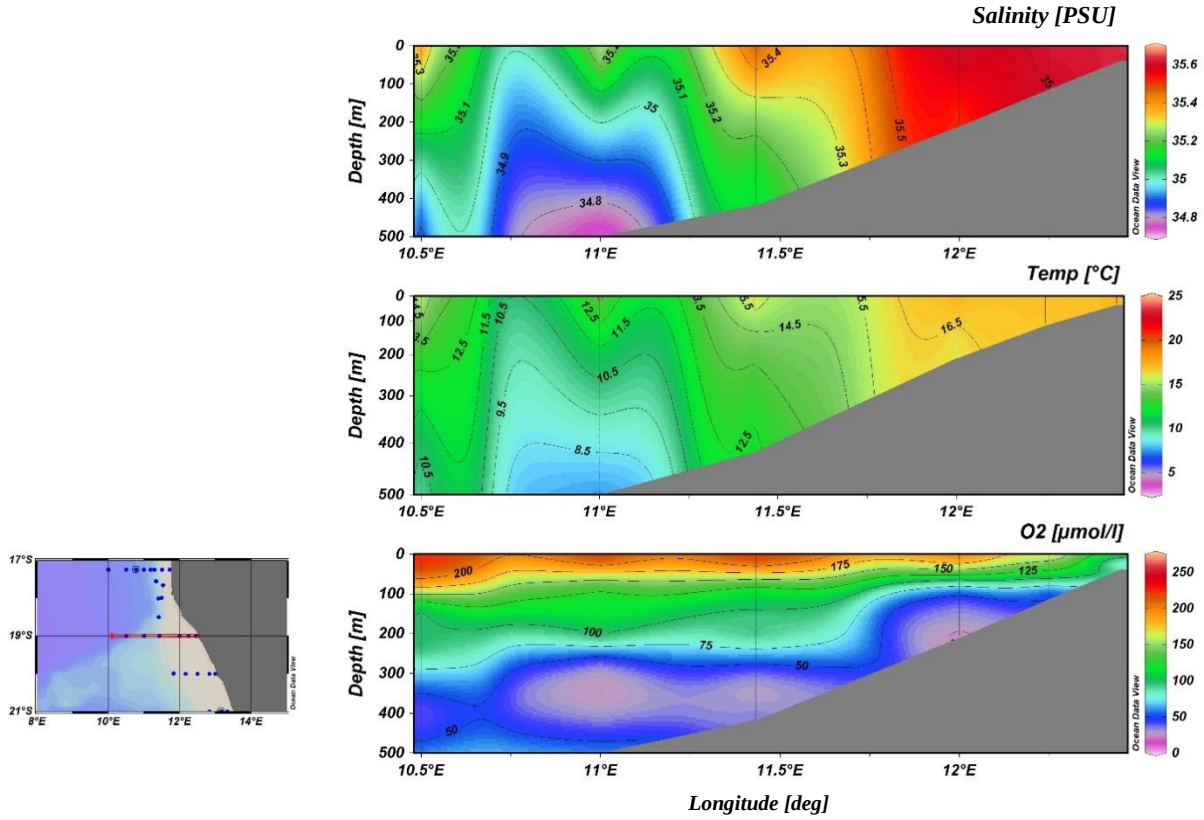

Figure 6: Distribution of salinity [PSU], temperature [°C] and oxygen [µmol/l] on the Rocky Point transect (14.-17.02.2011).

On the Rocky Point transect the salinity ranged from 35.7 to 34.8 PSU with a declining trend down the continental slope (Figure 6). Offshore the salinity was 35.2 PSU near the surface (0-50 m depth). A water body with salinity values of 34.8 to 35 PSU was detected between 100 m and 500 m at the upper slope (11° E), surrounded by saltier water. The water temperature was the highest (16.5 to 18.5 °C) near the coast. Offshore the temperature ranged between 17 °C near the surface and 12.5 °C at 100 m water depth. Temperature declined between 200 m and 500 m depth from 10.5 to 6 °C. The coldest temperature was reached below 400 m at the lower slope (11° E) showing a pattern similar to the salinity. At the inshore stations, anoxic water reached the surface (Figure 6) indicated by an oxygen

level of less than 50 µmol l^{-1} at 200 m depth. Further offshore oxygen concentrations ranged between 200 and 100 µmol l^{-1} in 50-200 m depth and dropped to less than 50 µmol l^{-1} between 300 m and 500 m depth.

3.1.3 Hydrography on the Kunene transect (17.5° S)

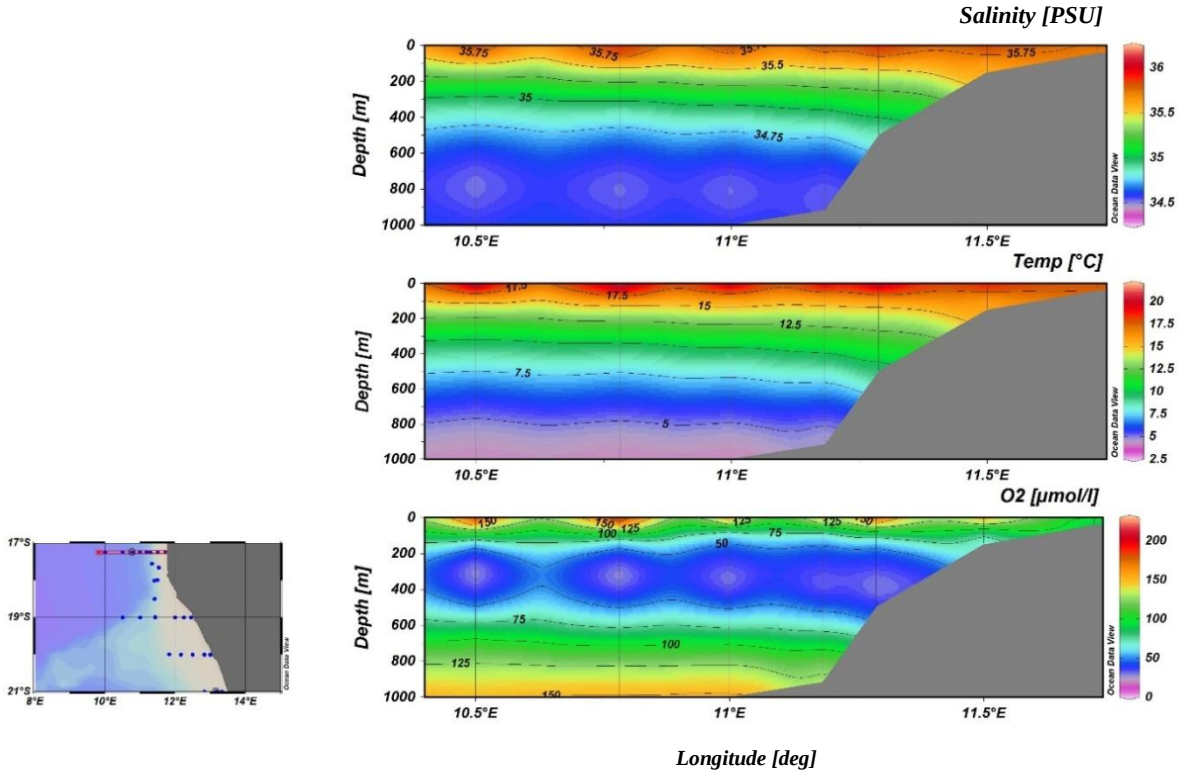

Figure 7: Distribution of salinity [PSU], temperature [°C] and oxygen [µmol/l] on the Kunene transect (19.-22.02.2011).

On the Kunene transect, salinity was about 35.8 PSU in the upper 100 m and declined to 34.6 PSU below 400 m water depth (Figure 7). Close to the surface and down to 200 m water depth the temperature was higher than 15 °C and decreased continuously with increasing depth to 2.5 °C at 1000 m. The oxygen level fluctuated from 150 µmol l^{-1} at the coast to 60 µmol l^{-1} at the open ocean site near the surface. An oxygen minimum zone with less than 1 µmol l^{-1} was located between 150 m and 600 m. Below 600 m oxygen rose again with increasing depth.

3.1.4 Summary of the hydrographical situation in the investigation area

The Terrace Bay transect is characterized by a stratified layer of salinity and oxygen with high concentrations near the surface. Furthermore, temperature and salinity were higher inshore than offshore. On the contrary, oxygen showed lower concentrations close to the coast. On the Rocky Point transect the physical parameters displayed similar patterns as on the Terrace Bay transect. However, the concentrations of those parameters were generally higher, except of a water body between 100 m and 500 m at the slope which had a low salinity and a low temperature. The Kunene transect was characterized by a stratified structure similar to the Terrace Bay transect. The main difference to the other transects was the oxygen minimum zone between 150 m and 600 m water depth.

3.2 Chlorophyll *a* concentrations

3.2.1 Chlorophyll a concentrations on the Terrace Bay transect (20° S)

During January 2011, the inshore chlorophyll *a* (Chl *a*) concentrations of the Terrace Bay transect were between 6 and 10 mg m^{-3} (Figure 8) and declined from the slope to the offshore area from 4 to 0.3 mg m^{-3}. Offshore the Chl *a* concentrations ranged from 0.3 and 0.03 mg m^{-3}. During the first week of January 2011, the Chl *a* concentrations were very high with 6 to 10 mg m^{-3} in the inshore area. On the slope and offshore the concentrations of Chl *a* decreased to 1 mg m^{-3} and 0.2 mg m^{-3}, respectively. In the middle of January (09.01.-24.01.) clouds made a detection of the surface Chl *a* concentrations impossible. At the end of January data was available only from the inshore area, where the Chl *a* concentrations were high with 5 to10 mg m^{-3}. At the shelf break the concentrations decreased to 0.3 to1 mg m^{-3}.

The general view of the Chl *a* concentrations indicated a higher primary production in February than in January 2011. At the beginning of February a detection of the Chl *a* concentrations were not possible due to overcast sky. In the middle of February (10.02.-17.02.) the concentrations of Chl *a* were measured between 1.5 and 3 mg m^{-3} above the slope. Offshore the distribution of the Chl *a* concentrations (0.2 to 0.03 mg m^{-3}) was similar to Janu-

ary. In the middle of February (18.02.-25.02.) the Chl *a* concentrations on the shelf were 4 to 10 mg m^{-3} and slightly decreased at the slope down to 0.3 to 1 mg m^{-3}.

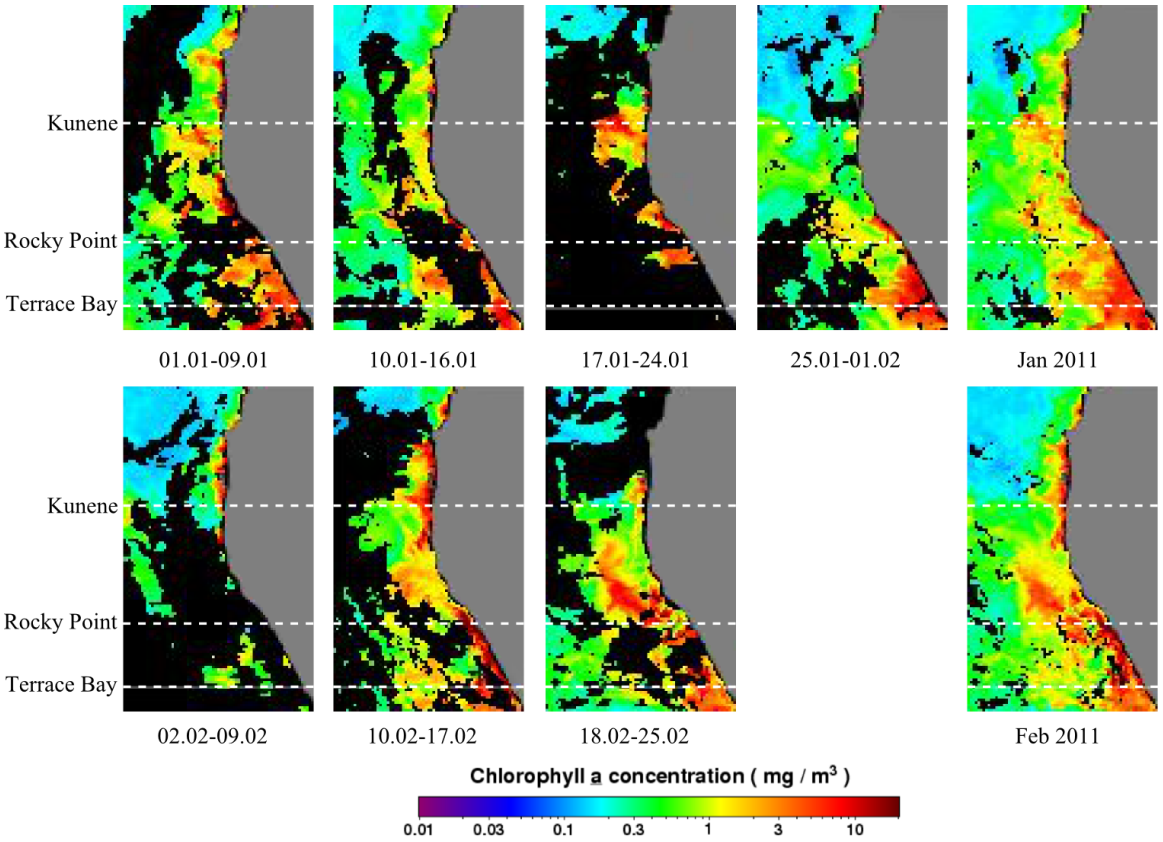

Figure 8: Chlorophyll a surface distribution detected via satellite (modified according to the data source: http://oceancolor.gsfc.nasa.gov/).

3.2.2 Chlorophyll a concentrations on the Rocky Point transect (19° S)

The Chl *a* concentrations on the Terrace Bay transect were generally higher than on the Rocky Point transect. At the beginning of January 2011 (01.01.-08.01.) the inshore Chl *a* concentrations of the Rocky Point transect (3-8 mg m^{-3}) were not as high as on the Terrace Bay transect (6-10 mg m^{-3}). Due to a lack of visual data above the shelf, it was not possible to define the concentrations of Chl *a* in this area. Chl *a* concentration decreased from onshore (10 mg m^{-3}) towards offshore (0.3 mg m^{-3}; Figure 8). In the latter area the concentrations of Chl *a* (0.1-1 mg m^{-3}) were higher than on the Terrace Bay transect. In the second week of January (09.01.-16.01.) data were obtained only near the coast and offshore with elevated Chl *a* concentrations with around 0.5 mg m^{-3} to around 8 mg m^{-3}. No data were available from the middle of January (17.01.) for the Terrace Bay transect. At the end of

January (25.01.) high Chl *a* concentrations (6-8 mg m-³) were detected inshore with a decreasing trend towards offshore on this transect, while the Rock Point transect showed a medium concentration of 1-3 over the whole transect.

In February 2011, high Chl *a* concentrations were detected at the coast. On the shelf, the Chl *a* concentrations reached around 10 mg m^{-3}. At the beginning of February (02.02.-09.02.) no data were available for this transect. In the middle of February (10.02-17.02.) only a few data points were measured inshore, indicating high Chl *a* concentrations of around 10 mg m^{-3}. On the shelf, the Chl *a* concentrations increased on both transect from 8-10 mg m^{-3} compared to the previous measurements in January. At the end of this month (18.02.-25.02.) the concentrations in the coastal area were similar to the previous period but slightly increased to 1-3 mg m^{-3} above the slope. At the end of February similar concentrations were found in the offshore region as at the end of January 2011.

3.2.3 Chlorophyll a concentrations on the Kunene transect (17.5° S)

The integrated data for January 2011 showed Chl *a* concentrations of 1-6 mg m^{-3} inshore of the Kunene transect (Figure 8). From the slope to the offshore area, the Chl *a* concentrations decreased from 3 to 0.3 mg m^{-3}. At the beginning of January (01.01.-08.01.) the inshore Chl *a* concentrations and slope concentration were lower with 0.3 to 3 mg m^{-3} than on the other transects. At the offshore region no data were available. During the second week of January (09.01.-16.01.) the Chl *a* concentrations on the slope could not be detected through the clouds in the inshore area. On the shelf and offshore the Chl *a* concentrations ranged between 0.2 and 1.0 mg m^{-3}. Merely in the third week of January (17.01.-24.01.) further detections were possible on the shelf with Chl *a* concentrations increased from 1 to 8 mg m^{-3}. At the end of January, the Chl *a* concentrations for this month ranged from 0.3 mg m^{-3} to 2 mg m^{-3} inshore and between 0.1 and 1 mg m^{-3} on the slope and in the offshore region. The slope showed Chl *a* concentrations between 0.3-1 mg m^{-3}. In the offshore area the Chl *a* concentrations were lower and ranged from 0.1 to 0.5 mg m-³. In the beginning of February (02.01.-09.02.) the Chl *a* concentrations reached 3 mg m-³ inshore and 0.1 mg m-³ offshore. However, in the middle of February a peak was measured with 1-10 mg m-³ on the shelf. Chl *a* concentrations slightly decreased down to 0.3 to5 mg m-³ on the shelf at the end of February 2011.

3.2.4 Summary of the chlorophyll a distribution in the investigation area

In general the Chl *a* concentrations were lower in February 2011 than in January 2011, and ranged between 3 and 6 mg m^{-3} inshore. The slope showed Chl *a* concentrations between 0.3-1 mg m^{-3}. In the offshore area the Chl *a* concentrations were lower and ranged from 0.1 to 0.5 mg m^{-3}. In the beginning of February (02.01.-09.02.) the Chl *a* concentrations reached 3 mg m^{-3} inshore and 0.1 mg m^{-3} offshore. However, in the middle of February a peak was measured with 1-10 mg m^{-3} on the shelf. Chl *a* concentrations slightly decreased down to 0.3 to5 mg m^{-3} on the shelf at the end of February 2011.

Chl *a* showed higher concentrations in February than in January 2011 and higher concentrations inshore (6-10 mg m^{-3}) than offshore (0.1-1 mg m^{-3}) on all transects. During both months, higher Chl *a* concentrations were observed on the Terrace Bay transect and on the Rocky Point transect than on the Kunene transect.

3.3 Microzooplankton abundance and vertical distribution

3.3.1 Microzooplankton abundance on the Terrace Bay transect (20° S)

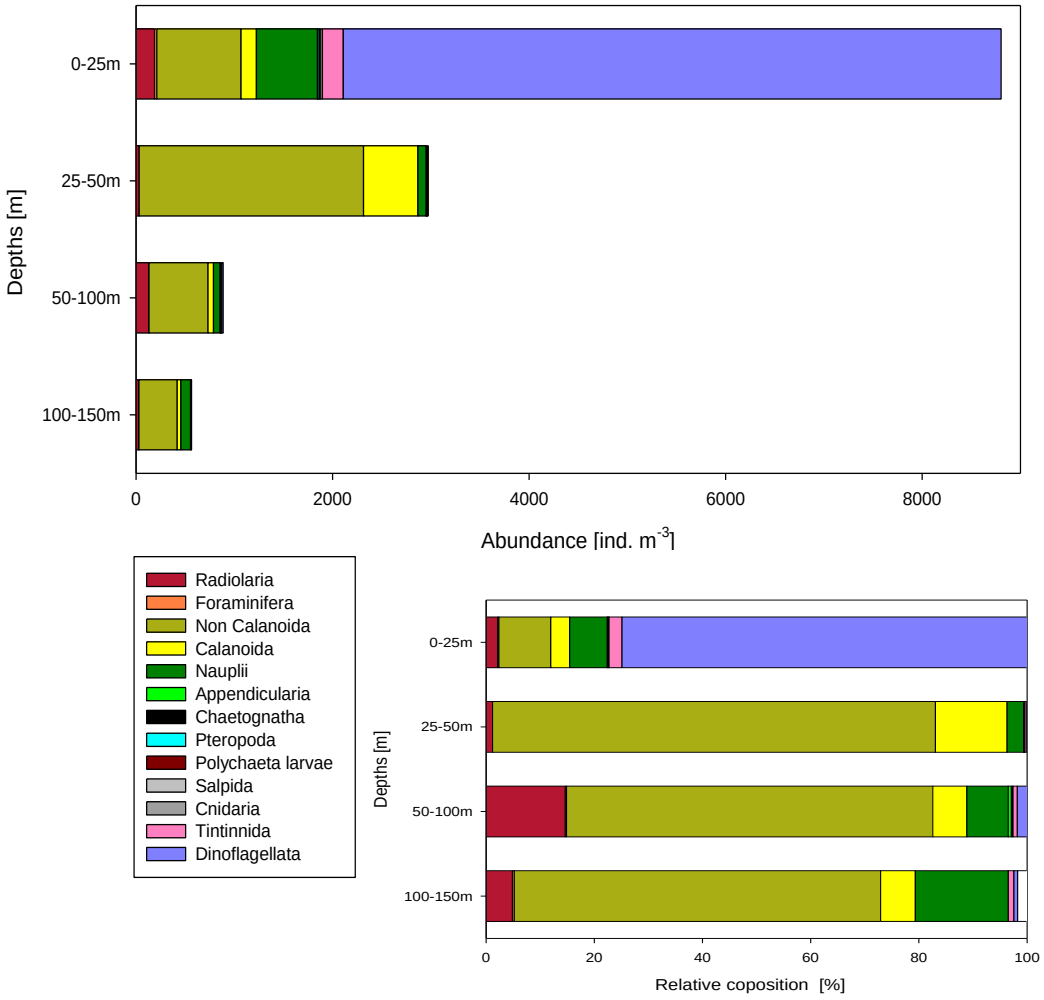

Figure 9: Microzooplankton abundance [ind. m^{-3}] in depth intervals and relative composition [%] at the Terrace Bay outer shelf station (st. 276) during daytime.

During daytime, the abundance of microzooplankton at the Terrace Bay outer shelf station (st. 276) was the highest with more than 8900 ind. m^{-3} in the depth interval between 0 m and 25 m (Figure 9) and decreasing with depth. The mentioned depth interval was dominated by Dinoflagellata with more than 79 % followed by non-Calanoida. Furthermore, the highest abundances of Nauplii were detected with a decreasing trend with depth but an increasing trend in relative composition. In the deeper water layers the abundance of microzooplankton decreased from 8900 ind. m^{-3} to 3000 ind. m^{-3}. The second lowest total

individual number of around 900 ind. m^{-3} was detected between 50-100 m, whereas the diversity was highest in this water layer. In the depth intervals 50-100 m and 100-150 m the non-Calanoida species dominated the composition in a range of 60 % to 65 % per interval, followed by Radiolaria with 32 %. Furthermore, 13 % of the individuals detected in these depth intervals were Calanoida. Further taxa found were Foraminifera, Chaetognatha, Appendicularia, Polychaeta larvae, Tintinnida, and Dinoflagellata. However, these taxa contributed less than 2 % each to the composition in these depth intervals.

3.3.2 Microzooplankton abundance on the Rocky Point transect (19° S)

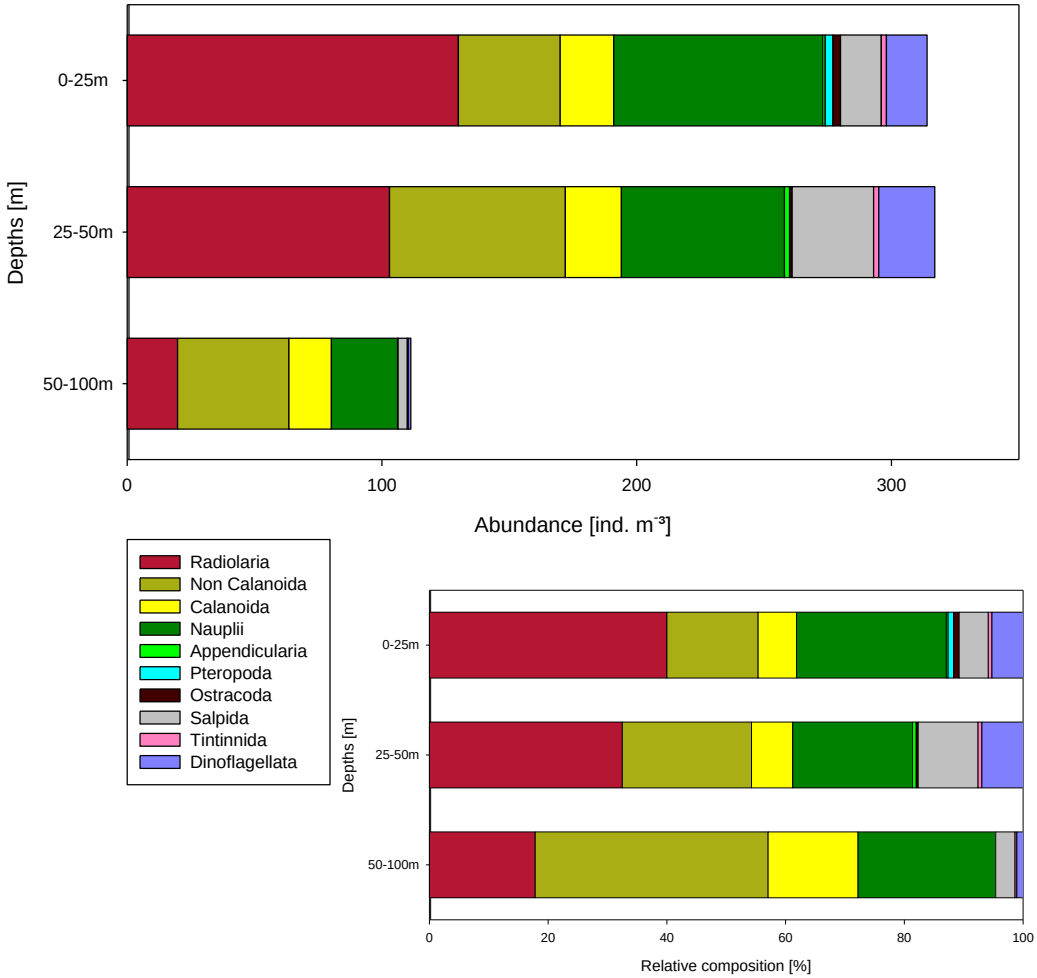

Figure 10: Microzooplankton abundance [ind. m^{-3}] in depth intervals and related composition [%] at the Rocky Point inner shelf station (st. 282) during night time.

At the inner shelf station (st. 282) on the Rocky Point transect three depth intervals down to 100 m water depth were sampled during night time (Figure 10). The abundances were the highest within the first two depth intervals (0-25 m and 25-50 m) with approximately 320 ind. m^{-3}. Radiolaria dominated the water layers with 50 % and 30 %. The contribution to the composition of non-Calanoida was 15 % (0-25 m) and 20 % (25-50 m). Further taxa with a high relative composition were Nauplii larvae with 10 % in 0-25 m and more than 23 % in 25-50 m depth. The total number of individuals decreased to 110 ind. m^{-3} in 50-100 m water depth where the non-Calanoida had the highest contribution with 35 %. Nauplii contributed up to 28 % (50-100 m), while Calanoida contributed with 8-13 % to the taxa's composition. For all depth intervals, further taxa like Salpida and Dinoflagellata showed a contribution of less than 10%. Appendicularia, Pteropoda, Ostracoda and Tintinnida obtained the lowest abundances with 1% or less.

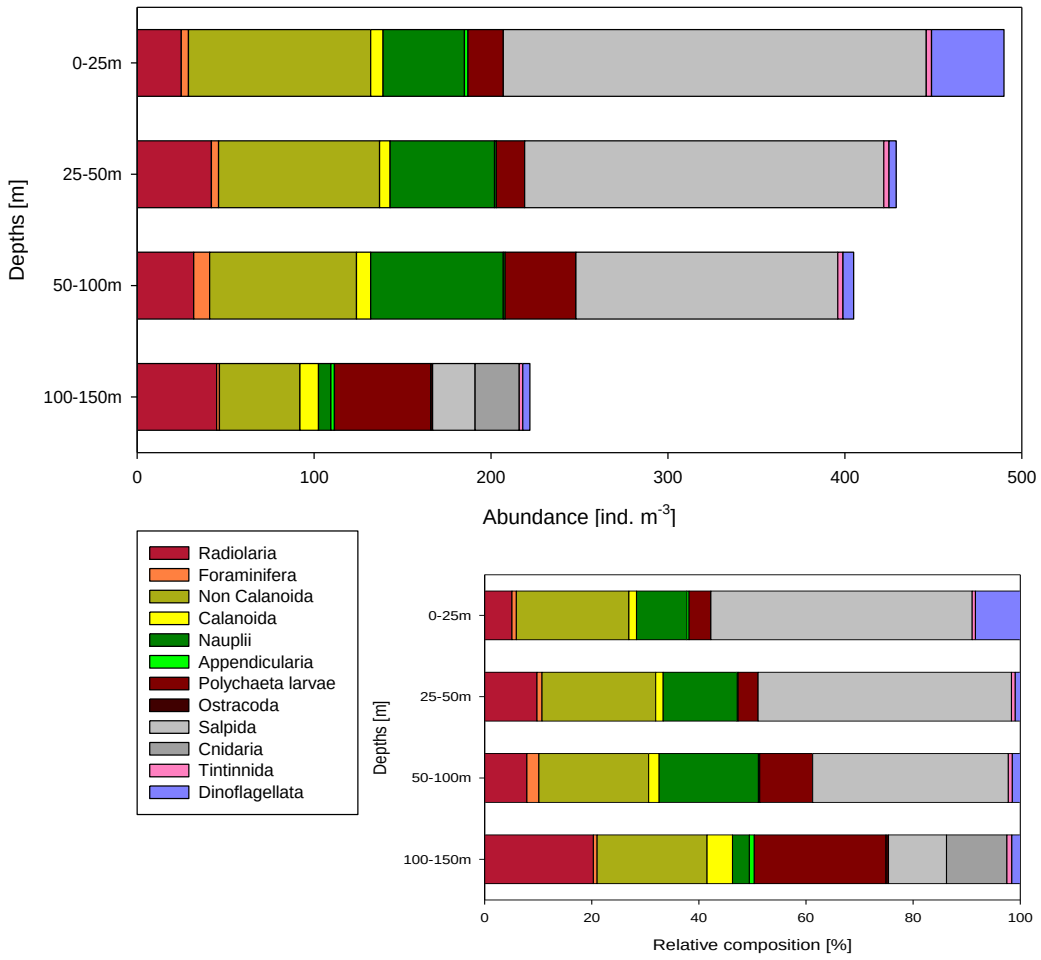

Figure 11: Microzooplankton abundance [ind. m^{-3}] in depth intervals and relative composition [%] at the Rocky Point outer shelf station (st. 285) during daytime.

At the outer shelf station (st. 285) of the Rocky Point transect the highest individual number (490 ind. m^{-3}) was detected in the interval from the surface down to 25 m water depth during daytime (Figure 11). The abundances in the depth intervals 25-50 m and 50-100 m were about 420 ind. m^{-3} and 405 ind. m^{-3}. In the first three depth intervals from the surface downwards Salpida were the main group with a high stake of 47 %, 48 % and 33 %. In the first two depth intervals, the second largest group was non-Calanoida with around 20 %. In the depth interval 50-100 m, the second major group was Nauplii with 24 %. In the surface layer, Dinoflagellata showed a higher abundance with 8-12 % than in the deepest interval with less than 1.5 %. In the deepest interval between 100-150 m, 220 ind. m^{-3} were counted. Polychaeta larvae were the dominant species with 20 % here. However, the dominance was not very distinct in this layer because the relative abundance of Radiolaria (17 %) and Calanoida (17 %) were similar.

In addition, the taxon Cnidaria (9 %) was caught in all intervals except from the deepest one. Additionally, Foraminifera (0.5 to 2 %), Calanoida (1 to 3 %), Appendicularia (less than 1 %), Ostracoda (less than 1%) and Tintinnida (less than 1 %) were caught in all depth intervals at this station.

3.3.3 Microzooplankton abundance on the Kunene transect (17.5° S)

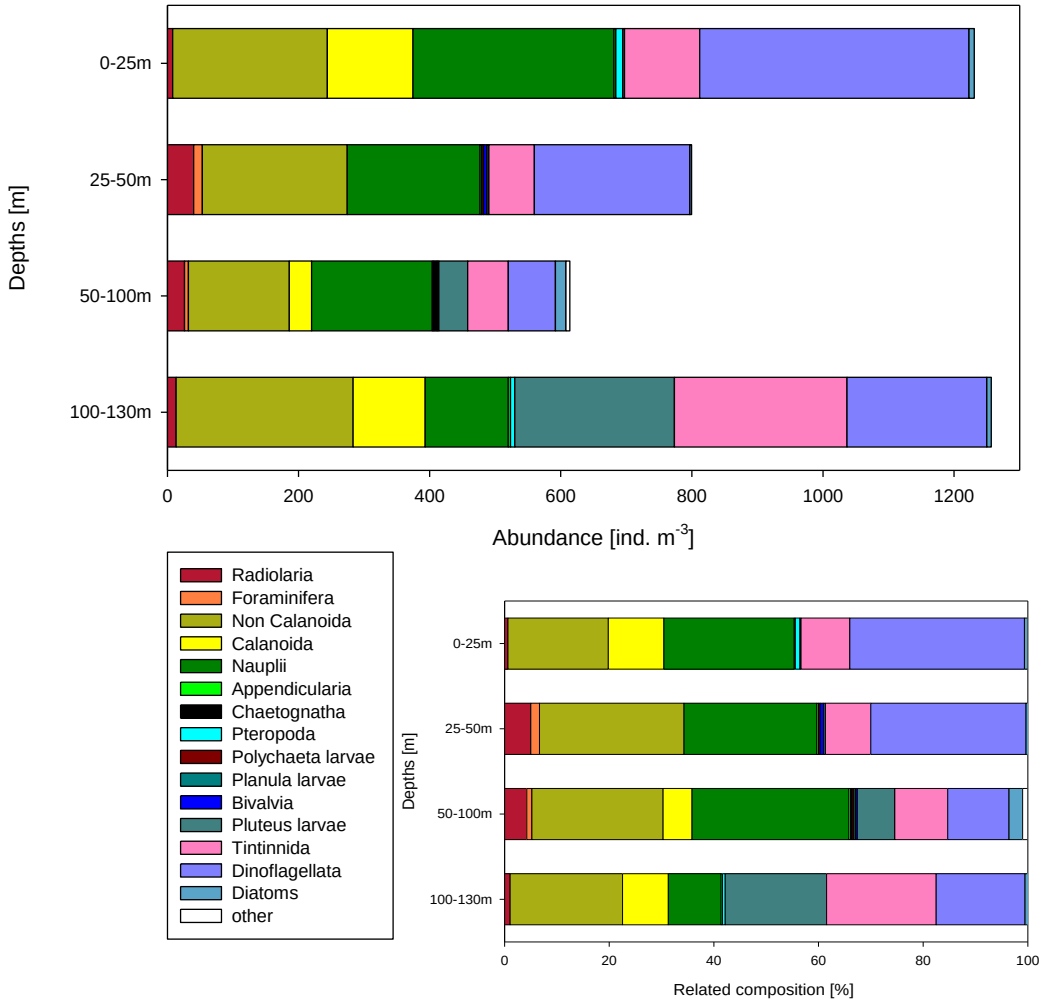

Figure 12: Microzooplankton abundance [ind. m^{-3}] in depth intervals and relative composition [%] at the Kunene shelf station (st. 305) during daytime.

At the shelf station (st. 305) on the Kunene transect the upper interval (0-25 m) was dominated by Dinoflagellata with 33 % during daytime (Figure 12). In the second depth interval (25-50 m) more than 880 ind. m^{-3} were measured. Non-Calanoida and Dinoflagellata contributed mainly with 29 %, followed by Nauplii (25 %) and Tintinnida (8 %). From 50- 100 m water depth 620 ind. m^{-3} were counted. In 100 - 300 m depth, the total abundance increased to 1250 ind. m^{-3}. Non-Calanoida showed the largest relative composition in this interval with 21 %. Pluteus larvae (19 %), Tintinnida (20 %) and Dinoflagellata (16 %) were also important groups. Radiolaria were caught in all depth intervals and ranged from 1 to 6 %. Taxa with an occurrence of 2 % or less were Foraminifera, non-

Calanoida, Appendicularia, Chaetognatha, Peteroptera, Polychaeta larvae, Planula larvae and others.

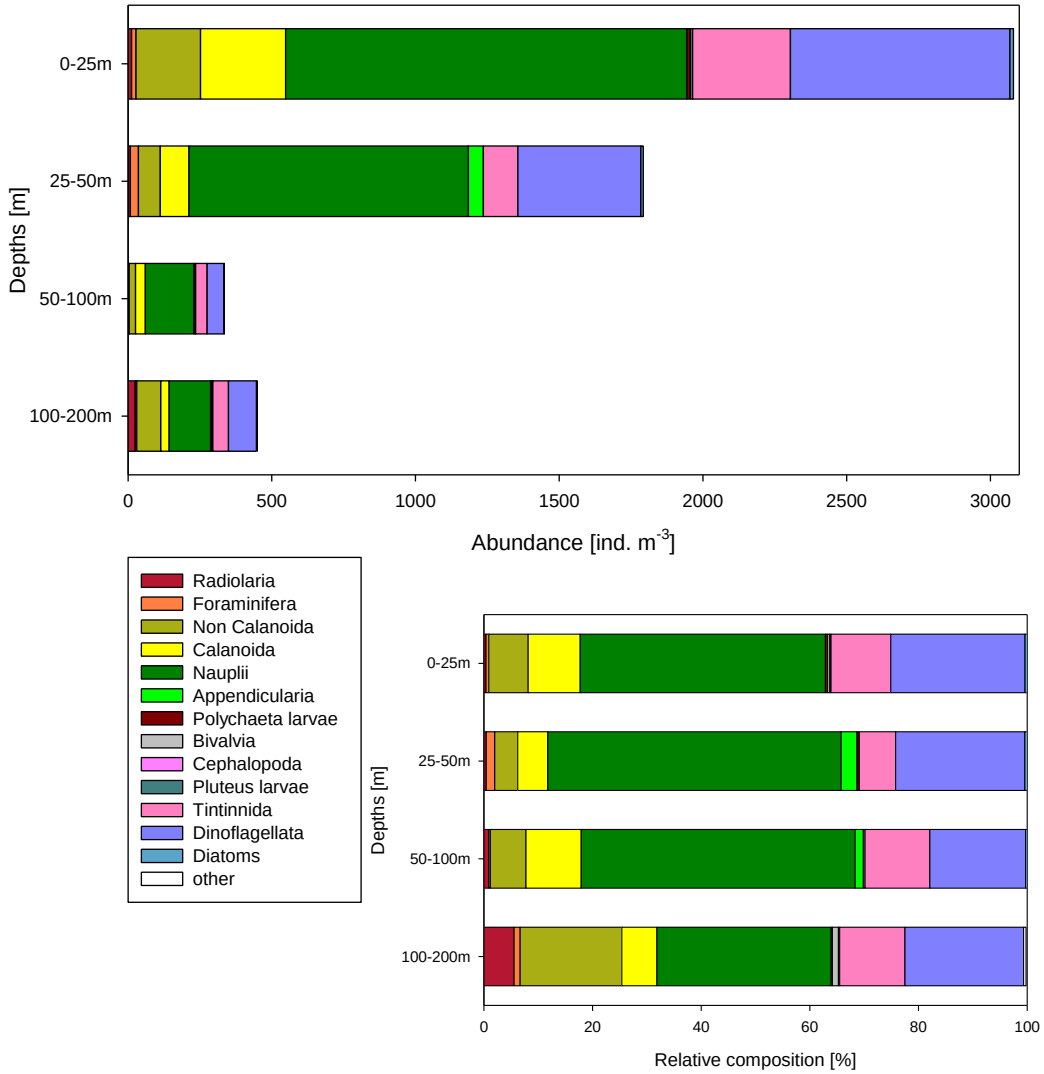

Figure 13: Microzooplankton abundance [ind. m^{-3}] in depth intervals and relative composition [%] at the Kunene upper slope station (st. 306) during daytime.

During daytime, at the slope station (st. 306) on the Kunene transect, the abundance declined from 3090 ind. m^{-3} in the surface layer (0-25 m) to about 400 ind. m^{-3} in 50-100 m but increased again to 450 ind. m^{-3} in the depth interval from 100-200 m (Figure 13). Nauplii built the main group of the relative composition in all depth intervals. In the relative composition, the contribution of Nauplii increased from the surface layer (0-25 m) with 35% to 50-54% in the depth intervals between 25-100 m and decreased again to 32 % in 100-200 m water depth. Calanoida and Tintinnida had abundances similar to each other

with around 9.5 %, 6 % and 11% in the upper three depth intervals. Only in the deepest interval (100-200 m) Tintinnida (12 %) represented a larger part than Calanoida (6 %). Non-Calanoida were detected in all depth intervals. They made up 4 to 7 % of the composition in the first three depth intervals. However, in the deepest water layer non-Calanoida represented the second largest group with 18 %. Radiolaria were found in the whole water column with an average raise from 0.5 % in the surface layer to 5 % in the deepest layer. Nevertheless, other taxa like Appendicularia, Foraminifera, Peteroptoda, Polychaeta larvae, Cephalopoda, Pluteus larvae and Diatoms were found with less than 3 % of the relative composition.

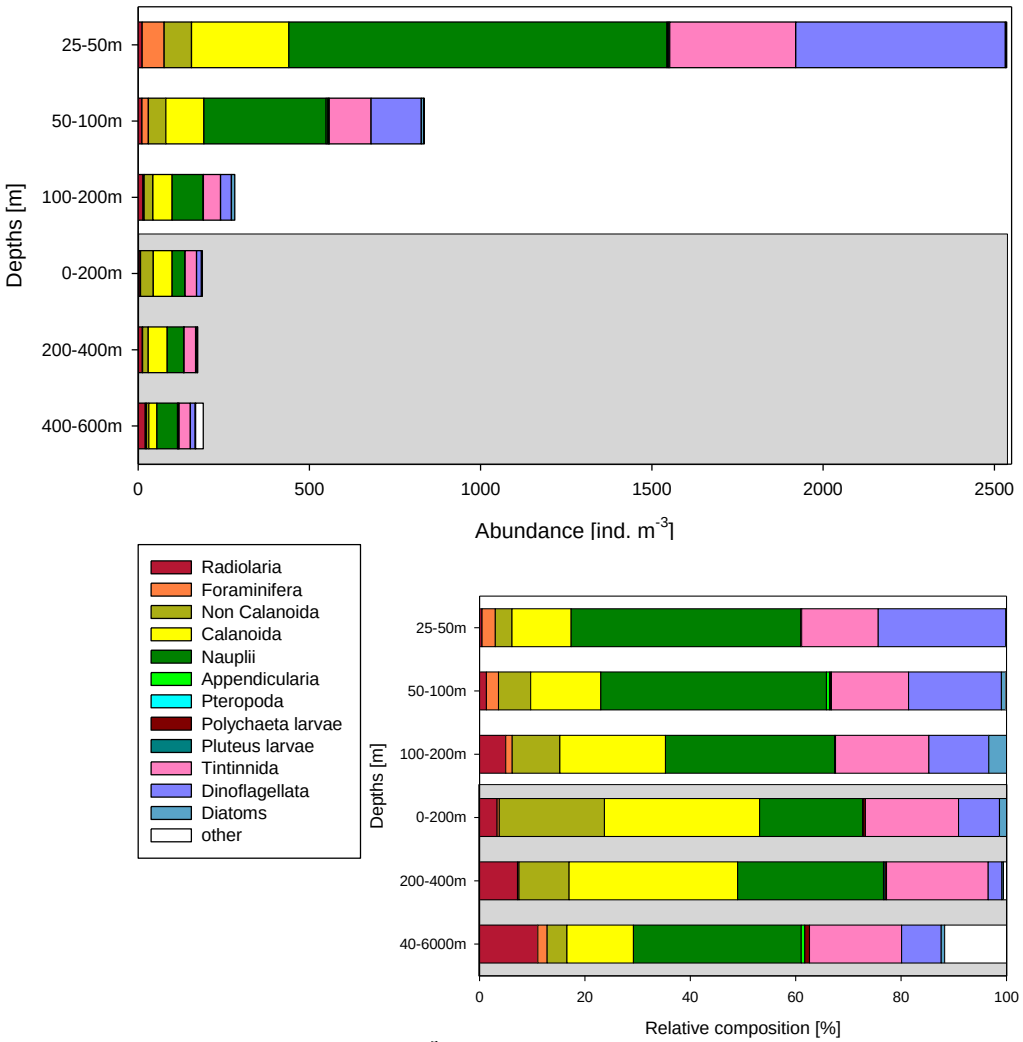

Figure 14: The abundance [ind. m^{-3}] and the relative composition [%] were displayed at two microzooplankton hauls with different depth intervals at the Kunene lower slope station 307 during daytime.

During daytime, at the lower slope station (st. 307) on the Kunene transect, the number of individuals decreased from 2500 ind. m^{-3} in the upper layer (25-50 m) to around 230 ind. m^{-3} in the two deepest layers (200-600 m; Figure 14). Nauplii made up the largest amount with 42 % of the composition in the depth intervals 25-50 m and 50-100m and decreased to 30 % (100-200 m). The Nauplii abundance increased again to 30 % in the deeper layers (200–600 m). Dinoflagellata showed a decreasing relative composition with depth till 400 m from 24 % to 5 %. Below 400 m the contribution of Dinoflagellata increased again slightly to 9 %. Calanoida and non-Calanoida showed a vertical distribution with an increasing trend with depth from 11 % and 3 % (0-25 m) to 20 % and 15 % (200-400 m), but decreased again to 12% and 3% below this depth. Tintinnida showed a similar distribution with small fluctuations around 17 % over all depth intervals. Moreover, Radiolaria contributed from 1% to 15 % to the composition with an increase with depth. The abundance of Radiolaria increased with depth from 0.5 % to 4 % in the depth interval 100-200 m. Foraminifera were obtained in the upper layer down to 200 m and in the deepest layer between 1 % and 3 %. Appendicularia, Pteropoda, Polychaeta larvae and Pluteus larvae had a relative composition of less than 1 %.

3.3.4 Summary of the microzooplankton distribution in the investigation area

The microzooplankton abundance presented a similar trend with decreasing numbers of individuals with depth at all stations, except of the Terrace Bay outer shelf station (st. 276) and the Kunene shelf station (st. 305). At both stations the individual numbers sharply increased again in the deepest depth interval. The highest individual numbers were obtained at the outer shelf station (st. 276) on the Terrace Bay transect. On the Rocky Point transect, the number of individuals on the shelf rose with increasing distance to the coast. In contrast to this, the numbers of individuals decreased from the shelf (st.305) to the lower slope (st.307) on the Kunene transect.

On the Terrace Bay transect the main taxa near the surface were non-Calanoida and Radiolaria. Three taxa dominated the relative composition on the Rocky Point transect. While at the inner shelf station (st. 282) Radiolaria and non-Calanoida illustrated the main fraction of the relative composition, Salpida were the dominating taxon in most depth intervals at

the outer shelf station (st.285) during night time. Non-Calanoida and Nauplii had a high individual abundance but the dominating taxon was Salpida except to the deepest interval. Nauplii were very abundant, the main abundance shown on the Kunene transect. At the shelf station (st. 305) of this transect non-Calanoida and Dinoflagellata presented the main fraction in some depth intervals. Besides the Nauplii, Copepoda (non-Calanoida and Calanoida) dominated the abundance in between 50-100 m depth intervals of the lower slope station (st.307). Generally, Copepoda and in particular non-Calanoida illustrated the highest individual numbers of the microzooplankton.

3.4 Mesozooplankton abundance and vertical distribution

3.4.1 Mesozooplankton abundance on the Rocky Point transect (19° S)

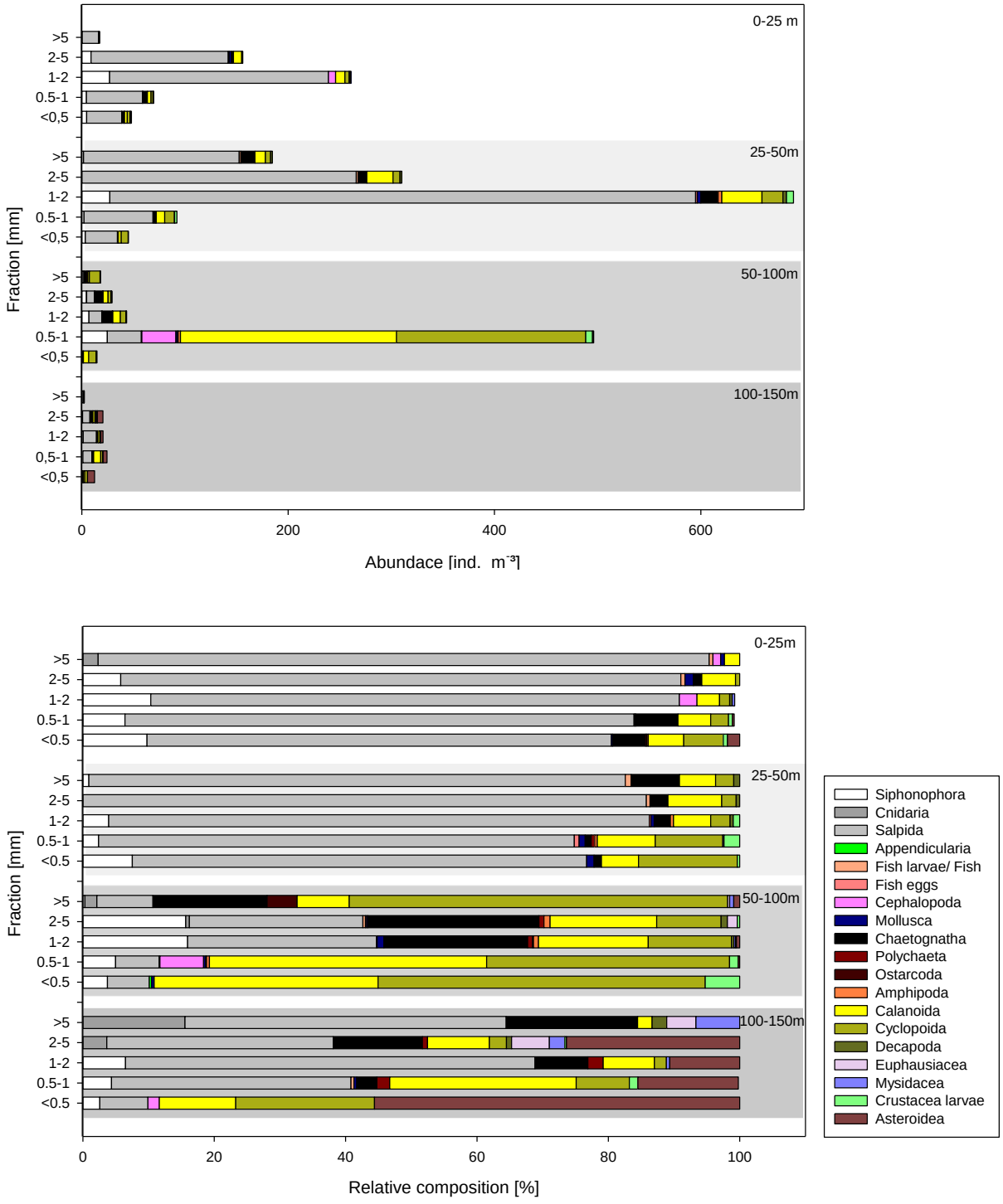

Figure 15: Mesozooplankton abundance [ind. m-3] in depth intervals and relative composition [%] at the Rocky Point outer shelf station (st. 285) at daytime.

During daytime at the lower shelf station (st. 285) on the Rocky Point transect, the total number of mesozooplankton individuals was the highest between 25-50 m (1370 ind.m^{-3}) and decreased to the deepest layer of 100-150 m (60 ind.m^{-3}; Figure 15). The second highest abundance of individuals was located between 0-25 m. Between 25-50 m depth the major fraction was detected in the size class 1-2 mm with more than 700 ind. m^{-3}. All size fractions were dominated by Salpida with approximately 70 % or more. In the 25-50 m depth intervals, Siphonophora (range 0-10 %), Cyclopoida (range 0-15 %), and Calanoida (range 2-8 %) and in some cases Chaetognatha (range 0-7 %) were common. Between 50-100 m depth the community was dominated by the 0.5-1 mm size class with around 500 ind. m^{-3}. Cyclopoida were the most frequent taxon with 49 % and 57 % of the fractions <0.5 mm and >5 mm. The fractions 1-2 mm and 2-5 mm were separated into two dominating taxa: Salpida (26-28 %) and Chaetognatha (21-26 %). The further most common taxa in these fractions were Siphonophora (15 %), Calanoida (16 %) and Cyclopoida (9-12 %). In the deepest water layer (100-150 m) the fraction < 0.5 mm contributed more than 35 ind. m^{-3}, whereas the other fractions amounted less than 18 ind. m^{-3}. Asteroidea were found abundantly, they dominated the <0.5 mm fraction with 55 %, but were also common in the fractions 0.5-1 mm (15 %), 1-2 mm (10 %) and 2-5 mm (26 %).

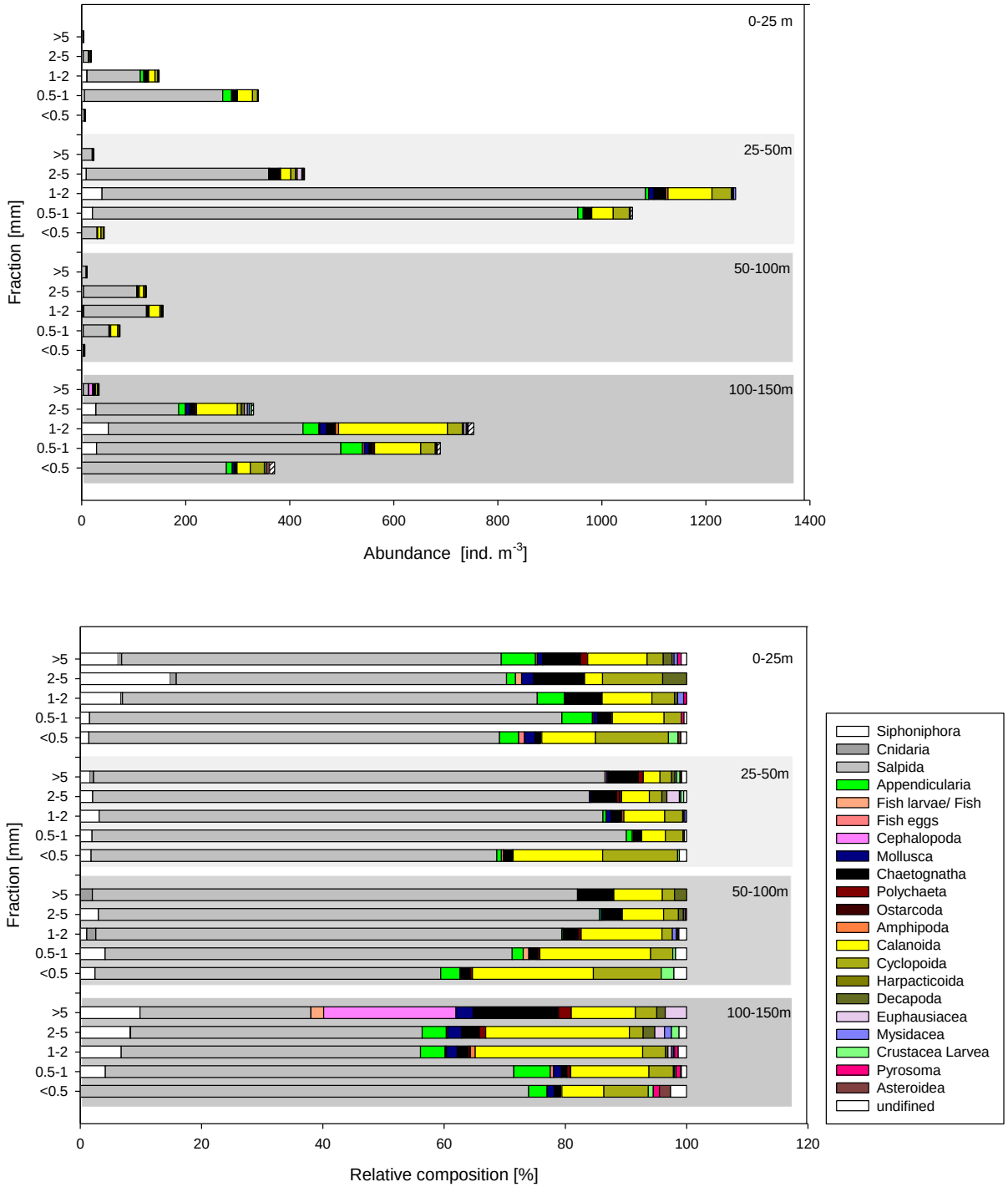

Figure 16: Mesozooplankton abundance [ind. m^{-3}] in depth intervals and relative composition [%] at the Rocky Point outer shelf station (st. 285) at night time.

At the outer shelf station (st. 285) on the Rocky Point transect in the water column between 0-50 m, the total number of individuals was higher during the night time with approximately 3.500 ind.m^{-3} than during the daytime with around 2000 ind. m^{-3} (Figure 16). The total abun-

dance of mesozooplankton was lower between 50 m and 100 m depth than between 100 m and 150 m with around half as much individuals as in the upper layers.

Salpida was the main determined group found on this station (54-88 % of the total) during the night in all depth intervals and size fractions except the size fraction < 5 at 100-150 m. Only in this fraction, Cephalopoda made 21 % of the total number of individuals. However, the number of Calanoida increased with depth. Cyclopoida were also found in all depths and fractions with a contribution to the relative composition between 2 % and 27 %. In contrast to the day sample where Appendicularia were detected only in the depth interval 100-150 m, this group (0.1-6 %) was found in all depth intervals during the night. In addition, less Asteroidea (0.2-1 %) were found in the water column than during the daytime.

3.4.2 Mesozooplankton abundance on the Kunene transect (17.5° S)

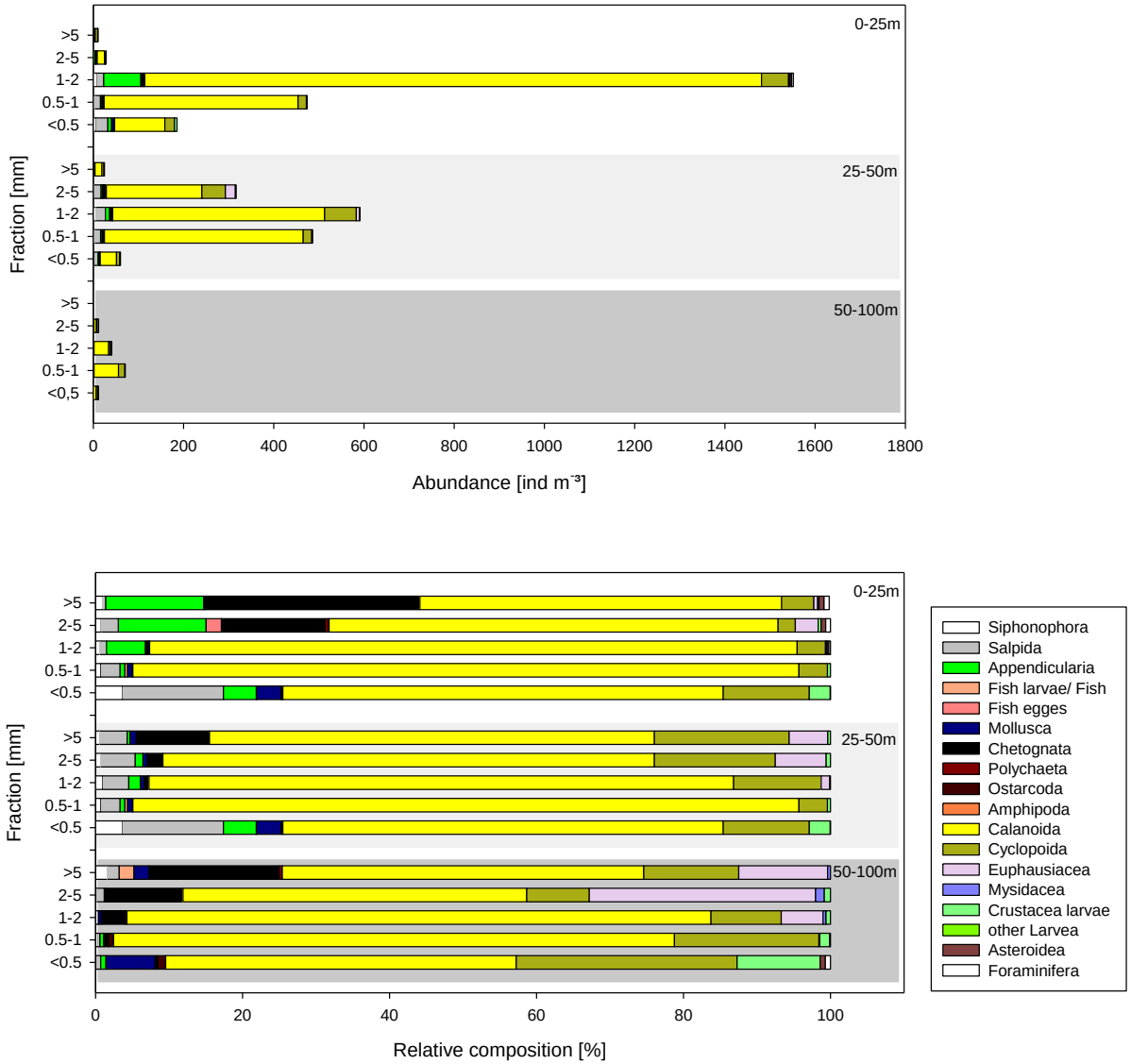

Figure 17: Mesozooplankton abundance [ind. m^{-3}] in depth intervals and relative composition [%] at the Kunene shelf station (st.305) during daytime.

During daytime on the shelf station (st. 305) on the Kunene transect the abundance of mesozooplankton decreased from the surface layer (2200 ind. m^{-3}) to the 50-100 m depth interval (135 ind. m^{-3}; Figure 17). In the upper 50 m the most abundant size fraction was the 1-2 mm with over 600 ind. m^{-3}. In 50-100 m depth, the size fraction 0.5-1 mm contained the most individuals with around 80 ind. m^{-3}.

In all depth intervals, Calanoida were the most abundant group with 47 % (100-150 m) and 90% (50-100 m), respectively. In all depths intervals and size fractions, Cyclopoida were obtained with an increasing trend in the relative composition from the surface (2-11 %) to the bottom (8-30 %). Moreover, the taxon Chaetognatha ranged from 10 % to 29 % in the size fraction > 5 mm and 2-5 mm between 0-25 m and 50-100 m depth. The relative abundance of Euphausiacea rose with increasing depth from 3 % (0-25 m) to 30 % (50-100 m). This group dominated the larger size fractions (> 5 mm, 1-2 mm). The highest abundance of Appendicularia was obtained in the upper water layers (4 %-13 %). In the other depth intervals, the relative abundance of Appendicularia ranged from 4 % (25-50 m) to less than 0.5 % (50-100 m). Most of the Salpida were detected in the two upper depth intervals with the highest relative abundance of 13 % in the size fraction < 0.5 mm.

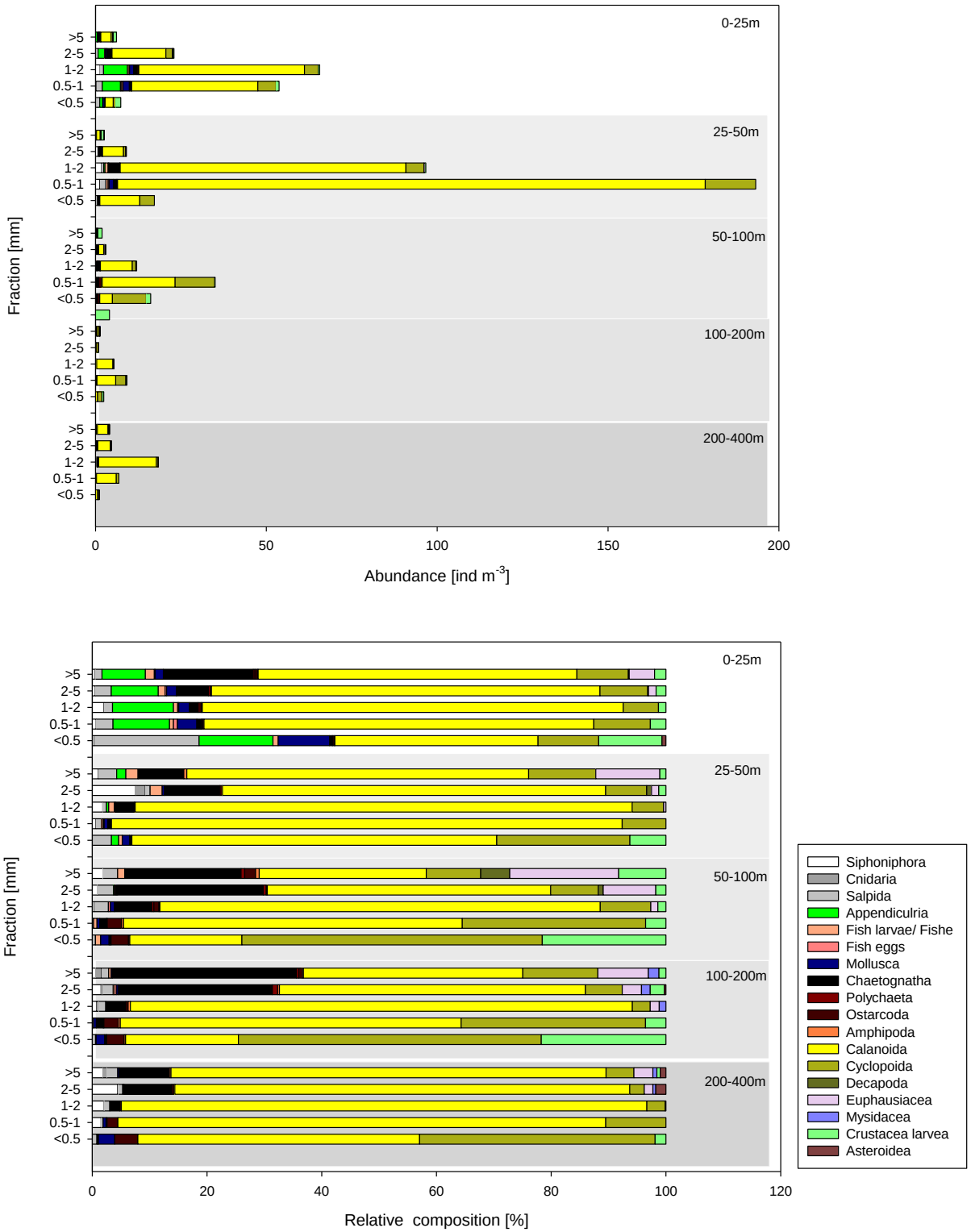

Figure 18: Mesozooplankton abundance [ind. m^{-3}] in depth intervals and relative composition [%] at the Kunene upper slope station (st. 306) at night time.

At the upper slope station (st. 306) of the Kunene transect the highest abundance of mesozooplankton was detected in the upper layer during the night (Figure 18). The highest abundance was detected in 25 to 50-m depth with around 350 ind. m^{-3}. The highest abundance in the size fraction 1-2 mm with 70 ind. m^{-3} was found in the surface layer (0-25 m). Copepoda (divided into Cyclopoida and Calanoida) were the most common taxon in all depth intervals, with a range from 31 % to 88 % of the total. This taxon was mainly dominated by Calanoida. Cyclopoida were more abundant in the size fraction <0.5 mm in 50-100 m and 100-150 m water depth than Calanoida. Besides this, Salpida were found in all depth intervals and size fractions with relative abundances between 7 % (depth: 200-400 m, fraction: 2-5 mm) and 36 % (depth: 0-25 m, fraction: <0.5 mm). Appendicularia were found in all size fractions in a range of 6-10 % at 0-25m and in the size fractions >5 mm (2 %) and <0.5 mm (1 %) at 25-50 m. In the second depth interval (25-50 m), the highest abundance of mesozooplankton was obtained with 180 ind. m^{-3} in the size fraction 0.5-1 mm. Chaetognatha showed a similar distribution in the whole water column with a decreasing trend from the larger size fraction (7-8.5 %) to the smaller size fraction with less than 3 % between 200m and 400 m. Furthermore, Chaetognatha were mainly detected in the larger size fractions (2-5 mm to 5 mm) with 16 % to 28 % between 50 m and 200 m. Near the bottom, the total abundance increased from 20 ind. m^{-3} (50-100 m) to around 40 ind. m^{-3} (200-400 m) with the highest abundance in the size fraction 0.5-1 mm (about 20 ind. m^{-3}). Euphausiacea were detected in all depth intervals mainly in the larger size fraction (1-15 %) with the highest relative abundance of 15 % (> 5 mm) between 50 m and 100 m. Other Crustacea larvae were mainly found between 50 m and 200 m water depth with 1-20 %. In the other depth intervals the relative abundance of the Crustacea larvae showed a decreasing trend with depth from 1.5 % to-8 % (0-25 m) over 0.5 % to 1.5 % (200-400 m) to 0-4 % (50-100 m).

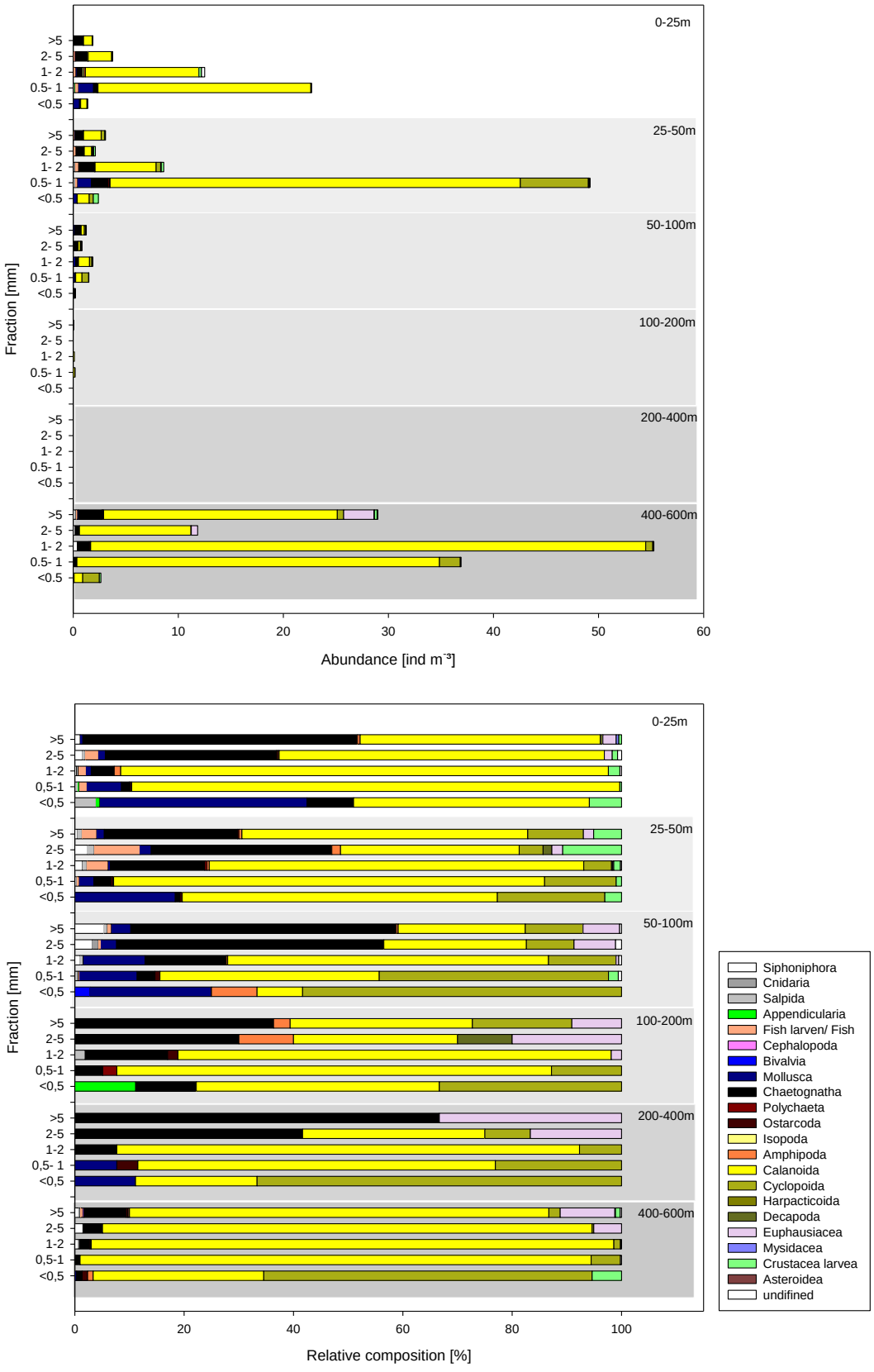

Figure 19: Mesozooplankton abundance [ind. m^{-3}] in depth intervals and relative composition [%] at the Kunene lower slope station (st. 307) at daytime.

During the daytime, samples at the lower slope station (st. 307) on the Kunene transect were taken in water depths down to 600 m (Figure 19). The surface interval (0-25 m) demonstrated quite a low total abundance of approximately 50 ind. m^{-3} in total. The depth interval below showed the second highest number of individuals with 50 ind. m^{-3} in the size fraction 0.5-1 mm. No more than 1 ind. m^{-3} per size fraction was found in the depth intervals 100-200 m and 200-400 m, respectively. Most individuals were obtained in the depth interval 400-600 m with about 150 ind. m^{-3} in total, where most of them (about 55 ind. m^{-3}) were part of the size fraction 1-2 mm.

Calanoida were the dominating group in most size fractions in a range of 32 % (25-50 m) to 95 % (400-600 m). From the latter depth interval down, Cyclopoida were the main taxon in the size fraction <0.5 mm. Chaetognatha were obtained in all depths intervals with the lowest abundance between 400-600 m (1-7 %). In the depth intervals 50-100 m and 200-400 m, Chaetognatha made the main part of the largest size fractions (24-50 %). Euphausiacea were found mainly in the larger size fractions, with an increasing trend from the surface down to 400 m water depth in a range of 1 to 33 % mainly in the larger size fractions. In the depth range from the surface down to 100 m fish larvae and fish eggs were found (0-8 %). Mollusca contributed to the relative composition in a range of 1 to 37 %.

3.4.3 Summery of the mesozooplankton abundance in the investigation area

The mesozooplankton distributions mainly showed a decreasing trend from the highest abundance in the second depth interval to a low abundance in the middle depth interval. The abundance increased again in the deepest interval at most stations.

The highest abundance of mesozooplankton was detected at the Rocky Point outer shelf station (st.285). On the Kunene transect, the mesozooplankton abundance decreased rapidly from the shelf to the slope. These distribution patterns were similar to the microzooplankton with the only difference that the abundance was less at the Rocky Point shelf station compared to the Kunene shelf station.

The Rocky Point shelf station was dominated by the group Salpida. In contrast, on the entire Kunene transect mainly Calanoida and Cyclopoida groups were found.

3.5 Biomass of mesozooplankton

3.5.1 Biomass of mesozooplankton on the Rocky Point transect (19° S)

Day

Night

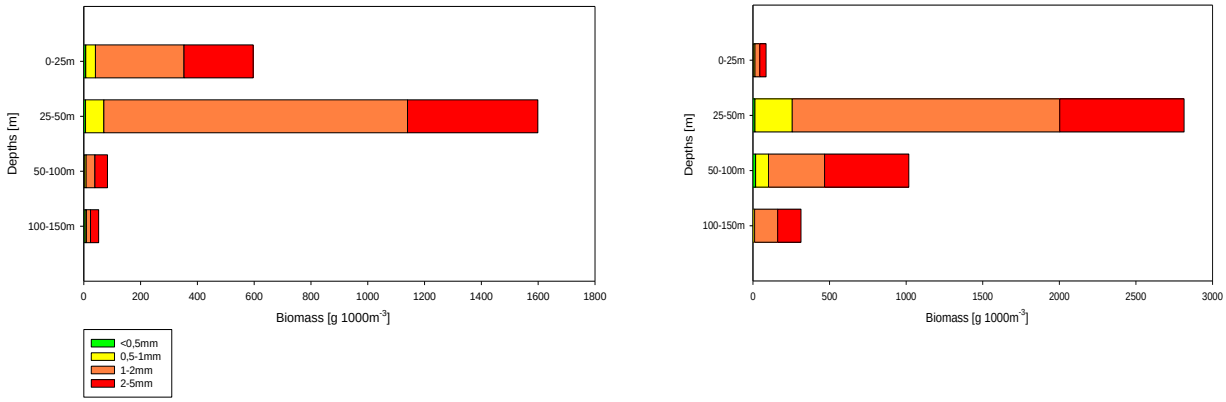

Figure 20: Mesozooplankton biomass [g 1000 m^{-3}] for all depth intervals at the Rocky Point outer shelf station (st. 285) at daytime and at night time.

During the daytime, at the outer shelf station (st. 285) on the Rocky Point transect, the biomass declined with decreasing depth from the second depth interval down (Figure 20). The second highest biomass was detected in the surface layer. The highest biomass was determined between 25 and 50 m (1600 g 1000 m^{-3}). The size fraction 1-2 mm dominated the first two depth intervals. The lowest biomass was observed between 100 and 150 m. In the two deepest intervals the biomass was mainly build by the two biggest size fractions in equal shares.

During the night, the highest biomass was as well found between 25 m and 50 m (2700 g 1000 m^{-3}). In contrast to the daytime, the second and third largest biomass values were found between 50 m and 100 m (1100 g 1000 m^{-3}) and 100 m to150 m (around 400 g 1000 m^{-3}).

3.5.2 Biomass of mesozooplankton on the Kunene transect (17.5° S)

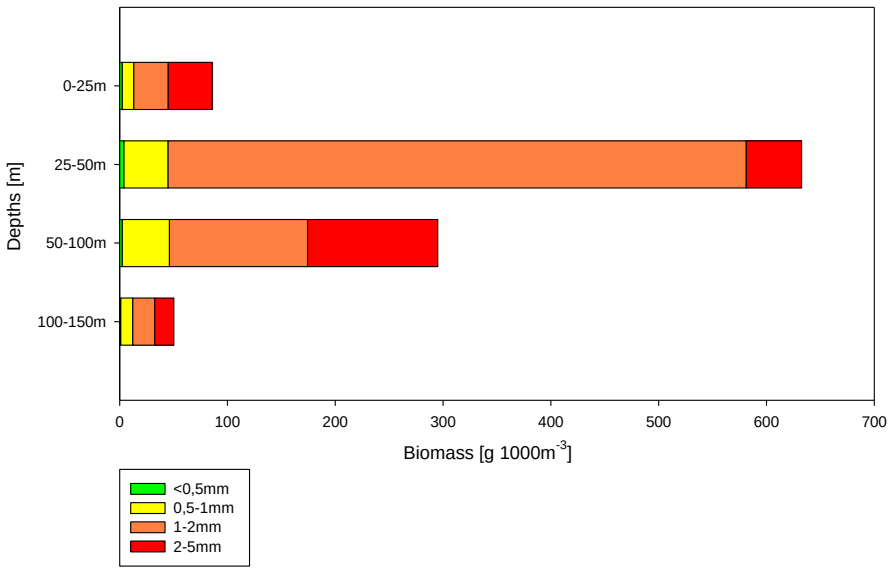

Figure 21: Mesozooplankton biomass [g 1000 m^{-3}] for all depth intervals at the Kunene shelf station (st. 305) at daytime.

At the shelf station (st. 305) on the Kunene transect the highest biomass was found between 25 m and 50 m depth (Figure 21). In deeper layers the biomass decreased to 300 g 1000 m^{-3} (50-100 m) and 50 g 1000 m^{-3} (100-150 m). However, the biomass structure in the different depth intervals was the same at the outer shelf station (st. 285) on the Rocky Point transect. This includes a high abundance of the size fraction 1-2 mm (around 500 g 1000 m^{-3}) in the 25 m to 50 m depth interval. Moreover, the size classes of 2-5 mm and 1-2 mm presented a similar relative abundance in the other depth intervals. In all depth intervals, the 0.5-1 mm fraction made up a smaller part of the biomass in a range of 10-40 g 1000 m^{-3} while the fraction < 0.5 mm only constituted a very small part with less than 4 g 1000 m^{-3} of the total biomass per depth interval in all water layers.

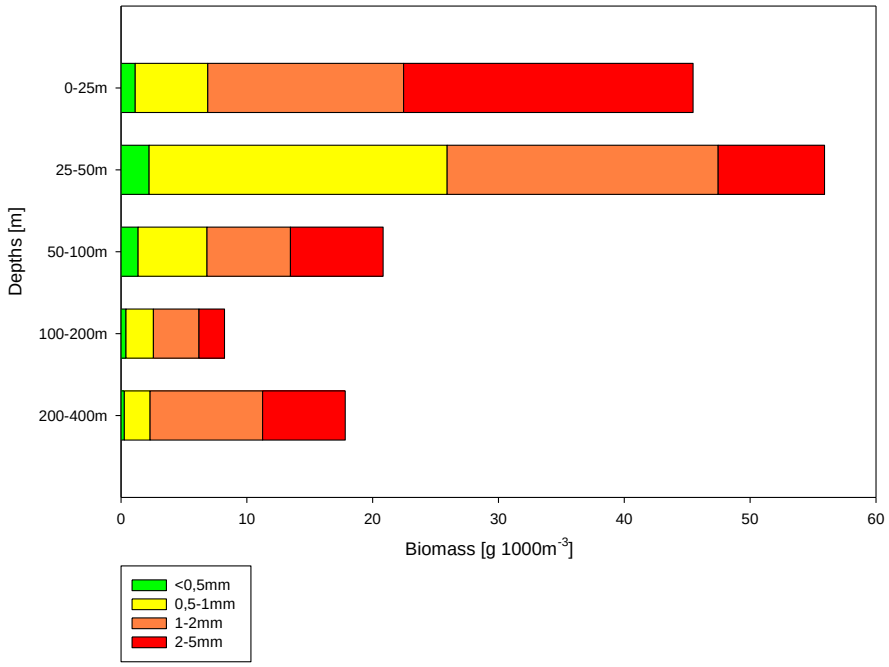

Figure 22: Mesozooplankton biomass [g 1000 m^{-3}] for all depth intervals at the Kunene upper slope station (st. 306) at night time

Less biomass with a range of 57 g 1000 m^{-3} (25-50 m) to 8 g 1000 m^{-3} (100-200 m) was detected at the upper slope station (st. 306) in comparison to the stations mentioned before (Figure 22). This low biomass led to a different composition of the biomass size fractions. In particular, the smaller size fractions constituted a larger part in relation to the bigger size fraction in a range of around 1 % to 10 % (<0.5 mm) and 10 % to 40 % (0.5-1 mm). The dominating size fractions in the second depth interval were the 2-5 mm fraction with around 25 g 1000 m^{-3} and the 0.5-1 mm fraction with 25 g 1000 m^{-3}.

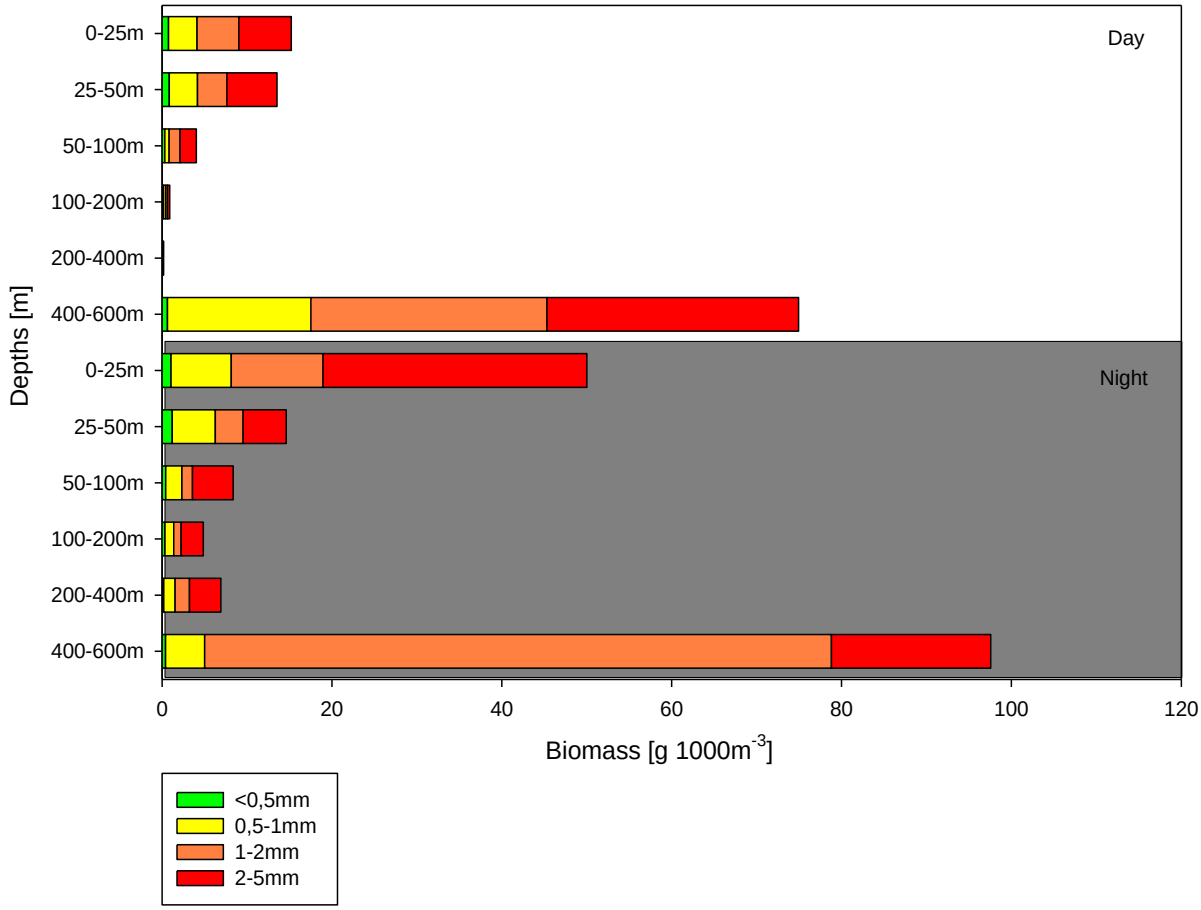

Figure 23: Mesozooplankton biomass [g 1000 m^{-3}] for all depth intervals at the Kunene lower slope station (st. 307) at daytime and night time.

In contrast to the other stations, the highest biomass was found in the deepest interval (400-600 m) at the Kunene lower slope station (st. 307) with 75 g 1000 m^{-3} during the day and 95 g 1000 m^{-3} during the night (Figure 23). The second highest biomass was found near the surface (day: 15 g 1000 m^{-3}; night: 50 g 1000 m^{-3}) and decreased with depth to less than 5 g 1000 m^{-3} (day) and 10 g 1000 m^{-3} (night). The composition of the size fractions was similar to the slope station (st. 306) with a dominance of the size fractions 1-2 mm and 2-5 mm. As at the station 306, the smaller size fractions made up a larger part of the total biomass compared to the bigger size classes, due to the small total biomass at this station.

3.5.3 Summary of the mesozooplankton biomass in the investigation area

The pattern of mesozooplankton biomass was similar to the mesozooplankton abundance. However, in contrast to the abundance pattern, the biomass increased from the intermediate depth intervals to the deepest depth interval at two stations on the Kunene transect. Another difference to the abundance pattern was the higher biomass at the lower slope station (st. 307) compared to the upper slope station (st. 306).

3.6 Biochemistry

Table 4: Bottom concentrations [µmol l-1] of the different elements: (PO_4), nitrite ion (NO_x), ammonium cation ($\mathbf{NO_2^-}$) ammonium ($\mathbf{NH_4^+}$), dissolved inorganic nitrogen (ammonium, nitrate, nitrite) (Din), inherited by A. Neumann

Station	Bottom c. [PO_4]	Bottom c. [NO_x]	Bottom c. [NO_2^-]	Bottom c. [NH_4^+]	Bottom c. [Din]
277					
278	3.28	23.40	0.49	6.85	30.25
279	5.91	19.23	0.93	11.54	30.77
305	2.16	13.45	-0.02	3.11	16.56
306	2.78	12.01	0.34	2.38	14.39
308	1.93	23.75	0.36	1.10	25.75

Data from stations nearby the ROV stations was evaluated for bottom nutrient concentration, fluxes and elemental composition (Table 4). The concentrations of phosphate (PO_4), nitrite ion (NO_x), ammonium cation (NO_2^-) and dissolved inorganic nitrogen (ammonium, nitrate, nitrite) (Din) at the Rocky Point inner shelf station (st. 279) illustrated the maximum bottom concentration of all stations. The bottom concentration of mono-nitrogen oxides (NO_x) was the highest at the offshore station (st. 308) and lowest at the shelf station (st. 305) and the slope station (st. 306) on the Kunene transect. The Kunene offshore station (st. 308) had the lowest concentration of PO_4 (1.93 µmol l-1), while NO_2^- was measured with the lowest concentration at the Kunene shelf station (st. 305; -0.02 µmol l^{-1}) and the second highest at the Terrace Bay innermost shelf station (st. 278; 0.49 µmol l^{-1}). Due to the influence of the concentrations of ammonium, nitrate and nitrite on Din it showed a similar pattern with the lowest concentration of 14 µmol l^{-1} at the Kunene slope station (st. 306). Generally, NH_4^- showed

an increasing trend from the shelf (st. 279: 11.54 µmol l^{-1}) down the slope (st. 308: 1.10 µmol l^{-1})

Table 5: Percentage of total nitrogen (N_{tot}) and organic carbon (C_{org}) in the sediment (molar ratio of both elements). Oxygen concentration compared to oxygen consumption, inherited by A. Neumann

Station	N_{tot} % (sediment)	C_{org} % (sediment)	C_{org} : N_{tot} (molar ratio)	Bottom water oxygen (µM)	Oxygen consumption (µmol m^{-2} d^{-1})
277	1.0	7.28	8.45	1.90	
278	0.5	3.57	8.83	1.33	769.48
279	0.22	1.59	8.62	16.38	
305	0.21	1.88	10.21	46.66	2023.06
306	0.14	1.00	10.33	42.58	2160.69
308	0.38	3.05	9.26	239.25	3065.04

N_{tot} and C_{org} contribution in the sediment were correlated to each other. For example, at the inner shelf station of Terrace Bay (st. 277) the highest N_{tot} (1.0 %) and also the highest C_{org} (7.3 %) were obtained. At the upper slope station (st. 306) on the Kunene transect the lowest percentages of N_{tot} (0.1 %) and C_{org} (1 %) were detected. At the shelf stations (st. 279, st. 305) of the Terrace Bay and Kunene transect the amounts of N_{tot} were very similar to each other (Table 5). However, the C_{org} presented a larger difference between these two stations. The C_{org} : N_{tot} ratio illustrated high values for the shelf station (st. 305) and the slope station (st. 306) with around 10.25 on the Kunene transect. The bottom water oxygen concentration increased from the shelf station (st. 277; 1.9 µM) to the lower slope station (st. 308; 239.25 µM). In comparison, the oxygen consumption presented the same trend: 769.48 µmol $m^{-2}d^{-1}$ (st. 278) and 3065.04 µmol $m^{-2}d^{-1}$ (st. 308) were measured.

Table 6: Fluxes and production of nitrogen, ammonium and phosphate (µmol m^{-2} d^{-1}) inherited by A. Neumann. Positive values demonstrating the uptake to the sediment and negative values the input into the water column.

Station	Nitrate flux	Nitrite flux	N_2 flux	Ammonium flux	Ammonium production	Phosphate flux	Phosphate production
277							
278	350.26	-0.16	-583.37	-411.75	359.53		
279		12.52	-718.68	-277.32	324.63	-77.29	58.06
305	472.70	-1.29	-353.03	-1885.38	507.84	-149.57	201.97
306	70.66	-20.44	-323.31	-20.44	35.46	-6.63	8.82
308	51.62	-0.14	-460.94	-89.92	65.11	-21.27	21.45

On the Terrace Bay transect at the inner shelf station (st. 278), the nitrate flux was 350 µmol m^{-2} d^{-1}, which indicates an uptake of nitrate into the sediment from the water column (Table 6). On the Kunene transect the absorption of nitrate from the water column decreased with increasing bottom depth of the three stations from 472 µmol m^{-2} d^{-1} on the shelf (st. 305) to 51 µmol m^{-2} d^{-1} offshore (st. 308).

The only positive measurement of the nitrite uptake of the sediment was detected at the inner shelf station (st. 279) on the Rocky Point transect. The biggest release of nitrite from the sediment was calculated for the Kunene slope station (st. 306).

Compared to the Kunene transect, the measured N_2 fluxes of the Terrace Bay transect were relatively low, which implicated an input from the sediment into the water column. Moreover, the highest input of N_2 into the water column was obtained with -719 µmol m^{-2} d^{-1} at the Rocky Point shelf station (st. 279). The highest release was obtained (-461 µmol m^{-2} d^{-1}) for the deepest offshore station (st. 308) on the Kunene transect.

The ammonium flux from the sediment into the water column decreased rapidly from -1885 µmol m^{-2} d^{-1} on the shelf (st.305) to -20 µmol m^{-2} d^{-1} at the slope station (st. 306) on the Kunene transect. Compared to this transect, the shelf regions of the other transects showed medium ammonium fluxes from the sea ground into bottom water.

A similar trend can be spotted for the ammonium production, where the stations of the Terrace Bay transect and Rocky Point were similar to each other and medium compared to the other transect, while the Kunene transect showed two extreme measures. Furthermore, the phosphate flux presented the same trend as the ammonium flux. It was correlated to the phosphate production, meaning that stations with a high phosphate production had also a high release of phosphate from the sediment.

3.6.1 Summary of the biochemistry

In summary, the bottom concentrations of the elements presented their maximums at the inner shelf stations (st. 278 and st. 279) on the Terrace Bay and the Rocky Point transect. In contrast to this, the maximum concentration of mono-nitrogen oxides (NO_x) on the Kunene transect was obtained at the offshore station (st. 308). On the Kunene transect, ammonium cation presented a decreasing trend. The nitrite ion concentration increased with water depth from

the shelf to the lower slope. The other detected concentration presents a maximum on the slope (st. 306).

The N_{tot} % and the C_{org} % were correlated to each other. The C_{org} : N_{tot} ratio was the lowest at the shelf on the Terrace Bay and the Rocky Point transect. On the Kunene transect, the C_{org} : N_{tot} ratio was the highest on the slope and decreased to offshore.

The oxygen consumption was related to the oxygen concentration. On the shelf the oxygen concentrations were low with increasing trends to the north (Terrace Bay → Kunene) and further offshore. The ammonium and phosphate productions were highest on the shelf. The ammonium and phosphate fluxes correlated positively with an increase of the sediment input accompanied by a higher productivity. However, the nitrate flux from the sediment presented a decreasing trend from the shelf sediment to the offshore sediment. In addition, the nitrite flux indicated no clear trend between the coastal areas and the offshore areas and on the shelf from south to north. The N_2 flux was the highest on the shelf with its maximum on the Rocky Point transect and a minimum on the Kunene transect. Furthermore, the Kunene transect indicated a higher N_2 flux from the sediment into the bottom water offshore than on the shelf.

3.7 Benthic macrofauna distribution

Benthic samples were evaluated at four stations on the Terrace Bay (st. 279), Rocky Point (st. 279) and Kunene transect (st. 305 and st. 308). All stations showed huge differences in taxa composition (Figure 24, 25). The selection of the stations was matched to the location of the ROV stations.

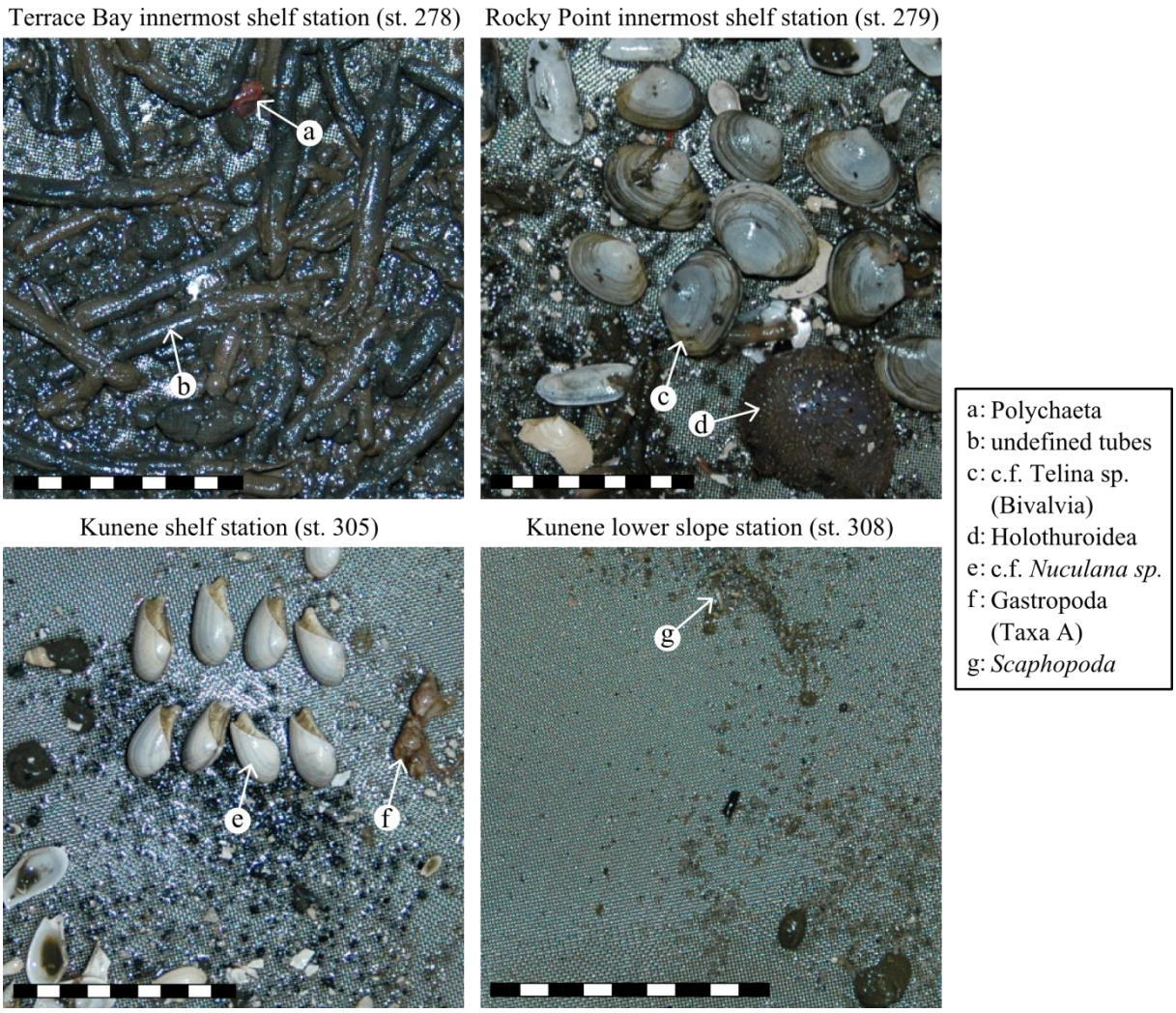

Figure 24: Benthic macrofauna taxa of the three transects. The scale is 5 cm.

The second highest individual number was detected at the inner shelf station (st. 278) on the Terrace Bay transect (approximately 122 ind. m^{-2}) but more than 60 % of the taxa were undetermined. Rather it was not possible to differentiate between all taxa, e.g. Holothuroidea or tubes of Polychaeta. The second largest fraction of the relative composition was undefined tubes (around 10 %). Holothuroidea and Polychaeta illustrated almost the same percentage with around 7 % of the relative composition. Moreover, c.f. *Telina sp.* (1 %) and not further identified Bivalvia shells (3 %) were found.

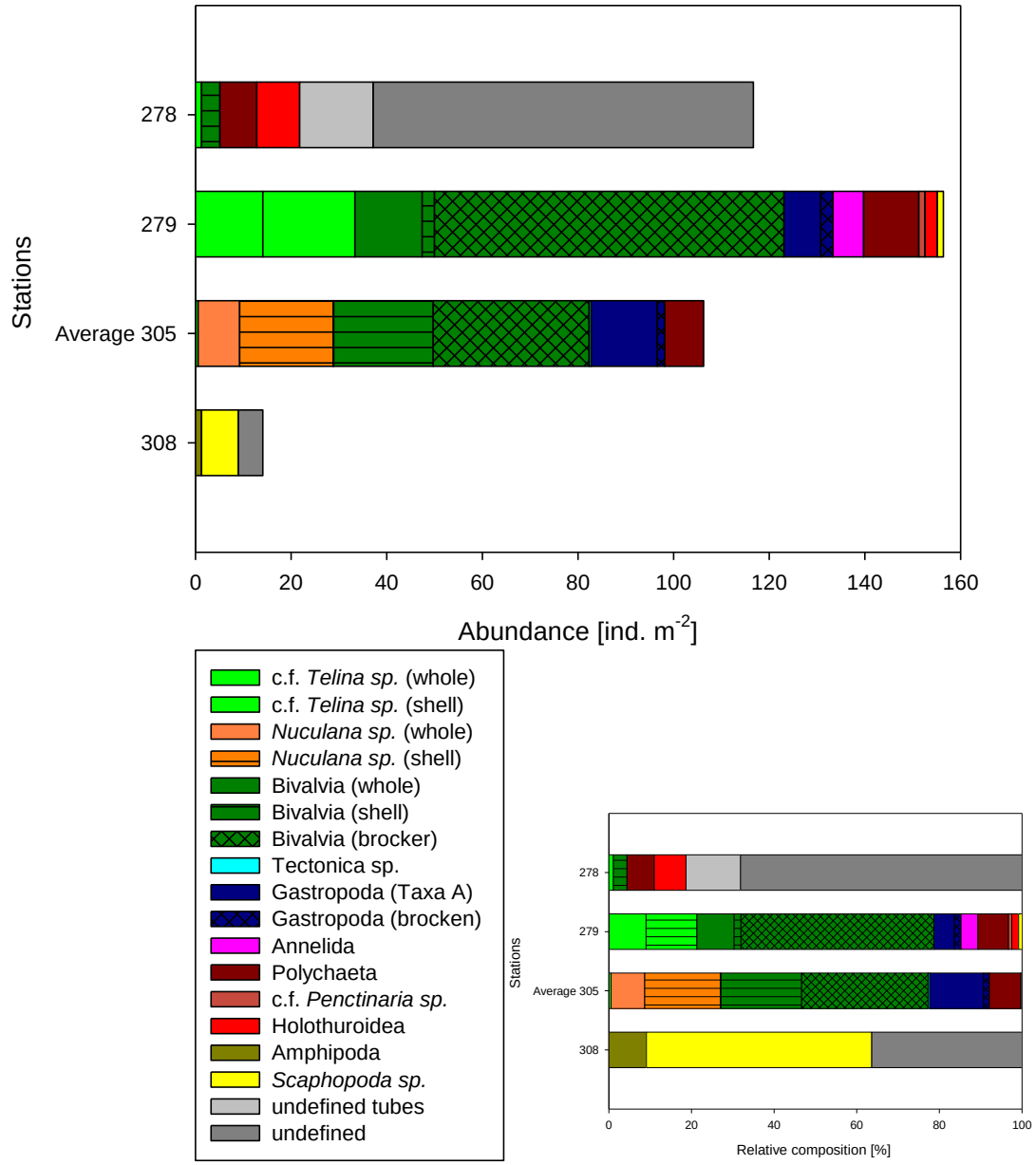

Figure 25: Benthic macrofauna abundance [ind. $^{m-2}$] and relative composition [%] at the Kunene shelf station (st.305).

The data showed that the highest abundance was found at the inner shelf station on the Rocky Point transect (155 ind. m^{-2}; st. 279). The dominating group was Bivalvia (80% of all). Most of them were undetermined and broken Bivalvia shells (~45 %). The remaining part consisted of whole Bivalvia (9 %), Bivalvia shells (1 %), whole c.f. *Telina sp*. (9 %), and shells of c.f. *Telina sp.* (12 %). Gastropoda were also found at these two stations. (1.5 % broken Gastropoda shells, 9 % of taxon A). Taxa A are Gastropoda which look like they plantain to the same species, but could not exactly be established via photos. A major part of the species composi-

tion at this station was represented by the group Polychaeta with 7 %. Moreover, Holothuroidea (1 %) and *Scaphopoda sp.* (0.8 %) were two of the seldom groups. On the Kunene transect at the shelf station (st. 305), the abundance of all determined individuals reached 110 ind. m^{-2}. The average of nine cores were analyzed. Similar to the Terrace Bay shelf station (st. 279) Bivalvia dominated the community with around 80 %. Unfortunately, 30 % of this group had broken shells and 19 % were empty shells. For the remaining Bivalvia the genus was determined, which led to a taxa composition as follows: whole c.f. *Telina sp*. (0.5 %), shells of c.f. *Nuculana sp.* (18 %) and whole c.f. *Nuculana sp.* (8 %). Gastropoda were found with around 1.5 % with broken shells, while 12 % were determined as taxa A and 0.5 % as cf. *Tectonatica sp*. Polychaeta contributed with 7 % to the taxa composition. The lowest abundance was observed at the deepest offshore station (st. 308) with less than 20 ind. m^{-2}. Here the main part of the taxa composition was determined as *Scaphopoda sp.* with 54 %, followed by unidentified species (36 %) and Amphipoda (9 %).

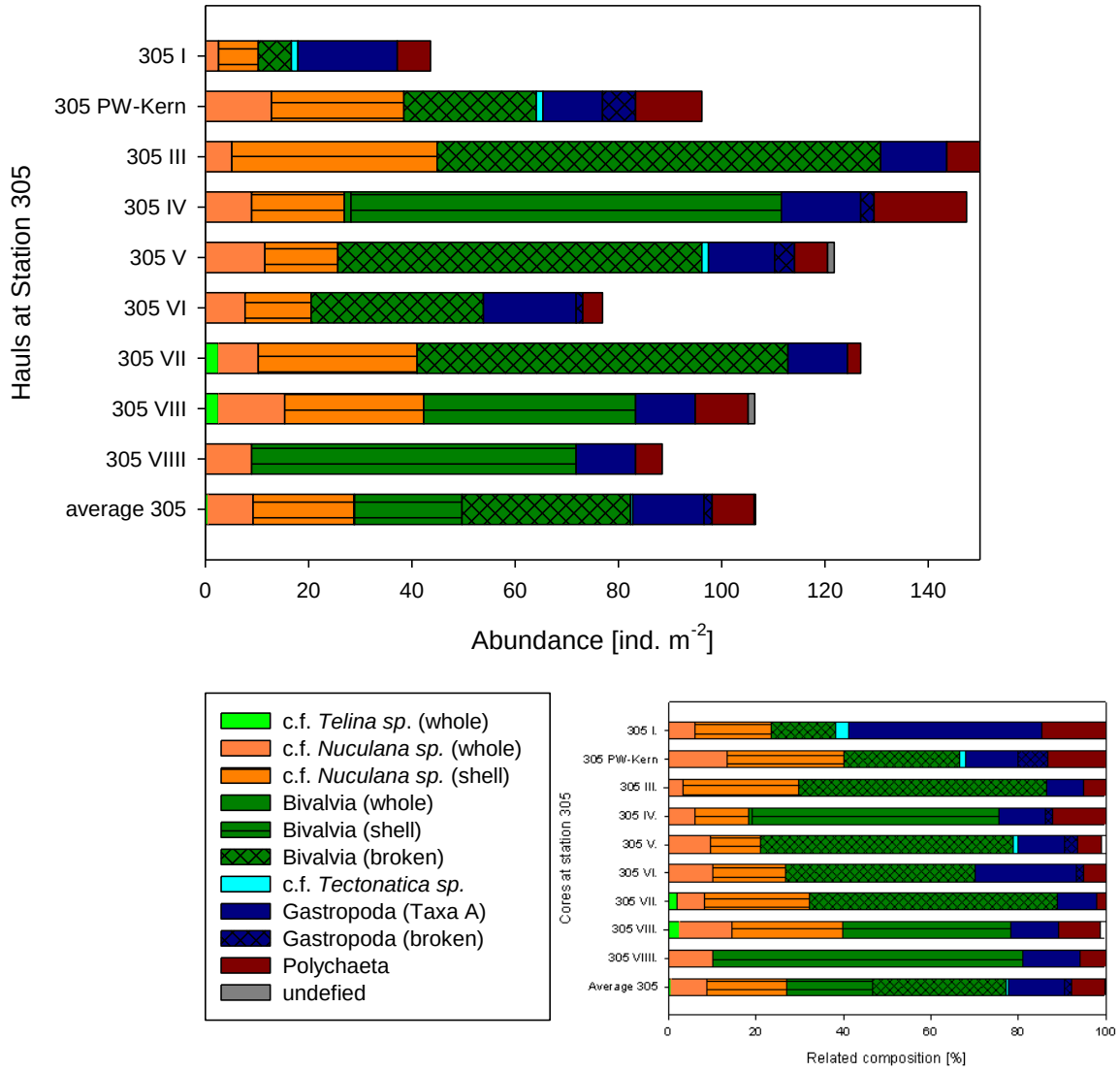

Figure 26: Benthos abundance and relative composition at the Kunene shelf station (st. 305) in nine different cores.

At the shelf station of the Kunene transect (st. 305) the different sediment cores showed an abundance of individuals of 50 ind. m^{-2} to 150 ind. m^{-2} (Figure 26). Except of the core 305 I, all cores were dominated by Bivalvia. Broken and undetermined Bivalvia presented the main part with a range of 40 % to 70 % of the taxa composition. The second largest part of this taxon consisted of whole organisms and/or shells of c.f. *Nuculana sp.* in a range of 10 % and 45 %. Furthermore, within the cores VII and VIII at the shelf station (st. 305) c.f. *Telina sp.* were detected with around 5 %. However, at core 305 I. Gastropoda made up the major part with around 3 % c.f. *Tectonatica sp.* and 44 % Gastropoda of taxa A. At the cores 305 PW.

and 305 V. c.f. *Tectonatica* sp. were obtained with around 1 %. At the other cores the Gastropoda taxon A was detected in a range of 8 % (305 III) to 23 % (305 VI). The Polychaeta were detected in a range of 2-14 % in all cores.

3.7.1 Summary of the benthic macrofauna abundances in the investigated area

All stations of the three transects showed large differences in taxa composition of the benthic macrofauna. The shelf stations of all three transect showed high abundances compared to the Kunene offshore station (st. 308). On the Terrace Bay shelf station (st. 278), the composition of all organisms was dominated by Polychaeta and Holothuroidea. The main fraction made the undefined tubes that could not clearly be assigned to one of those two taxa. The Rocky Point and Kunene shelf stations (st. 279 and st. 305 average) presented a higher abundance of Bivalvia taxa than the other stations. At the station 305, more cores were sampled that illustrated a dominance of the taxon Bivalvia which was split into c.f. *Telina sp*., c.f. *Nuculana sp.* and not further classified Bivalvia. All Bivalvia taxa and the other main taxa Gastropoda (Taxa A) and Polychaeta presented different abundance fractions between the different cores. In addition, *Scaphopoda sp*. was the dominating taxon at the Kunene offshore station (st. 308).

3.8 ROV video analysis of the benthic megafauna

3.8.1 Benthic megafauna abundance on the Terrace Bay transect (20° S)

The benthic megafauna diversity on the ROV videos was analyzed at the six stations on the three transects (Appendix, Table 8Table 9; Figure 27).

At the shelf station (st. 277) of the Terrace Bay transect, the observed track was 119 m long and located in a water depth of 100 m. Mainly Medusa were detected with an abundance of 203 ind. 100 m^{-1} (Table 9). Most of the Medusa had their tentacles pointed up to the surface. One unidentified Actinopterygii was detected; unfortunately a detailed classification was not possible. One Blackbelly Rose fish (*Helicolenus dactylopterus*) was found per 100 m route length.

3.8.2 Benthic megafauna abundance on the Rocky Point transect (19° S)

The inner shelf station (st.282) of the Rocky Point transect was situated at the shelf (110 m) and the route length was 284 m long (Figure 27). The most common taxa were the Asteroidea with 124 ind. 100 m^{-1}. Medusa and *Sufflogobius bibarbatus* (Bearded Gobies) were the second most common taxa with 21 individuals each on a track length of 100 m. Furthermore, Actiniaria was detected (2 ind. 100 m^{-1}) and Gastropoda (Table 9).

The outer shelf station (st. 285) was situated at a depth of 205 m and the track length was 351 m. Actiniaria was the most common taxon with 56 ind. 100 m^{-1}. Gobies (*Sufflogobius bibarbatus)* presented 10 ind. 100 m^{-1} track route. Compared to the shelf station on this transect, Medusa abundance was low with 2 ind. 100 m^{-1}. Gastropoda with 1 ind. per 100 m track length occurred as rarely as on the inner shelf station. In contrast to the other station on this transect, the unidentified taxa of Actinopterygii (3 ind. 100 m^{-1}), Pennatulacea (7 ind. 100 m^{-1}) and *Merluccius capensis* (hake) (1 ind. 100 m^{-1}) were also found at outer shelf station. Only on this transect, bacteria mats were observed. At the inner shelf station (st.282) the bacteria mats were frequently with a rare coverage at the outer shelf station (st. 285) on the Rocky Point transect.

3.8.3 Benthic megafauna abundance on the Kunene transect (17.5° S)

The shelf station (st. 305) on the Kunene transect was 150 m deep and the corrected track length was 430 m (Figure 27 and Figure 28). Most common group was the Pennatulacea with 2397 ind. 100 m^{-1} (Table 9). The second most abundant taxon was Gastropoda with 728 ind. 100 m^{-1}. Furthermore, the unidentified taxa of Actinopterygii (9 ind. 100 m^{-1}) were detected. The taxa Actiniaria, *Sufflogobius bibarbatus* and Shrimp were recorded, but only with 1 or less individuals per 100 m track route.

At the upper slope station (st. 314; 500 m depth), the track route had a length of 500 m. Like at the shelf station, Gastropoda (4463 ind. 100 m^{-1}) and Pennatulacea (1278 ind. 100 m^{-1}) were the most common taxa. Moreover, higher abundance of shrimps (15 ind. 100 m^{-1}) was observed compared to the shelf station (st. 305) on the Kunene transect. Macrouridae (Rattails) were also found (16 ind. 100 m^{-1}) where 8 ind. 100 m^{-1} were further classified as *Callorhinchus spp*., other unidentified Actinopterygii (2 ind. 100 m^{-1}) were less common at the

slope station compared to the shelf station. *Sufflogobius bibarbatus*, *Merluccius capensis*, Helicolenus dactyloperus (blackbelly rosefish), *Selachophidium guenthir* (barbed brotula), Type 16 (fish not clearly defined) and Coleoidea were found with an amount of 1 or less individuals per 100 m.

The deepest ROV station was the Kunene lower slope station (st. 315) on the continental slope (775 m). The track length was 339 m. The most common taxon was the Macrouridae with 49 ind. 100 m^{-1}, 8 of them were determined as *Callorhinchus spp.* One was defined as *Coelorinchus simorhynchus*.

With 2 ind. 100 m^{-1} the same number of other Crustacea was detected as at the upper slope station. However, less shrimps (13 ind. 100 m^{-1}) were detected than at the upper slope station. In contrast to the other stations on this transect, no Gastropoda were found and only 8 ind. 100 m^{-1} of Pennatulacea were observed. However, more unidentified Actinopterygii were found with 16 ind. 100 m^{-1}.

3.8.4 Summary of the megafauna abundances in the investigation area

The highest benthic megafauna abundance was found at the Kunene lower slope station (st. 306). The distribution pattern on this transect presented a high abundance at the shelf station (st.305) with a peak at the slope station (st. 306). Nevertheless, minor abundances were obtained at the lower slope station (st. 307). On the Terrace Bay transect at the shelf station (st. 277), the abundance was less than on the Kunene shelf station but higher than the Rocky Point shelf station (st. 282). The inner shelf station (st. 282) presented a lower abundance than the outer shelf station (st. 285) on the Rocky Point transect. At the Terrace Bay shelf station (st. 277) mainly Medusa were recorded.

On the Rocky Point transect, *Sufflogobius bibarbatus* and Medusa formed the main organisms at the inner shelf station (st. 282) while Actiniaria were the dominating species at the outer shelf station (st. 285). On the Kunene transect, Pennatulacea and Gastropoda illustrated the main taxa at the shelf station (st.305) and the upper slope station (st. 306). In particular, Pennatulacea dominated the shelf and Gastropoda the slope. At the lower slope, the main found taxon was Macrouridae. In contrast to the inner stations, no Gastropoda and Pennatulacea were obtained.

Kunene shelf station (st. 305)

Terrace Bay shelf station (st.277)

Rocky Point inner shelf station (St. 282)

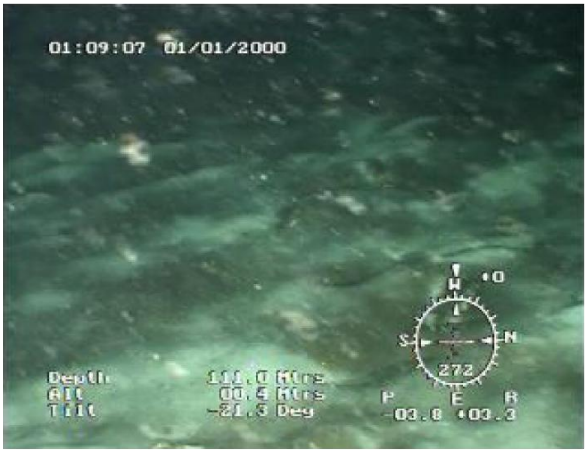

Rocky Point inner shelf station (St. 282)

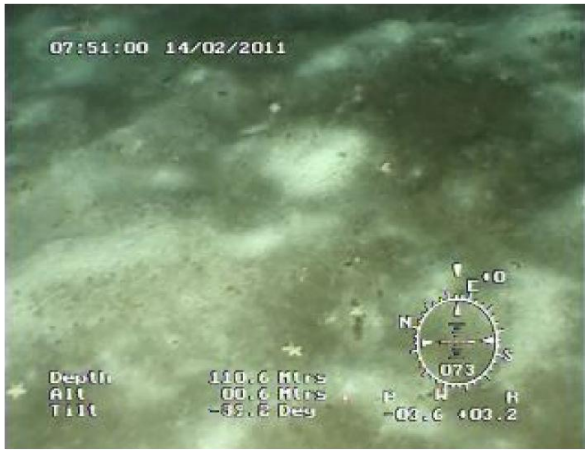

Rocky Point outer shelf station (St. 285)

Rocky Point outer shelf station (St. 285)

Figure 27: Overview of the benthic megafauna on the northern Namibian shelf.

Upper shelf station (st. 314)

Upper shelf station (st. 314)

Lower shelf station (st. 315)

Figure 28: Overview of the benthic megafauna on the Kunene slope.

3.9 Correlation of benthic megafauna abundance with different biotic and abiotic parameters

The benthic megafauna abundance is displayed in relation to the chemical and physical components measured in the water column as well as the abundance of benthic macrofauna, mesozooplankton and microzooplankton (Figure 29).

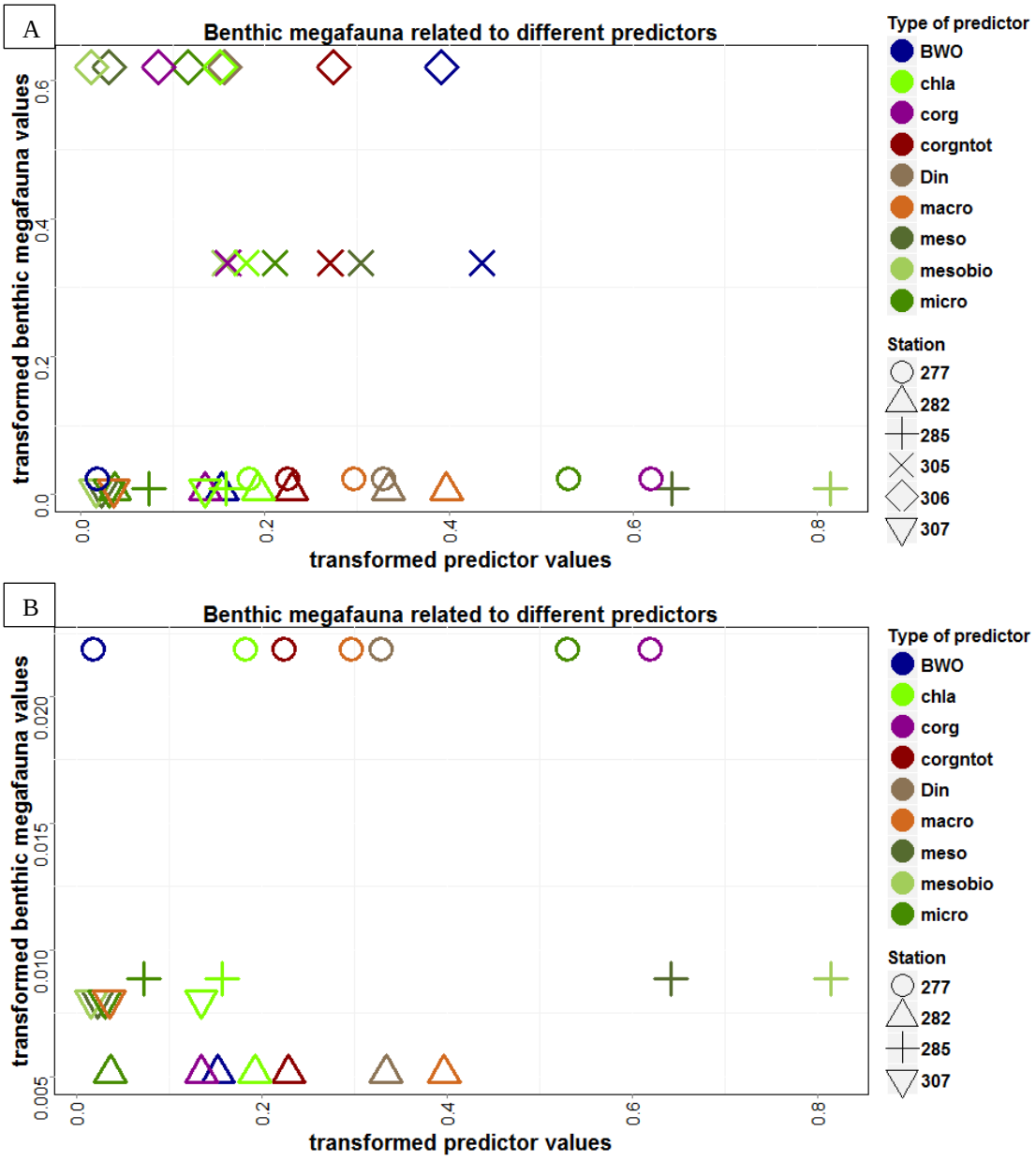

Figure 29: A: Megafauna values related to physical and chemical parameters and the values of benthic macrofauna, mesozooplankton and microzooplankton at all stations of the three transects. **B**: magnification of the relations of the three stations with the lowest benthic megafauna abundances. chla: Chlorophyll a, micro: microzooplankton, meso: mesozooplankton, mega: benthic megafauna, macro: benthic macrofauna, Corg: benthic organic carbon, Din: dissolved inorganic nitrogen (ammonium, nitrate, nitrite), BWO: bottom water oxygen.

3.9.1 Correlation pattern of benthic megafauna in the investigated area

By comparison of the benthic megafauna abundance of the different transects it became apparent that the station on the shelf (st. 305) and at the upper slope (st. 306) of the Kunene transect showed the largest abundance value of benthic megafauna (0.61 and 0.33). Compared to these high values, all stations on the Terrace Bay (st. 277) and Rocky Point (st. 282 and 285) transect as well as the lower slope station (st. 307) of the Kunene transect demonstrated very low benthic megafauna values in a range of 0.008 and 0.022 (Figure 29 A). Within these low values, the Terrace Bay shelf station (st. 277) had the highest abundance (0.022) while the Rocky Point inner stations (st. 282; st.285) had intermediate values (0.018–0.009). The lowest abundance was obtained at the Kunene lower slope station (st. 307)

3.9.2 Correlations at the Terrace Bay transect (20° S)

The chlorophyll *a* showed the second highest value (0.18) at the Terrace Bay shelf station (st.277) after the Rocky Point shelf stations while the bottom water oxygen (BWO) concentration was the lowest compared to the other stations. At the Terrace Bay shelf station no data was available for mesozooplankton abundance and biomass (Figure 29 B). The microzooplankton abundance was higher (0.529) compared to the other stations, while the value for the benthic macrofauna was the second highest (0.290). Moreover, the highest benthic organic carbon (Corg) value was detected (0.619) compared to all other stations. Furthermore, the Corg : Ntot (molar ratio) was the second highest and as high as at the Rocky Point inner shelf station (st.282). The value for Din was the second highest at this station, while the bottom water oxygen (BWO) concentration was the lowest compared to the other stations. At the Terrace Bay shelf station no data was available for mesozooplankton abundance and biomass.

3.9.3 Correlations at the Rocky Point transect (19° S)

On the Rocky Point transect the inner shelf station (st. 282) and the outer shelf station (st. 285) both displayed low values of benthic megafauna, while higher values were displayed at the inner shelf station (st. 282). This pattern is visible vice versa in the microzooplankton abundance, which showed a slightly higher abundance at the outer shelf station

(0.0734; st. 285) than at the inner shelf station (0.036; st. 282). Compared to the other transects, these values were the second lowest after the Kunene lower slope station (st.307; Figure 29 B). The Chl *a* concentration was higher at the inner shelf station and decreased to an intermediate value at the outer shelf station (st.285). Mesozooplankton was merely observed at the outer shelf station (st.285) and had the highest abundance (0.64) and biomass (0.815) compared to the Kunene transect stations. No data of benthic macrofauna and benthic biochemistry was available for the outer shelf station (st.285). The inner shelf station (st. 282) was characterized by the lowest benthic megafauna of all stations, while the benthic macrofauna abundance showed the highest value (0.397). Biochemistry measurements showed the second lowest values for the C_{org} concentration, the C_{org} : N_{tot} (molar ratio) and the BWO compared to the Terrace Bay shelf station (st. 277). The Din concentration was the highest at the inner shelf station (st.282).

3.9.4 Correlations at the Kunene transect (17.5° S)

On the Kunene transect the three stations showed very different values. While the highest benthic megafauna abundance of all transects was recorded at one of the slope stations (st. 306), the second highest abundance was recorded at the shelf station (st. 305; Figure 29 A). The lower slope station (st. 307), displayed the second lowest value of all transects. The chlorophyll *a* concentrations decreased from the coast to the continental slope. On the shelf, the value was higher than at the Rocky Point shelf and lower than at the Terrace Bay shelf.

In addition, the microzooplankton abundance (0.211-0.03) as well as the mesozooplankton abundance (0.30-0.02) and the benthic macrofauna abundance (0.27-0.0358) at the stations 305, 306 and 307 decreased from the coast towards the offshore waters (0.197-0.029). In comparison to the other transects, the microzooplankton on the shelf had an intermediate abundance that laid between the abundances of the Terrace Bay transect (0.529) and the Rocky Point transect (0.07). The mesozooplankton abundance at the same station was half as high as the abundance at the Rocky Point outer shelf station (st.285). The Kunene shelf station (st.305) showed the lowest benthic macrofauna abundance of the shelf stations of the two other transects. For the biochemistry comparison, data was available only for the shelf station (st. 305) and shallower slope station (st. 306) of the Kunene transect, the Rocky Point inner

shelf station (st. 282) as well the Terrac Bay shelf station (st. 277). The C_{org} concentration on the shelf (0.16; st. 305) showed an intermediate value that laid between the values of the inner shelf stations of the Terrace Bay shelf station (0.620; st. 277) and the Rocky Point shelf station (0.135; st. 282). The C_{org}:N_{tot} ratio was the highest with around 0.272 compared to the other transects. At the Kunene shelf station (st. 305) the DIN was lower than at the shelf stations of the other transect and decreasing further in the direction of the slope (st. 306). Only the BWO increased from the shelf to the offshore area (0.454-0.393) and the values were all higher than on the other two transects.

3.9.5 Sperman' rho correlation

The two sided Spearman's rho correlation of the benthic and the pelagic parameters showed no significant correlation ($p < 0.05$) for any combination (Table 7). However, there could be weak relations, even if they are not significant, between Chl *a* and microzooplankton (r_s = -0,374). Furthermore, the megafauna has a weak relation as well to Chl *a*, mesozooplankton and benthic macrofauna (r_s = 0.2). A moderate relationship was found between microzooplankton and mesozooplankton (r_s = 0.4) and between benthic macrofauna and microzooplankton (r_s = 0.4). The microzooplankton and the benthic megafauna showed a strong relation (r_s = 0.714) and an even stronger relationship was detected between mesozooplankton and Chl *a* (r_s = 0.8) and between mesozooplankton and benthic macrofauna (r_s = 1).

Table 7: Two sided Spearman's rho correlation test for all standardized abundance and concentration values of the pelagical and benthos with the associated p-values ($p < 0.05$). Black boxes display the separation of the rho- and p-values.

		Spearman's rho values				
		Chl *a*	Microzoo-plankton	Mesozoo-plankton	Benthic meg-afauna	Benthic macrofauna
p -values	Chl *a*	-	0.374	0.8	-0.2?	1
	Microzooplankton	0.497	-	0.4	0.714	0.4
	Mesozooplankton	0.333	0.75	-	0.2	1
	Benthic megafauna	0.7139	0.1631	1	-	0,2
	Bnethic macrofauna	0.083	0.75	1	0.9167	-

3.9.6 Relation of the biological and chemical parameters in the pelago-benthic coupling

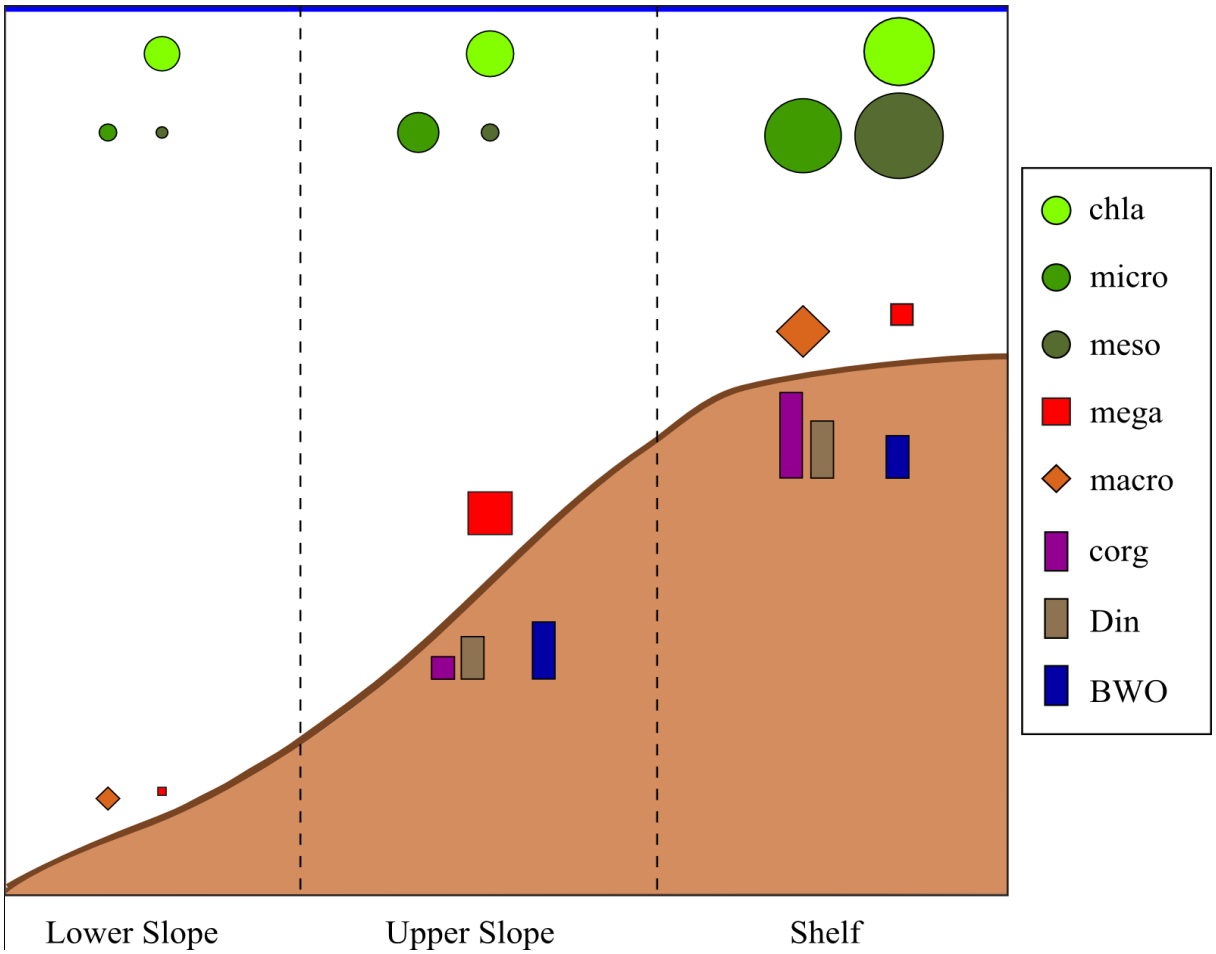

Figure 30: Relation of the different biological and chemical parameters in the pelagial and benthos. chla: Chlorophyll a, micro: microzooplankton, meso: mesozooplankton, mega: benthic megafauna, macro: benthic macrofauna, Corg: benthic organic carbon, Din: dissolved inorganic nitrogen (ammonium, nitrate, nitrite), BWO: bottom water oxygen.

Generally, all parameters Chl *a*, microzooplankton, mesozooplankton, benthic megafauna, benthic macrofauna, dissolved inorganic nitrogen and benthic organic carbon except the oxygen were higher on the shelf and decreased down the slope (Figure 30). Chl *a* as well as the microzooplankton abundance showed a decreasing trend from the shelf towards the open ocean. The decline of mesozooplankton abundance between the shelf and the upper slope was more intense than for microzooplankton. This pattern indicates a high biomass in the pelagic realm on the shelf, which leads to a stronger sedimentation on the shelf than at the upper slope and lower slope. The result is a higher C_{org} and Din concentration on the shelf, while simultaneously a reduced oxygen concentration was detected due to bacterial decomposition of organic matter. Down the slope the values of Chl *a*, microzooplankton and mesozooplankton abundance decreased constantly with a declining trend of the chemical concentration

(C_{org} ;Din) at the bottom and the benthos abundances, merely the upper slope demonstrate the highest benthic megafauna abundance in contrast to the shelf and lower slope. The lower slope presents the lowest pelagic and benthic organism abundances.

3.9.7 Corellation of the benthos and pelagial at all stations of the three transects

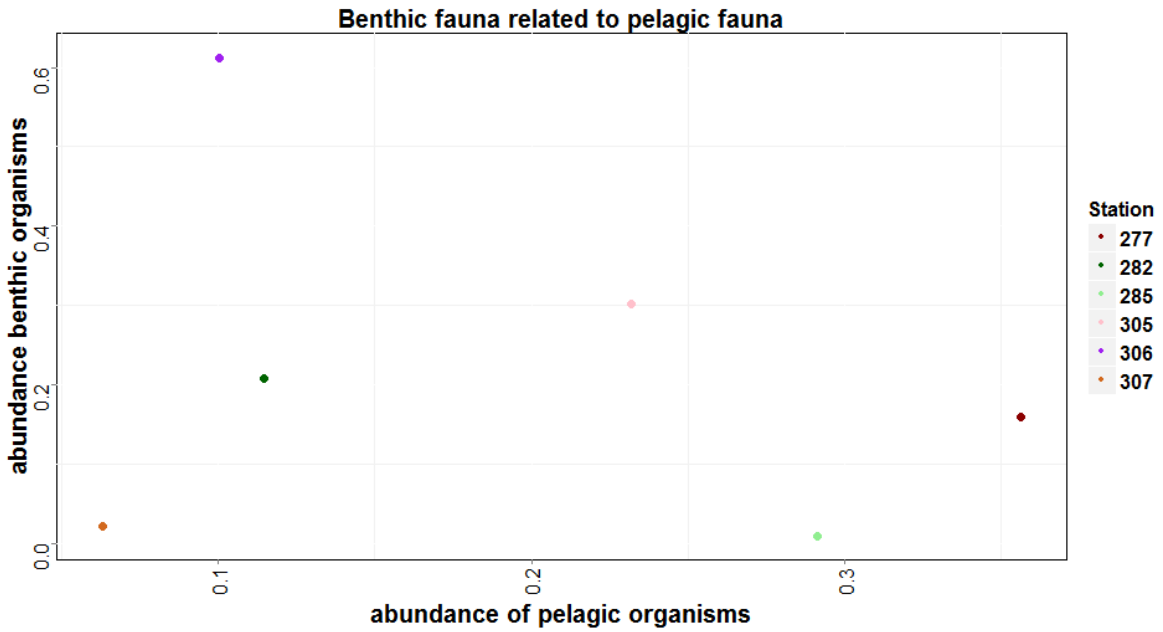

Figure 31: The correlation of the sum of all benthic abundances (macrofauna and megafauna) and the sum of all pelagic concentrations and abundances (chlorophyll a (phytoplankton), microzooplankton and mesozooplankton) at all stations of the three transects.

The by far highest benthos abundance and the second lowest pelagic abundance were detected on the Kunene transect at the upper slope station (st. 306; Figure 31). On this transect the second highest abundance of the benthic fauna and the third highest abundance of the fauna of the water column were obtained at the shelf station (st. 305). The two inner shelf station of the Terrace Bay and the Rock Point transect showed an intermediate abundance of the benthos ranging between 0.159-0.201. However, the Rocky Point inner shelf station (st. 282) showed a much lower pelagic abundance (0.114) than the Terrace Bay shelf station which had the highest pelagic abundances (0.356). Nevertheless, the lowest benthic abundances were detected at the Rocky Point outer shelf station (st. 285; 0.009) and the Kunene lower slope station (st. 307; 0.0219). In contrast to this, the pelagic abundances were the second highest at this shelf station and the lowest at this lower slope station.

4 Discussion

In the present study, the pelagic-benthic coupling (Graf, 1989) in the Namibian upwelling area was investigated from the shelf down the slope. At the continental margins, Jahnke (1990) stated that local topography may have some influence on deposition and the remineralisation rates. However, these local effects are generally much smaller than large scale regional trends like injections of water mass from the southern and northern currents. Nevertheless, this study identifies local factors structuring the benthic community in the northern Benguela Upwelling System. Three transects in this area which are between 60 and 89 NM apart from each other showed clear differences in benthic abundance and composition of megafauna and macrofauna. Abiotic and biotic data from the overlying water column were correlated with the benthic data, assuming that the benthos is depending on the input of organic material (OM) from the upper water layers (see also Parsons et al., 1984; Roughgarden, 2006)

4.1 Hydrography

Hydrography data were used for the detection of the upwelling phenomena, which cause the input of nutrients from deeper layers into the eutrophic zone. Additionally, oxygen minimum zones (OMZ) were detected. The hydrographic profiles indicated a recent or active coastal upwelling along the entire Namibian coast typical during the summer season, at all three transects throughout the investigation (Figure 5, Figure 6 and 7). However, in the northern Benguela upwelling system, a maximum upwelling occurs between April and September and is reduced in January and February between 17° S and 21° S (Demarcq et al., 2007). During this study, higher water temperatures than usual in this season were recorded during the southern summer and the salinity showed a decreasing trend to the south caused by saltier SACW in the north and less salty water in the south introduced by the Eastern South Atlantic Central Water (ESACW; (Mohrholz et al., 2007). This indicates that water masses from the north (Angola Current) were displaced into the northern Namibian area.

On the Terrace Bay transect, the detected moderate upwelling conditions were underlined by an absence of an intermediate salinity maximum, which is typical for intense upwelling condi-

tions (Mohrholz et al., 2007). Offshore, at above 240 m depth, the influence of the ESCAW was indicated by high oxygen concentrations. In contrast, the central water layer was dominated by low oxygenated SACW below 240 m and at the inner stations. Similar findings were also detected near the bottom of the Rocky Point transect. Those suboxic to anoxic zones have an influence on the distributions of organisms (Bertrand et al., 2010). On the Rocky Point transect, downward sloping isopycnals near the shelf edge point to a poleward undercurrent in a depth layer between 100 m and 200 m (Lahajnar et al., 2012). In addition to the two southern transects mentioned above, the highest fraction of oxygen poor SACW was detected on the Kunene transect between 200 and 400 m water depth. Between 100 m and 400 m, in the central water layer, a strong downward sloping of isotherms and isohalines towards the coast was depicted, which is typical for a strong geotropic adjusted southward flow along the shelf edge (Lahajnar et al., 2012). Compared to the offshore surface layer, different patterns of temperature, salinity and oxygen in inshore surface waters indicate a coastal upwelling from water layers between 50 m and 80 m on the Kunene transect. On this transect, the center position of the Angola Benguela frontal zone (ABFZ) was detected. Above the thermocline the transect was partly covered by warm saline surface water of tropical origin, which implies a southward shift of the ABFZ (Lahajnar et al., 2012). On the Kunene shelf this front acted as a physical barrier and limited the extension of the OMZ (Monteiro and van der Plas, 2006). The outflow of the Kunene River is located on this transect and on its annual minimum in October (monthly flow rates (mfr): 99 million m^3; 29 years average) and highest in March and April (975-1153 million m^3; 29 years average), but with a high variability between the years (Nogueira et al., 1997).This could be a reason for the high particle flux rate during the investigation in February (mfr: 554; 29 years average; Eggers, 1990). Moreover, the estuary of the Kunene River may have an influence on the ecosystem in this coastal area (Lass et al., 2000).

4.2 Plankton abundances

4.2.1 Phytoplankton distribution detected by satellite

Nutrients are transported in high concentrations into the eutrophic zone mainly from the sub-thermocline by upwelling. This supports an immensely powerful biological pump and maintains phytoplankton blooms (Malone, 1980; Berger et al., 1989; Diffenbaugh et al., 2004). In this study, the phytoplankton concentration was monitored as Chl *a* concentrations by satellite data. On all transects the Chl *a* concentrations presented the same trend with the highest concentration at the coast and a decrease with increasing distance from the coast, exhibiting a strong negative offshore gradient, which was also observed by Demarcq et al. (2003) and Weeks and Shillington (1995).

During the sampling period of this study, the upwelling activity was low but contrary to this the phytoplankton abundance demonstrated a high concentration near the coast. Barlow et al., (2005) detected that the phytoplankton bloom is variable, but there are indications that the phytoplankton abundance is generally elevated during winter and spring time in the northern BUS (Demarcq et al., 2007). In the Peruvian upwelling system only a weak relation between the seasonal maximum of the Chl *a* concentrations and the seasonal maximum of the upwelling activity was detected (Nixon and Thomas, 2001). In a more specific study of these coherences, Carr and Kearns (2003) determined that the primary production is mainly influenced by large-scale circulations, responsible for up to 60 % of the variance in primary production, while the physical forcing in terms of upwelling and temperature variability affects only 18 % of the variance. On all three transects, upwelling events were detected, but in contrast to the Kunene transect the upwelled water on the southern transects (Terrace Bay and Rocky Point) had its origin in nutrient rich water below 100 m depth (Shannon, 1985). This fact could lead to a lower nutrient supply which could be the reason for the lower chlorophyll *a* concentration on the Kunene shelf than in the shelf region of the two other transects (Nogueira et al., 1997).

4.2.2 Microzooplankton abundance

Phytoplankton abundance is not only controlled by nutrient supply but also by grazing pressure (Flynn, 1989). The main grazer of phytoplankton in upwelling areas are microzooplankton (Calbet and Landry, 2004). This could be the reason for the high abundance of microzooplankton at the Terrace Bay shelf station (st. 277) and the low abundance at the Kunene lower slope station (st. 307), despite that each site showed the same value in Chl *a*. The microzooplankton abundance on the Rocky Point shelf was lower than on the Kunene shelf, although the Chl *a* concentrations were higher. This could be caused by other elements of the diet of microzooplankton like bacteria, detritus and other microzooplankton animals (Jarre-Teichmann et al., 1998). Another reason for the higher abundance of microzooplankton in proportion to a low Chl *a* concentration on the Kunene shelf could be the absence of OMZ in this region. OMZ have an enormous influence on the species abundance since only a few species can tolerate these extreme oxygen deficiencies, thereby constraining the vertical habitat of most marine organisms (Prince and Goodyear, 2006; Bertrand et al., 2010). A further explanation for a lower abundance of microzooplankton at a lower Chl *a* concentrations could be the predation by other zooplankton (Kleppel, 1993).

At the Terrace Bay shelf station (st. 277) below 50 m and at the Rocky Point shelf stations from 80 m downwards oxygen minimum zones were located, probably causing a decrease in microzooplankton abundance. At the Kunene shelf station (st. 305) with well oxygenated water masses, the number of individuals increased again below 100 m. However, at the lower Kunene slope station (st.307), where an OMZ is located between 200 and 400 m water depth, the abundance of microzooplankton was stable throughout the whole water column. A constant species abundance below an OMZ in these water depths could not be observed at the other stations due to shallower depths. In addition to that, the Kunene slope station (st. 305) showed the same distribution pattern as the Terrace Bay outer shelf station (st. 276) and the Rocky Point shelf stations (st. 282 and st.285), with a decline of microzooplankton abundance with depth, probably caused by an OMZ. The different sampling times of the day demonstrated no obvious difference in the vertical distribution.

Microzooplankton (in a size range of 20-125 µm) is mainly composed of Dinoflagellata and Tintinnida (Laybourn-Parry, 1992). In this study, a large size fraction (55-300 µm) was analyzed and the taxon Dinoflagellata was detected with high abundances only at the Terrace Bay outer shelf station (st. 276; Figure 9) and at the Kunene shelf station (st. 305; Figure 12). The

microzooplankton taxa composition demonstrated a structure different from to the one observed by Laybourn-Parry (1992) at many stations, with a dominance of Copepoda. This taxon was found more often on the shelf than at the slope in the present study. The reason for this could be that Copepoda feed on phytoplankton during active upwelling (Timonin et al., 1992) with an average of 25% of the available daily phytoplankton (Verheye et al., 1992). A maximum abundance of Copepoda was also recorded by Hansen et al. (2005) on the central shelf (40 NM from the coast) at the further south Walvis Bay transect (23° S). Radiolaria were the main taxon at the Rocky Point shelf station (st. 282). This taxon is often found in nutrient-rich water with a high Chl *a* concentrations (McMillen and Casey, 1978; Dworetzky and Morley, 1987) like on the inner shelf.

4.2.3 Mesozooplankton abundance

Mesozooplankton and microzooplankton revealed a similar distribution pattern since mesozooplankton consumes microzooplankton (Iirigoien et al., 2005). The concentration declined from high abundance inshore (st. 305) over intermediate abundance at the continental slope (st. 306) to the lowest abundance offshore (st. 307). However, in contrast to the microzooplankton abundance the mesozooplankton abundances were higher at the Rocky Point outer shelf station (st. 285) than at the Kunene shelf station (st. 305).

Mesozooplankton day-night vertical distributions on the Rocky Point transect (st. 285) indicated a higher abundance of individuals in the upper water layer at daytime than during the night. These distribution patterns are contrary to the common vertical migration of mesozooplankton (Vinogradov, 1968). While during night time mesozooplankton emerges from deeper water into the upper more food-rich water layers to feed, it migrates into deeper layers to prevent predation at daytime (Stich and Lampert, 1981; Steinberg et al., 2000).

The impact of the OMZ on the mesozooplankton abundance in the different depth intervals seemed more obvious than for the microzooplankton distribution. A decrease in the abundance and biomass of the mesozooplankton was observed between water depths of 100 m to 400 m where an OMZ was located at the Kunene lower slope station (st. 307). Below the OMZ, the individual number of the mesozooplankton sharply increased again. Due to the location of the OMZ close to the bottom, it could not be detected whether depth or the OMZ was the reason for decreasing mesozooplankton abundance (Auel and Hagen, 2002).

4.3 Sedimentation

The pelago-benthic coupling is important for supply of food to the benthic community. The abundance and sinking velocities of organic particles determine the magnitude of carbon flux which reaches the benthos (Fowler and Knauer, 1986). Microzooplankton and mesozooplankton are important food web members in epi- and upper mesopelagic zones of the oceans. They consume large amounts of particles including phytoplankton and protozoans (see Robison et al., 2010) and contribute largely to the particle flux in the ocean by modifying marine snow (Alldredge and Silver, 1988), by sinking faecal pellets (Bruland and Silver, 1981) and by the sinking of dead bodies. This causes a higher particle flux on the shelf than offshore, caused by a higher abundance of microzooplankton and mesozooplankton as consumers of chlorophyll *a*.

The primary turnover could be estimated by the quantitative importance of new nitrogen to primary production. This is given by the f-ratio, the ratio of NO_3^- uptake to the combined uptake of NO_3^- and NH_4^- (Eppley and Peterson, 1979). Upwelling systems typically have higher f-ratios of about 0.5 than offshore regions (Eppley, 1981). At the Namibian coast, f-ratios of 3-5 indicated maxima in near-surface waters (25 % light penetration) and lower values indicated a minimum towards the boarder of the euphotic zone and the lower water masses (James et al., 1989). This increase could lead to a high primary production as estimated by Summerhayes et al. (1995). The authors measured a shelf-edge productivity of 175-240 mmol C m^{-2} d^{-1}. These sedimentation of plankton and particle transport more organic material into the benthic zone (Rogers and Bremner, 1991) and organic matter accumulates as mud belts (Inthorn et al., 2006). In the present study higher concentrations of marine snow were observed with the ROV at the inner shelf station at Terrace Bay and the Rocky Point and at the Kunene shelf stations (st. 305) than at the Kunene lower slope station (st. 307). Please note, that these particle concentrations were not quantified. The predominance of sediments enriched by organic matter across the shelf and upper slope of the northern BUS indicates that the new productions are consistent with long-term trends in sedimentation (Calvert and Price, 1970) (Bremner, 1983). Furthermore, Jahnke (1996) suggested that continental margins account for ~40% of the particulate organic carbon flux in to the deep ocean (at > 1,000 m water depth).

4.4 The sediment structure

Differences in the flux lead to a diverse sediment structure from the shelf downwards the continental slope. Bremner (1978) divided the seafloor off Namibia's coast into three zones with high organic matter deposits: firstly the inner mud belt in 50-140 m water depth with the highest concentration of organic matter deposits (7-25 %), especially diatom mud (to 150 m). The second area is located on the middle shelf in 200-300 m depth in a sandy-muddy substrate region with a depth range of 150 m to 400 m. The outermost belt, which is the third area, is located at a depth of 500-1400 m on the slope with a muddy seabed below 1000 m. The areas are additionally supplied with organic material by lateral transport due to the high concentration of organic material caused by the high phytoplankton production (Steffani, 2012).

Transferring this pattern onto the analyzed transects, the Terrace Bay and Kunene shelf stations (st. 277 and st. 305) as well as the Rocky Point inner shelf station (st. 282) were located in the inner mud belt. The amount of mud increased with depth from the shelf down the slope (see also Werner, 2012). Furthermore, the outer Rocky Point shelf station (st. 285) was estimated to be located in the sandy-mud area. Both slope stations (st. 306 and st. 307) of the Kunene transect were in the alternate belt. The recordings of the ROV did not detect the sediment structure, but sandy sediment seems to be observed at the Terrace Bay shelf station (st. 277). The amount of mud increased with depth from the shelf down the slope (Werner, 2012).

The shelf is seasonally exposed to relatively warm bottom water (SACW), which permits intensive microbial activity and results in high rates of nutrient turnover (Neumann, 2012). A frequent consequence of high remineralisation rates is the successive consumption of available electron acceptors such as oxygen, nitrate and sulphate etc. by bacteria. Moreover, high remineralisation rates should be positively correlated with the water temperature which influences polikilothermal bacteria and invertebrates (Kristensen et al., 1992). In particular, the shelf stations of the transects Rock Point and Terrace Bay present a high concentration of nitrogen compounds and high C_{org} concentrations, which is in contrast to the Kunene transect with decreasing concentrations of these elements with bottom depth. High temperatures enhance the accumulation reaction into carbon dioxide, dinitrogen, hydrogen sulphide and methane in the surface sediment and the bottom water (Neumann, 2012). These reactions were

accompanied by a low oxygen concentration on the shelf (Terrace Bay and Rock Point) with an increasing trend downwards the continental slope as measured on the Kunene transect. A further reason for the higher oxygen concentration at the Kunene lower slope station (st. 308) might be the introduction of NADW into the bottom water: the highest oxygen concentrations with up to 238 µmol l^{-1} were detected at this lower slope station (Neumann, 2012).

4.5 Sediment flux

Fluxes of nitrate, nitrite, ammonium, N2 and phosphate in the sediment display less temporal variability than water column fluxes. However, phosphate and ammonium fluxes between the bottom water and the sediment are increasingly exponential by increasing temperature (Smith et al., 1992). These higher flux rates are driven by the activity of bacteria and invertebrates (Kamp-Nielsen, 1975; Neumann, 2012). The present study agrees with these results: much higher phosphate and ammonium fluxes between the sediment and the bottom water were detected on the warmer shelf than at the colder, deeper stations on all three transects. Generally, flux rate decrease with lower temperature and increasing depth (Zabel et al., 1998; Schulz and Schulz, 2005; Goldhammer et al., 2011). Neumann et al. (2012) pointed out, that the C_{org} : N_{tot} ratio is affected by the release of ammonium from the sediment. This implies that fresh organic material with a low C_{org} : N_{tot} ratio as detected at all shelf stations investigated in this study releases more ammonium than refractory organic material with high C_{org} : N_{tot} ratio like at both Kunene slope stations (st. 306 and st. 307).

The ratio of released ammonium and phosphate is shifted towards phosphate by nitrification if oxygen is present (Goldhammer et al., 2011). This might be the case at the Kunene slope stations (st. 306 and st. 307). Here, the nitrate uptake from the bottom water into the sediment is higher than on the shelf while at the same time the ammonium flux decreased from the sediment into the water. Thus, N_2 production is more controlled by bottom water oxygen concentration than by nitrate concentration. At higher temperatures and lower oxygen concentrations, as it was detected on the shelf in the present study, the ammonium-nitrate balance is shifted towards ammonium. Füssel et al. (2012) mentioned that nitrification was displaced from the sediment into the water column by a higher nitrate flux of > 10 µmol l^{-1} even in the OMZ. Moreover, Kalvelage et al. (2011) observed a high rate of nitrate reduction in the OMZ of the

Namibian and Peru/Chile upwelling system and suggested that the produced nitrite reduction is coupled to anaerobic ammonium oxidation (annammox) (Kuypers et al., 2005; Ward et al., 2008). Competing reoxidation of reduced nitrite would explain why nitrate was not fully consumed during the sampling of the present study.

Veraart et al. (2011) stated that microbial oxygen consumption and thus the availability of oxygen within the sediment is temperature-dependent. The availability of oxygen ultimately controls oxygen dependent processes such as nitrification and denitrification. In the present study, nitrite fluxes as proxy of nitrification and denitrification suggest that internal nitrification apparently ceased at temperatures above 11°C which are predominant on the shelf.

4.6 Bacteria mats

The largest surface coverage of bacteria mats was observed at the inner shelf station (50-79 %; st. 282) and showed a decreasing trend to the outer shelf station (20-49 %; st. 285). This pattern could be influenced by a higher decomposition of organic material generated by greater plankton abundance in the pelagic at the inner shelf station (st. 282). On the inner shelf the diatom mud belt is associated with a high organic matter input and a high sulphur concentration. Moreover, the higher amount of diatoms in the mud increased the sulphur concentrations via decomposing. Such conditions are preferred by *Thiomargarita namibiensis.* (Steffani, 2012).

Thiomargarita namibiensis is located in the upper centimeters of the sediment and stores phosphate at an oxygen concentration above 40 µmol O_2 l^{-1} (Schulz and Jørgensen, 2001). At a temperature of 12-15 °C and < 40 µmol O_2 l^{-1} the highest phosphate fluxes from the sediment into the water column were detected at the shelf station. This was also recorded by Schulz and Schulz (2005) and Goldhammer et al. (2011). The authors attributed intensive phosphate releases to the abundance of *Thiomargarita namibiensis*. This bacteria and *Beggiatoa* are facultative aerobic sulphur bacteria which oxidize bottom water sulphide out of the covered bottom water into environmentally harmless colloidal sulphur and sulphate (Lavik et al., 2009). The metabolism of these bacteria turns anaerobic on the shelf due to the low oxygen concentration; hence a larger coverage of bacterial mats on the inner shelf than on the outer shelf was detected. Under the conditions mentioned above the bacteria oxidize up to

55% sulphide into sulphur and sulphate on the Namibian shelf. Thus, the bacterium is able to flexibly adapt its metabolism to the conditions on the shelf off Namibia (Schulz and Schulz, 2005). According to this, bacteria mats were observed via ROV only at the two anoxic Rocky Point stations (st. 282; st. 285) in the present study.

4.7 Benthic macrofauna abundance

The benthos has the highest diversity within the marine species (Gray, 1997) and the seafloor presents the largest continuous ecosystem on earth (Snelgrove et al., 1997). The high overall productivity and mineralization on the Namibian shelf results in high benthic biomasses and a benthic community well adapted to a constant and massive organic material input (Aspetsberger et al., 2007). This pattern of particle flux rates may explain the findings of the present study that the benthic macrofauna abundance decreased from the shelf towards the lower slope, matching results from other deep benthic environments (Martin and Sayles, 2004; Aspetsberger et al., 2007; Heip et al., 2001). One reason for this pattern could be the significant correlation between the abundance and biomass of the macrofauna, the silt content and the TOC (total organic carbon) in the sediment detected by Kröncke and Türkay (2003). This indicates that the C_{org} concentration on the shelf is higher compared to the lower slope and influences the macrofauna density. Carbon is an important component for the basic metabolism of the deep-sea community and even refractory organic material is sufficient to meet the energy demand in the deep sea (Tenore and Chesney, 1985). Macrofaunal contribution to total metabolism is reported to be high on the shelf and upper slope sediments in the Benguela Upwelling System (Heip et al., 2001; Aspetsberger et al., 2007). In particular, Steffani (2010) stated that the species richness inshore and offshore of Namibia showed a strong dominance of Polchaeta followed by Crustacea and Mollusca. This is in contrast to the findings of this study, which indicate a dominance of Mollusca followed by Polychaeta, except for the Terrace Bay inner shelf station, where the major species were Polychaeta and Holothuroidea.

The two inner shelf stations of the Terrace Bay and Rocky Point transect (st. 277 and st. 282) ROV stations were approximately at 105 m depth, but the benthic macrofauna sampling stations were at 34 m depth at both sites. At the anoxic Terrace Bay innermost shelf station

(st. 278), Holothuroidea and Polychaeta indicated a high abundance. Similar findings detected by Zettler et al. (2009) in an OMZ at depths between 150 m and 201 m on the Namibia shelf. The shelf area was covered by the diatomaceous mud (Bremner, 1978), which causes a reduction in benthic macrofauna, although it contains high concentrations of organic matter and reduced sulphur. Sako (1998) and Sanders (1968) detected that the macrofauna species diversity was reduced in OMZ off Namibia, but higher abundances and biomasses exist at the edge of the OMZ. This could not be confirmed in the present study since the highest taxa diversity and abundances were found at the anoxic innermost shelf station of Rocky Point (st. 279). Furthermore, the not further defined Gastropod taxon A was observed at this station. The animals look very similar to *Nassarius vinctus*, which is a long-living species and seem to be adapted to the occurrence of nearly anoxic and hypoxic conditions in this region. This species can be used as an indicator species of OMZ. The high abundances of this species in the OMZ were also detected by Zettler (2009). Nevertheless, the main taxon at this station was Bivalvia. At the Kunene upper slope station (st. 305) at the lower shelf break ROV observations recorded less particle flux, this could result in the low C_{org} sediment concentrations compared to the shelf. This feature has an effect on the taxa composition resulting in high abundances of the anoxic adapted Bivalvia *Nuculana* sp. (might be *N. bicuspidata*) and taxon A (might be *Nassarius vinctus*) in the present study (Zettler et al., 2009; Eisenbarth, 2012). Generally, organisms living in OMZ are more restricted by the lack of oxygen than by the supply of POM (particulate organic matter). However, Sibuet et al. (1989) described the flow of particulate material as a parameter, which mainly influences the distribution of the deep-sea fauna (Eisenbarth, 2012).

Please note, that the ROV lower slope station (st. 307) was at 800 m depth and hence 1000 m shallower than the well oxidized deepest Kunene offshore station (st. 308). In this deep sea area the upwelling has no influence (Thiel, 1978). This leads to a more stable physically balanced environment in the deeper layer, where organisms could easily build stable communities (Sanders, 1977; Sanders, 1968). Benthic abundance and diversity were low in the oxygenated bottom water at low temperatures and intermediate C_{org} concentrations. Additionally, Rowe (1981) notion that benthic biomass is function of surface productivity and tends to decrease with distance from the shore and with depth. Moreover, the low bottom temperature did not show any measurable effects on the benthic bacterial processing rates, which were recorded during the in situ experiments of Aspetberger et al. (2007) in the Benguela Upwelling System. It has to be pointed out that the analysis of the abundance and diversity of

the macrofauna was merely based on pictures; identification was only possible on the group or family level.

4.8 Benthic megafauna abundances

It is presumed that differences in the habitat structure of the benthos are caused by physical, chemical and biological processes (Narvarrete et al., 2005; Siegel et al., 2008). This could be the reason why the three transects demonstrate a very different benthic megafauna community structure in small scaled areas (150 NM). The benthic megafauna distribution showed a similar decreasing trend from inshore to offshore as recorded by the ROV (Figure 32).

At the Terrrace Bay shelf station (st. 277) the third highest abundance of megafauna was recorded concerning the major taxon Medusa (203 ind. 100 m^{-1}). This high abundance was also detected by Flynn et al. (2012) who indicated a peak of jellyfish abundance over the central region of the Namibian shelf, which is characterized by a broad shelf (Shannon, 1985). It has been considered as a semi-permanent convergence zone and could lead to the accumulation of jellyfish (Boyer et al., 2001). The Medusa pointed their tentacles to the surface to catch marine snow, which had a higher concentration on the shelf than at the slope (Berryman, 2005; Calvert and Price, 1970). The higher concentration of particles was caused by higher phytoplankton (Estrada and Marrasé, 1987; Brown et al., 1991) and zooplankton biomass (Shannon and Pillar, 1986; Olivar and Barange, 1990). Jellyfish are probably more abundant in areas with a high particle concentration (Bailey and Batty, 1984). Nevertheless, the Medusa found in the present study were not identical with the two common species *Chrysaora fulgida* and *Aequorea forskalea* on the Namibian shelf (Gibbons, 2011) which did not show this kind of feeding behavior.

The hypoxic conditions detected at the Terrace Bay station were tolerated by polyps and Medusa. The adaptation to low oxygen condition on the shelf and the decreasing abundances of small pelagical fishes since the 1970s (Gibbons, 2011; Boyer et al., 2001) lead to an increase in the abundance of Jellyfish over the whole length of the Namibian coast from the Kunene River in the north to the Orange River in south (Venter, 1988; Fearon et al., 1992) with the

greatest abundances in water depths of < 200 m. The main predators on jellyfish are turtles, sunfish and the bearded gobies on the shelf (Flynn et al., 2012). The Rocky Point transect was the only transect where bacteria mats (*Thiomargarita namibiensis)* were recorded. The covering decreased from the inner shelf to the outer shelf and the major taxon *Sufflogobius bibarbatus* showed a similar trend. This fish lives in a depth up to 340 m and at a temperature between 11°C and 15°C (Martin and Sayles, 2004). The decomposition of the diatom mud results in hydrogen sulphites (H_2S) and methane (CH_4).The aerobic activity of bacteria and decomposing processes lead to hypoxic conditions; *Sufflogobius bibarbatus* could survive under these conditions (Utne-Palm et al., 2010). This environment is a safe refuge zone for *Sufflogobius bibarbatus* due to the absence of the main predators like *Merluccius capensis* (Utne-Palm et al., 2010) *Sufflogobius bibarbatus* mainly feeds on zooplankton, Medusa and benthic species like Polychaeta and diatom mud which are associated with *Thiomargarita namibiensis* (Utne-Palm et al., 2010).

The lower coverage of bacteria at the other shelf station could be a reason for the detected higher oxygen concentration compared to the inner shelf station (st. 282). This oxygen concentration could further lead to the finding of 1 ind. 100 m^{-1} of *Merluccius capensis* (hake).

Asteroidea were found in a range of 124 (inner shelf st. 282) to 56 ind. 100 m^{-1} (outer shelf st. 285). This pattern was also detected by Brand et al. (2006), with a higher abundance of Echidodermata on the shelf compared to the deep sea. One reason for a higher abundance inshore is that the taxa live in areas depending mainly on organic matter supply from the euphotic zone (Gooday and Turley, 1990). A higher abundance of plankton and an assumed higher particle flux were detected at the inner shelf station (st. 282). In the Southern Ocean the Anthozoa species distribution is driven by depth (Brandt et al., 2006). Octocorallia were mainly found on the shelf, whereas Hexacorallia dominated the deep sea (Brandt et al., 2006). These taxa orders are suspension feeders which have a high abundance in regions with high particle flux rates (Berryman, 2005).

Pennatulacea belong to the Octocorallia. In the present study a smaller amount of Pennatulacea were detected at the Rocky Point outer shelf station (st. 285) compared to the upper Kunene transect. Actinaria, which belong to the Hexacoralia were also detected at both Rocky Point shelf stations with a higher abundance at the outer shelf station (st. 285). Werner (2012) assumed that this distribution pattern is driven by a positive oxygen concentration. The strong geotropic adjusted southward flow along the shelf edge (Lahajnar et al., 2012) may transport

particle rich water from the Kunene River to the Rocky Point shelf break. This could lead to the occurrence of Pennatulacea at the outer shelf station on the Rocky Point transect.

Nevertheless, the highest abundance of Octocorallia were recorded on the Kunene transect with a decreasing trend from the shelf through the slope to the lower slope, where Vertillidae were detected mainly on the shelf and Pennatulacea at the slope station (Figure 32Figure 33). This distribution followed the same trend as the particle flux. The highest particle flux was detected on the Kunene shelf and could be driven by the Kunene river outflow (Eggers 1990). The marine snow in this region consisted of large flakes although there was a low seasonal input from the Kunene River (Nogueira et al., 1997), which could be the main reason for the high abundance of Pennatulacea on the Kunene transect. For the link between the megafauna abundances and the biochemical sediment conditions it has to be recognized that higher concentrations of the $C_{org,}$: N_{tot} ratio and DIN were detected at the Kunene lower slope station compared to shelf and slope. This low element concentration on the shelf and upper slope might be influenced by the large colonies of Pennatulacea which filtrate most nutrients out of the bottom.

Gastropoda were observed on the same transect with the highest abundance at the slope. This is in contrast to the calculation of a higher abundance of Gastropoda on the Kunene shelf by Werner (2012). The difference could be caused by different ways of calculating subsamples, Werner (2012) used a camera frame for the surface-calculation method, whereas the individuals were counted every 10 minutes for 30 seconds in the present study and the distance traveled during this time frame was also determined. However, at the Kunene lower slope station Werner (2012) also detected the lowest abundance of Gastropoda. Brand et al. (2006) described a Gastropod pattern with a decreasing trend of the individual number with depth, which was only recorded with the same trend between the Kunene slope station and the lower slope station in this study.

Merely at the upper and lower slope station (st. 315) of the Kunene transect, Crustacea were observed. At the upper slope, higher abundances of undetermined other Crustacea and shrimps were found than at the lower slope. Similar patterns were detected by Werner (2012).

At the Kunene lower slope station (st. 315) the highest diversity and abundance of fish was detected. This could be caused by the increasing oxygen concentration down the slope which includes no detection of bacteria mats. The higher particle flux rate provided more food and

hence a higher abundance of fish. At the upper slope station (st. 314) only 1 ind. 100 m^{-1} of each, the predator *Merluccius capensis* and its prey *Sufflogobius bibarbatus* were recorded, which could be substantiated by the lack in food availability. Another reason for the low abundance of *Merluccius capensis* was mentioned by Werner (2012), when detecting this species at a depth of 500 m, while Cohen (1990) classified this species as a shallower species living between 100 to 200 m near the bottom.

Macrouridae are dominating the habitats near the bottom at depth from < 2000 to at least 4000 m of the deep sea (Martin and Christiansen, 1996; Marschall and Iwamoto, 1973). In the present study, the highest abundance was found at the deepest ROV station (st. 315) at the Kunene lower slope. Eight of them were determined as *Callorhinchus spp.* and one as *Coelorinchus simorhynchus*. At the upper slope on the same transect, Macrouridae were also detected with 16 ind. 100 m^{-1} of which eight were further classified as *Callorhinchus spp*.

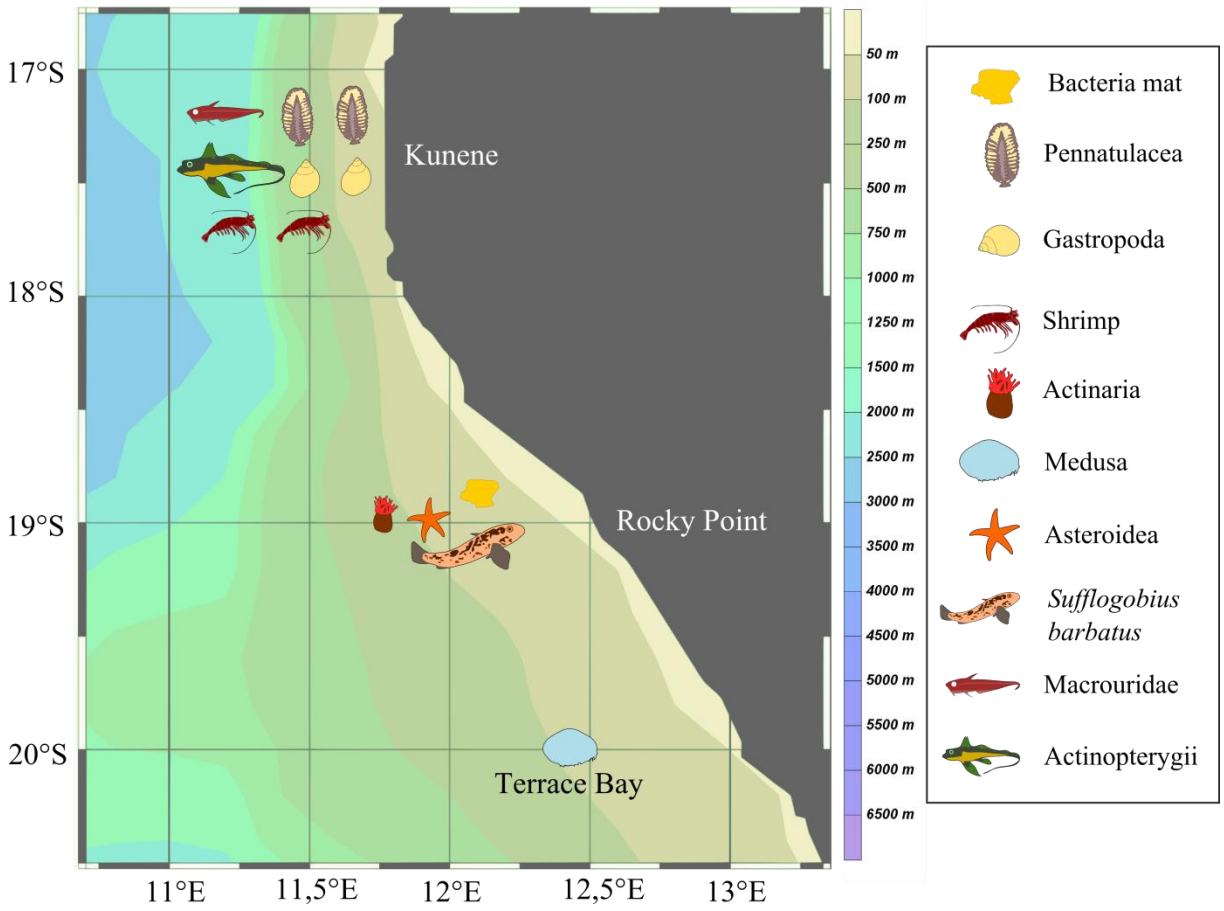

Figure 32: Main taxa composition on the tree transects

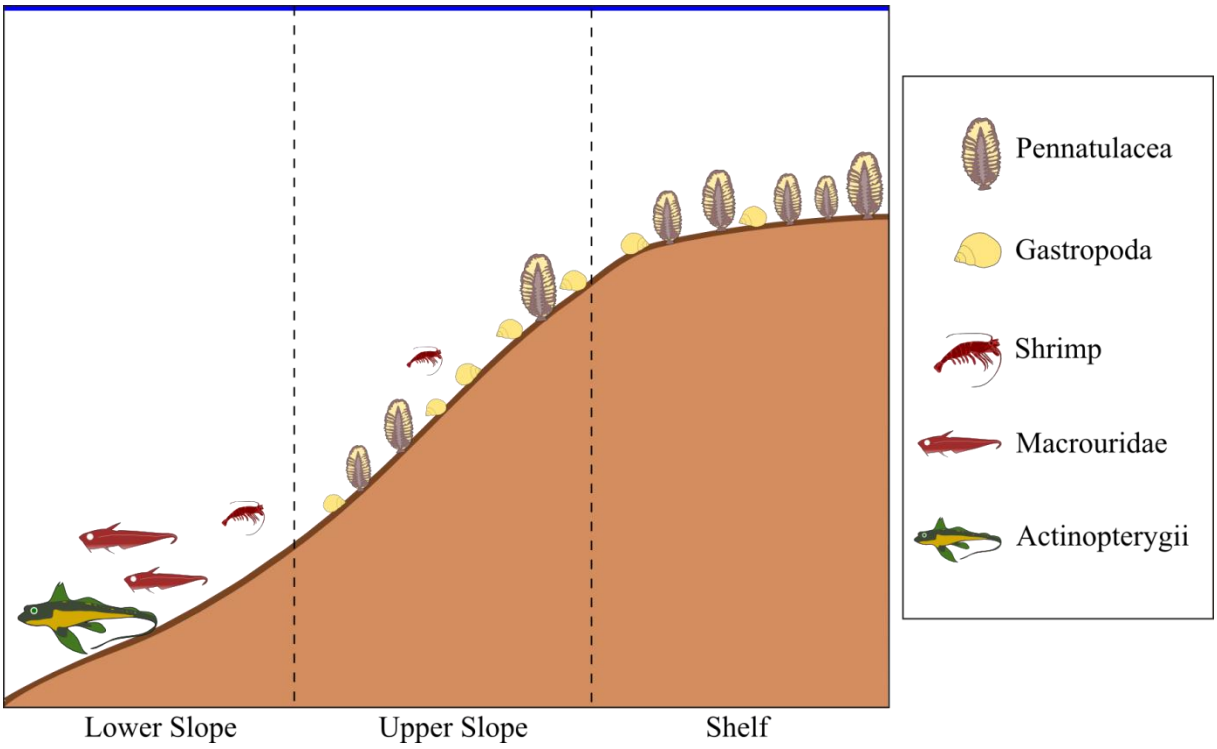

Figure 33: Main taxa composition on the Kunene transect

5 Conclusion

Other oceanic upwelling systems with high food concentrations have shorter trophic food chains and a lower number of links per species (Dunne et al., 2004). This makes them more sensitive to extinctions or changes in the basal species composition (Dunne et al., 2004). Considering this background information, it is crucial to understand how the pelagic components impact the benthic structure in the different regions and depths off the Namibian coast. No significant correlation between the different benthic and pelagic parameters was detectable. Even though no significant correlation was detected, the trend between the chlorophyll *a* concentration and the microzooplankton and mesozooplankton abundances implied a connection between mesozooplankton and microzooplankton. This could be related to the food chain, which is structured through the different trophic levels from phytoplankton over microzooplankton to mesozooplankton. The link between the water column and the benthic structures was shown by an overall trend between higher values of parameters and a higher benthic abundance and vice versa, probably caused by the particle flux and the resulting increase of food. However, benthos communities are more stable than the pelagic communities and changes in particle flux may be burred (Aspetsberger et al., 2007). In particular, this indicates that an earlier pelagic sampling has to take place since there is a time lag between food consumption and the benthic reactions. Overall for a better understanding of the linkage between the water column and the sea bottom, more sampling effort has to be implemented with different time periods between the pelagic and the benthic investigations.

However, the present study demonstrated a positive correlation between microzooplankton abundance and Chl *a* concentrations, despite that high microzooplankton abundance was also found on the slope of the Kunene transect. As the mesozooplankton consumed microzooplankton and phytoplankton, the abundances of these groups showed similar decreasing trends from inshore to offshore. Concurrently with the lower plankton abundance in the offshore region, the particle flux also decreased which results in a lower organic matter input on the sea floor. The low particle flux in the deep sea restricted the high abundance of macro- and megafauna. The higher abundance of megafauna at the Kunene slope stations compared to the shelf might be explained by the Kunene River outflow, which leads to a higher organic sedimentation and lateral advection. Extrapolations of benthic animals at the Kunene stations may cause a different estimation compared to direct counting.

The three transects showed a large diversity in the benthic macro- and megafauna which was mainly driven by the differences in particle flux and by the OMZ. Moreover, the sediment structure and the chemical process at the sediment-water-interface, the width of shelf and the Kunene River outflow are further factors for the diverse benthic community structures. In a future study it would be interesting to record the megafauna also at the upper slope and lower slope stations of the Rocky Point and Terrace Bay transects for a better understand of the slope habitat without an influence by river discharge. The visualization by the ROV allows a recording of a large area in a short time period by a very low impact on the habitat in comparison to other sampling gears.

6 Acknowledgement

At the end of my thesis I would like to thank all those people who made this master thesis possible and an unforgettable experience for me.

First of all, I would like to express my thanks to my first supervisor Prof. Dr. Christian Möllmann for the statistical support and his comments on my work.

I would like to thank my second supervisor Dr. Rolf Koppelmann who offered me this thesis and for the continuous perfect advice and encouragement during my master thesis. His guidance throughout the laboratory work and writing were an amazing help. Also I would like to thank him as well for the opportunity to become a part of a research survey at the Namibian Cost.

Furthermore, I would like to thank very much Dr. Bettina and Karolina Bohata (PhD Student) for the help by the analysis of the mesozooplankton and the microzooplankton samples and the support during the process of writing my master thesis.

I am thankful for the provision of data by Dr. Volker Mohrholz (Hydrographic data), Dr. Andreas Neumann (benthic macrofauna and biochemical sediment data), Karoline Bohata (part of the microzooplankton data) and Dr. Betina Martin (part of the mesozooplankton data).

Also I would like to express my gratitude towards Miriam Püts, Inga Rau, Dominique Aichele, Julie Sabau, Jan Tersteegen, Patricia Hüdepohl and Alex Keth for the assistance during the written and graphical realization of my thesis.

Last but not least, I would like to thank my family and friends for moral support and that they always believed in me.

7 References

Alldredge, A. L. and Silver, M. W. (1988). *Characteristics, dynamics and significance of marine snow*. Progress in Oceanography, 20: 41-82.

Al-Mutairi, H. and Landry, M. R. (2001). *Active export of carbon and nitrogen at Station ALOHA by diel migrant zooplankton.* Deep-Sea Research II, 48(8–9): 2083-2103.

Aspetsberger, F., Zabel, M., Ferdelman, T., Struck, U., Mackensen, A., Ahke, A. et al. (2007). *Instantaneous benthic response to different organic matter quality: In situ experiments in the Benguela Upwelling System.* Marine Biology Research, 3(5): 342-356.

Auel, H. and Hagen, W. (2002). *Mesozooplankton community structure, abundance and biomass in the central Arctic Ocean*. Marine Biology, 40(5): 1013-1021.

Bailey, K. M. and Batty, R. S. (1984). *Laboratory study of predation by Aurelia aurita on larvae of cod, flounder, plaice and herring: development and vulnerability to capture.* Marine Biology, 83: 287-291.

Baltar, F., Arístegui, J., Gasol, J. M., Sintes, E. and Herndl, G. J. (2009). *Evidence of prokaryotic metabolism on suspended particulate organic matter in the dark waters of the subtropical North Atlantic.* Limnology and Oceanography, 54: 182-193.

Barlow, R., Sessions, H., Balarin, M., Weeks, S., Whittle, C. and Hutchings, L. (2005). *Seasonal variation in phytoplankton in the southern Benguela: pigment indices and ocean colour.* African Journal of Marine Science, 27(1): 275-287.

Berger, V. S., Smetacek, V. S. and Werfer, G. (1989). *Productivity of the ocean. Present and past.* Wiley, 44.

Berryman, M. (2005). *Marine Invertebrates of Bermuda, Upside-down Jellyfish Cassiopea xamachana*.http://www.thecephalopodpage.org/MarineInvertebrateZoology/Cassiopea xamachana.html (10.10.2013).

Bertrand, A., Ballón, M. and Chaigneau, A. (2010). *Acoustic observation of living organisms reveals the upper limit of the oxygen minimum zone.* PLoS ONE, 5: e 10330.

Boyd, P. W., Sherry, N. D., Berges, J. A., Bishop, J. K., Calvert, S. E., Charette, M. A.et al. (1999). *Transformations of biogenic particles from the pelagic to the deep ocean realm.* Deep-Sea Resarch II, 46: 2761-2792.

Boyer, D. C., Boyer, H. J., Fossen, I. and Kreiner, A. (2001). *Changes in abundance of the northern Benguela sardine stock during the decade 1990–2000, with comments on the relative importance of fishing and the environment.* South African Journal of Marine Science, 23: 67-84.

Brandt, A., Broyer, C. D., Mesel, I. D., Ellingsen, K. E., Gooday, A. J., Hilbig, B. et al. (2006). *The biodiversity of the deep Southern Ocean benthos.* Biological Science, 362: 39-66.

Bremner, J. (1983). *Biogenic sediments on the South West African (Namibian) continental margin.* Plenum, New York: In: Thiede, J., Suess, E., Coastal Upwelling: Its Sedimentary Record, Part B: Sedimentary Records of Ancient Coastal Upwelling, 73-104.

Bremner, J. M. (1978). *Sediments on the continental margin off south west Africa between the latitudes 17° and 25° S.* South Africa: Ph.D. Thesis University of Cape Town, 233 pp.

Brown, P. C., Painting, S. J. and Cochrane, K. L. (1991). *Estimates of phytoplankton and bacterial biomass and production in the northern and southern Benguela ecosystems.* South African Journal of Marine Science, 11: 537-564.

Brüchert, V. (2006). *In Past and Present Water Column Anoxia.* Springer Netherlands.

Bruland, K. W. and Silver, M. W. (1981). *Sinking rates of fecal pellets from gelatinous zooplankton (Salps, Pteropods, Doliolids).* Marine Biology, 63: 295-300.

Buitenhuis, E., Le Quéré, C., Aumont, O., Beaugrand, G., Bunker, A., Hirst, A. et al. (2006). *Biogeochemical fluxes through mesozooplankton.* Global Biogeochemical Cycles, 20: 0886-6236.

Burd, A. B. and Jackson, G. A. (2009). *Particle aggregation.* Annual Reviews of Marine Science, 1: 65-90.

Calbet, A. (2001). *Mesozooplankton grazing effect on primary production: a global comparative analysis in marine ecosystems.* Limnology and Oceanography, 46: 51-57.

Calbet, A. and Landry, M. (2004). *Phytoplankton growth, microzooplankton grazing and carbon cycling in marine systems.* Limnology and Oceanography, 49: 51-57.

Calbet, A. and Saiz, E. (2005). *The ciliate-copepod link in marine ecosystems.* Aquatic Microbial Ecology, 38: 157-167.

Calvert, S. E. and Price, N. B. (1970). *Minor metal contents of recent organic-rich sediments off South West Africa.* Nature, 227: 593-595.

Carr, M. (2002). *Estimation of potential productivity in eastern boundary currents using remote sensing.* Deap Sea Research II, 49: 58-80.

Carr, M.-E. and Kearns, E. J. (2003). *Production regimes in four Eastern Boundary Current systems.* Deep-Sea Research II, 50: 3199-3221.

Chapmann, P. and Shannon, L. V. (1985). *The Benguela ecosystem. Part II. Chemistry and related processes.* Oceanography and Marine Biology, Annual Review 23: 183-251.

Cohen, D. M., Inada, T., Iwamoto, T. and Scialabba, N. (1990). *Merluccius paradoxus Franca 1960 Deep-water Cape hake.* FAO Fisheries Synopsis, 125(10): 442 pp.

de Villiers, S. (1998). *Seasonal and interannual variability in phytoplankton biomass on the southern African continental shelf: evidence from satellite-derived pigment concentrations.* In: Pillar, S. C., Moloney, C. L., Payne, A. I. L., Shillington, F. A. (Eds). South African Journal of Marine Science, 19: 169-179.

Demarcq, H., Barlow, R. G. and Hutchings, L. (2007). *Application of a chlorophyll index derived from satellite data to investigate the variability of phytoplankton in the Benguela ecosystem.* African Journal of Marine Science, 29: 271-282.

Demarcq, H., Barlow, R. and Shillington, F. A. (2003). *Climatology and variability of sea surface temperature and surface chlorophyll in the Benguela and Agulhas ecosystems as observed by satellite imagery.* African Jounal of Marine Science, 25: 363-372.

Diffenbaugh, N. S., Snyder, M. A. and Soloan, L. C. (2004). *Could CO2-Induced Land Cover Feedbacks Alter Near-shore Upwelling Regimes?* Proceedings of the National Academy of Sciences, 337: 220-223.

Dunne, J. A., Williams, J. R. and Martinez, N. D. (2004). *Network structure and robustness of marine food webs.* Marine Ecology Progress Series, 273: 291-302.

Dworetzky, B. A. and Morley, J. J. (1987). *Vertical distribution of Radiolaria in the eastern equatorial Atlantic: analysis of a multiple series of closely-spaced plankton tows.* Marine Micropleontology Journal, 12: 1-19.

Eisenbarth, S. (2012). *Zusammensetzung und Verteilung der Makrozoobenthosgemeinschaften auf einem quer zur Küste verlaufenden Transekt vor Namibia.* Master Thesis Univerisity of Rostock.

Ekman, V. (1905). *On the influence of the earth´s rotation on ocean currents.* Archeological. Mathematical Astronomical and Physical Journal, 11: 2.

Emeis, K. C., Brüchert, V., Currie, B., Endler, R., Ferdelman, T., Kiessling, A. et al. (2004). *Shallow gas in shelf sediments of the Namibian coastal upwelling ecosystem.* Continental Shelf Research, 24: 627-642.

Eppley, R. W. (1981). *Autotrophic production of particulate matter.* In: Longhurst, A. R., Analyses of marine ecosystems (Ed.), Academic Press, 343-361.

Eppley, R. W. and Peterson, B. J. (1979). *Particulate organic matter flux and planktonic new production in the deep ocean.* Nature, 282: 677-680.

Estrada, M. and Marrasé, C. (1987). *Phytoplanktonbiomass and productivity of the Namibian coast in the Benguela and comparable ecosystems.* South African Journal of Marine Science, 5: 347-356.

Fearon, J. J., Boyd, A. J. and Schülein, F. H. (1992). *Views on the biomass and distribution of Chrysaora hysoscella (Linne, 1766) and Aequorea aequorea (Forskal, 1775) off Namibia, 1982-1989.* Indian Journal Marine Science, 56(1): 75-85.

Feldman, G. C. and McClain, C. R. (2012). *Ocean color web. Monthly aqua MODIS chlorophyll (4 km grids).* NASA Goddard Space Flight Center, Available from http://oceancolor.gsfc.nasa.gov/ (10.10.2011).

Flynn, B., Richardson, A., Brierley, A. S., Boyer, D. C., Axelsen, B. E., Scott, L. et al. (2012). *Temporal and Spatial Patterns in the Abundance of Jellyfish in the Northern Benguela Upwelling Ecosystem and their Link to Thwarted Pelagic Fishery Recovery.* African Journal of Marine Science, 34(1): 131-146.

Flynn, K. J. (1989). *Interaction between nutrient and predator limitation of production in the marine euphotic zone.* Chemistry and Ecology, 4: 21-36.

Forward, R. B. (1988). *Diel vertical migration: zooplankton photobiology and behaviour.* Oceanography and Marine Biology Annual Review, 26: 361-393.

Fowler, S. W. and Knauer, G. A. (1986). *Role of large particles in the transport of elements and organic compounds through the oceanic water column.* Progress in Oceanography, 16: 147-194.

Füssel, J., Lam, P., Lavik, G., Jensen, M. M., Holtappels, M., Günter, M. et al. (2012). *Nitrite oxidation in the Namibian oxygen minimum zone* The ISME Journal, 6: 1200-1209.

Gibbons, M. (2011). *Specialist Study of Jellyfish in the environs of the proposed dredging of Phosphate Deposits in the Sandpiper Phosphate Mining Licence Area off the coast of Central Namibia.* Draft Report for the dreging of marine phosphate entriched sediments from Mining Licence Area No. 170., 2-21.

Goldhammer, T., Brunner, B., Bernasconi, S. M., Ferdelman, T. G. and Zabel, M. (2011). *Phosphate oxygen isotopes: Insights into sedimentary phosphorus cycling from the Benguela upwelling system.* Geochimica et Cosmochimica Acta, 75: 3741-3756.

Gooday, A. J. and Turley, C. M. (1990). *Responses by benthic organisms to inputs of organic material to the ocean floor. a review.* Philosophical Transactions of the Royal Society London A, 331.

Graf, G. (1989). *Benthic-pelagic coupling in a deep-sea benthic community.* Nature, 341: 437-439.

Gray, J. S. (1997). *Marine Biodiversity: Patterns, threats and conservation needs.* Biodiversity and Conservation, 6: 153-175.

Gruber, N. and Sarmiento, J. L. (1997). *Global patterns of marine nitrogen fixation and denitrification.* Global Biogeochemical Cycles, 11: 235-266.

Hamukuaya, H., O'Toole, M. J. and Woodhead, P. M. (1998). *Observations of severe hypoxia and offshore displacement of Cape hake over the Namibian shelf in 1994.* South African Journal of Marine Science, 19: 57-59.

Hansen, F., Cloete, R. R. and Verheye, H. M. (2005). *Seasonal and spatial variability of dominant copepods along a transect off Walvis Bay (23° S), Namibia*. African Journal of Marine Science, 27(1): 55-63.

Hart, T. J. and Currie, R. I. (1960). *The Benguela Current.* In: Discovery reports. issued by the National Institute of Oceanography. Discovery Report, 31: 123-298.

Heip, C. H., Duineveld, G., Flach, E., Graf, G., Helder, W. and Herman, P. M. (2001). *The role of the benthic biota in sedimentary metabolism and sediment-water exchange processes in the Goban Spur area (NE Atlantic).* Deep Sea Research Part II: Topical Studies in Oceanography, 48: 32-43.

Huggett, J. A. and Bradford-Grieve, J. (2007). *Guide to some common copepods in the Benguela Current Large Marine Ecosystem.* Swakopmund, Namibia: Regional Zooplankton Taxonomy and Identification Training Workshop.

Huggett, J. A., Boyd, A. J., Hutchings, L. and Kemp, A. D. (1998). *Weekly variability of clupeoid eggs and larvae in the Benguela jet current: implication for recruitment.* (Bd. 19). In: Pillar, S. C., Moloney, C. L., Payne, A. I. L. and Shillington, F. A. (Eds.). Benguela Dynamics: Impact of Variability on Shelf-Sea Environments and their Living Resources. South African Journal of Marine Sience, 19: 97-210.

Hutchings, L., van der Lingen, C. D., Shannon, L. J., Crawford, R. J., Verheye, H. M., Bartholomae, C. H. et al. (2009). *The Benguela Current: An ecosystem of four components.* Progress in Oceanography, 83: 15-32.

Iirigoien, X., Flynn, K. J. and Harris, R. P. (2005). *Phytoplankton blooms: a 'loophole' in microzooplankton grazing impact?* Journal of Plankton Research, 27(4): 313-321.

Inthorn, M., Wagner, T., Scheeder, G. and Zabel, M. (2006). *Lateral transport controls distribution, quality and burial of organic matter along continental slopes in high-productivity areas.* Geology, 34(3): 205-208.

Jahnke, R. A. (1990). *Ocean flux studies: A statusreport.* Reviews of Geophysics, 28: 381-398.

Jahnke, R. A. (1996). *The global ocean flux of particulate organic carbon: areal distribution and magnitude.* Global Biogeochemical Cycles, 10: 71-88.

James, A. G., Probyn, T. A. and Huchtings, L. (1989). *Laboratory-derived carbon and nitrogen budgets for the omnivorous planktivore Engraulis capensis Gilchrist.* Journal of Experimental Marine Biology and Ecology, 131: 125-145.

Jarre-Teichmann, A., Shannon, L. J., Moloney, C. L. and Wickens, P. A. (1998). *Comparing trophic flows in the southern Benguela to those in other upwelling ecosystems.* South African Journal of Marine Science, 19: 391-414.

Kalvelage, T., Jensen, M. M., Contreras, S., Revsbech, N. P., Lam, P., Günter, M. et al. (2011). *Oxygen sensitivity of anammox and coupled N-cycle processes in oxygen minimum zones.* PLoS ONE, 6(12): e 29299.

Kamp-Nielsen, L. (1975). *A kinetic approach to the aerobic sediment-water exchange of phosphorus in Lake Esrom.* Ecological Modelling, 1(2): 153-160.

Kiorboe, T., Kaas, H., Kruse, B., Mohlenberg, F., Tiselius, P. and Aetebjerg, G. (1990). *The structure of the pelagic food web in relation to water column structure in the Skagerrak.* Marine Ecology Progress Series, 59: 19-32.

Kleppel, G. S. (1993). *On the diets of calanoid copepods.* Marine Ecology Progress Series, 99: 183-195.

Koppelmann, R. and Frost, J. (2008). *The Ecological Role of Zooplankton in the Twilight and Dark Zones of the Ocean.* In: Mertens, L. P. (Ed.), Biological Oceanography Research Trends, Nova: 67-130.

Koppelmann, R. and Weikert, H. (1992). *Full-depth zooplankton profiles over the deep bathyal of the NE Atlantic.* Marine Ecology Progress Series, 86: 263-272.

Koppelmann, R., Schäfer, P. and Schiebel, R. (2000). *Organic carbon losses measured by heterotrophic activity of mesozooplankton and CaCO3 flux in the bathypelagic zone of the Arabian Sea.* Deep-Sea Research II, 47: 169-187.

Kristensen, E., Andersen, F. Ø. and Blackburn, T. H. (1992). *Effects of benthic macrofauna and temperature on degradation of macroalgal detritus: The fate of organic carbon.* Limnology and Oceanography, 37(7): 1404-1419.

Kröncke, I. and Türkay, M. (2003). *Structural and functional aspects of the benthic communities in the deep Angola Basin.* Marine Ecology Progress Series, 260: 43-53.

Kuypers, M. M., Lavik, G., Woebken, D., Schmid, M., Fuchs, B. M., Amann, R. et al. (2005). *Massive nitrogen loss from the Benguela upwelling system through anaerobic ammonium oxidation.* USA: Proceedings of the National Academy of Sciences, 102(18): 6478-6483.

Lahajnar, N., Ankele, M., Annighöfer, M., Bode, M., Bohata, K., Buchholz, M. et al. (2012). *Geochemistry and Ecology of the Namibian Upwelling System*. MARIA S. MERIAN Cruise: No. 17, Leg 3 (2011) report.

Lass, H. U., Schmidt, M., Mohrholz, V. and Nausch, G. (2000). *Hydrographic and Current Measurements in the Area of the Angola – Benguela Front.* Journal of Physical Oceanography, 30: 2589-2609.

Lavik, G., Strührmann, T., Brüchert, V., Van der Plas, A., Mohrholz, V., Lam, P. et al. (2009). *Detoxification of sulphidic African shelf waters by blooming chemolithotrophs.* Nature, 457: 581-584.

Laybourn-Parry, J. (1992). *Protozoan Plankton Ecology.* London: Chapman and Hall.

Leibold, M. A. (1995). *The niche concept revisited: Mechanistic models and community context.* Ecology, 76: 1371-1382.

Malone, T. C. (1980). *Algal size.* London: In: Morris, I. (Ed.), The Physiological Ecology of Phytoplankton. Blackwell Scientific Publications, 433-463.

Marschall, N. B. and Iwamoto, T. (1973). *Family Macrouridae.* In: Cohen, D. M., Fusches of the Western North Atlantic.

Martin, B. and Christiansen, B. (1996). *Diets and standing stocks of benthopelagic fishes at two bathymetrically different midoceanic localities in the northeast Atlantic.* Deep-Sea Research I, 44(4): 496-655.

Martin, J. H., Kanauer, G. A., Karl, D. M. and Broenkow, W. W. (1987). *VERTEX: carbon cycling in the northeast Pacific*. Deep-Sea Research I, 34(2): 541-558.

Martin, W. R. and Sayles, F. L. (2004). *Organic matter cycling in sediments of the continental margin in the northwest Atlantic Ocean.* Deep Sea Research Part I: Oceanographic Research Papers, 51: 45-89.

McMillen, K. J. and Casey, E. (1978). *Distribution of living polycystine radiolarians in the Gulf of Mexico and Caribbean Sea and comparison with the sediment record.* Marine Micropaleontology Journal, 3: 121-145.

Meeuwis, J. and Lutjeharms, J. (1990). *Surface thermal characteristics of the Angola-Benguela Front.* South African Journal of Science, 9: 261-279.

Miller, P. J. (1990). *Sufflogobius bibarbatus (from Bonde, 1923) Pelagic goby.* Check-list of the fishes of the eastern tropical Atlantic.

Mohrholz, V., Bartholomae, C. H., van der Plas, A. K. and Lass, H. U. (2007). *The seasonal variability of the northern Benguela undercurrent and its relation to the oxygen budget on the shelf.* Continental Shelf Research, 28: 224-234.

Mohrholz, V., Schmidt, M. and Lutjeharms, J. R. (2001). *The hydrography and dynamics of the Angola-Benguela Frontal Zone and environment in April 1999.* South African Journal of Marine Science, 97: 424-441.

Monteiro, P. M. and van der Plas, A. K. (2006). *Low oxygen water (LOW) variability in the Benguela system: Key processes and forcing scales relevant to forecasting in Large Marine Ecosystems.* Elsevier, 14: 71-90.

Navarrete, S. A., Wieters, E. A., Broitman, B. R. and Castilla, J. C. (2005). *Scales of benthicpelagic coupling and the intensity of species interactions: From recruitment limitation to top down control.* Proceedings of the National Academy of Sciences, 102: 18046-48051.

Nelson, L. and Hutchings, G. (1983). *The Benguela Upwelling Area.* Oceanography, 12: 333-356.

Neumann, A. (2012). *Elimination of reactive nitrogen in continental shelf sediments measured by membrane inlet mass spectrometry.* Germany: Ph.D. Thesis University Hamburg, 81-108.

Nival, P., Carlotti, F. and Sciandra, A. (1988). *Modelling of recruitment of marine species.* In: Rothschild, B. J. (Ed.), Toward at theory of biological-physical interactions in the world ocean. NATO series in marine sciences. Kluwer-Academic Publishers, 321-342.

Nixon, A. C. and Thomas, A. (2001). *On the size of the Peru upwelling ecosystem.* Deep-Sea Research I, 48: 2521-2528.

Nogueira, E., Pérez, F. F. and Ríos, A. F. (1997). *Seasonal patterns and long-term trends in an estuarine upwelling ecosystem (Ria de Vigo, NW Spain).* Estuarine Coastal Shelf Science, 44: 285-300.

Olivar, M. P. and Barange, M. (1990). *Zooplankton of the northern Benguela upwelling system in a quiescent upwelling period.* Journal of Plankton Research, 12: 1023-1044.

Parsons, T. R., Takahashi, M. and Hargrave, B. (1984). *Biological oceanographic*.. Headington Hill Hall, Oxford: England: Pergamon Press, 330 pp.!

Pearre., S. (1979). *Problems of detection and interpretation of vertical migration.* Journal of Plankton Research, 1: 20-44.

Perry, R. I., Harding, G. C., Loder, J. W., Tremblay, M. J. and Sinclair, M. M. (1993). *Zooplankton distributions at the Georges Bank frontal system: retention or dispersion?* Continental Shelf Research, 13(4): 357-383.

Peterson, R. G. and Stramma, L. (1991). *Upper-level circulation in the South Atlantic Ocean.* Progress in Oceanography, 26: 1-73.

Pillar, S. C., Armstrong, D. A. and Hutchings, L. (1989). *Vertical migration, dispersal and transport of Euphausia lucens in the southern Benguela current.* Marine Ecology Progress Series, 53: 179-190.

Poole, R. and Tomczak, M. (1999). *Optimum multiparameter analysis of the water mass structure in the Atlantic Ocean thermocline.* Deep-Sea Research I, 46: 1895-1921.

Prince, E. D. and Goodyear, P. (2006). *Hypoxia-based habitat compression of tropical pelagic fishes.* Fisheries Oceanography, 15: 451-464.

Reinthaler, T., van Aken, H., Veth, C., Aristegui, J., Robinson, C., Williams, P. J. et al. (2006). *Prokaryotic respiration and production in the meso- and bathypelagic realm of the eastern and western North Atlantic basin.* Limnology and Oceanography, 51: 1262-1273.

Ricklefs, R. E. (1987). *Community diversity: Relative roles of local and regional processes.* Science, 235: 167-171.

Risgaard-Petersen, N., Nielsen, L. P., Rysgaard, S., Dalsgaard, T. and Meyer, R. L. (2003). *Application of the isotope pairing technique in sediments where anammox and denitrification coexist.* Limnology and Oceanography, Methods 1: 63-73.

Robison, B. H., Sherlock, R. E. and Reisenbichler, K. R. (2010). *The bathypelagic community of the Monterey Canyon.* Deep-Sea Research II, 57(16): 1551-1556.

Rogers, J. and Bremner, J. M. (1991). *The Benguela ecosystem Part VII. Marine-geological aspects.* Annual Review of Oceanography and Marine Biology, 29: 1-85.

Rollwagen Bollens, G. C. and Penry, D. I. (2003). *Feeding dynamics of Acartia spp. copepods in a large, temperate estuary (San Francisco Bay, CA).* Marine Ecology Progress Series, 257: 139-158.

Roughgarden, J. (2006). *Foreward.* In: Kritzer, J. and Sale, P. (Eds.), Marine metapopulations. Elsevier.17-20.

Rowe, G. T. (1981). *The deep-sea ecosystem.* In: Longhurst, A. R. (Ed.), Analysis of marine ecosystems. Marine Ecology, 1: 235-267.

Sako, A. L. (1998). *The influence of the Benguela upwelling system on Namibia's marine biodiversity.* Biodiversity and Conservation, 7: 419-433.

Sanders, H. L. (1968). *Marine benthic diversity: a comparative study.* American Naturalist, 102: 223-243.

Sanders, H. L. (1977). *Evolutionary ecology and the deep-sea benthos.* Philadelphia, Pennsylvania: In: Goulden, C. E. (Ed.), Changing scenes in natural sciences. Academy of Natural Sciences, 243-282.

Schulz, H. N. and Schulz, H. D. (2005). *Large sulfur bacteria and the formation of phosphorite.* Sicence, 307: 493-495.

Schulz, H. N., Brinkhoff, T., Ferdelman, T. G., Mariné, H. M., Teske, A. and Jørgensen, B. B. (1999). *Dense populations of a giant sulphur bacterium in Namibian sediments.* Science, 284: 416-418.

Schulz, H. and Jørgensen, B. B. (2001). *Big bacteria.* Annual Review of Microbiology, 55: 105-137.

Shannon, C. E. and Weaver, W. (1949). *The mathematical theory of comunication.* Champaign II: University of Illinois Press.

Shannon, L. V. (1985). *The Benguela ecosystem. 1. Evolution of the Benguela, physical features and processes.* Annual Review of Oceanography and Marine Biology, 23: 105-182.

Shannon, L. V. and O'Toole, M. J. (2003). *Sustainability of the Benguela: ex africa semper aliquid novi.* Amsterdam. In: Hempel, G. and Sherman, K. (Eds.), Large Marine Ecosystems of the World: Trends in Exploitation. Protection and Research. Elsevier, 423pp.

Shannon, L. V. and Pillar, S. C. (1986). *The Benguela ecosystem. 3. Plankton.* Annual Review of Oceanography and Marine Biology, 24: 65-170.

Sibuet, M., Lambert, C. E., Chesselet, R. and Laubier, L. (1989). *Density of the major size groups of benthic fauna and trophic input in deep basins of the Atlantic Ocean.* Journal of Marine Science, 47: 851-867.

Siegel, D. A., Mitarai, S., Costello, C. J., Gaines, S. D., Kendall, B. E., Warner, R. R. et al. (2008). *The stochastic nature of larval connectivity among nearshore marine populations.* Proceedings of the National Academy of Sciences, 105: 8974-8979.

Smith, D., Simon, M., Alldredge, A. L. and Azam, F. (1992). *Intense hydrolytic enzyme activity on marine aggregates and implications for rapid particle dissolution.*. Nature, 359: 139-142.

Snelgrove, P. V., Blackburn, T. H., Hutchings, P., Alongi, D., Grassle, J. F., Hummel, H. et al. (1997). *The importance of marine sediment biodiversity in ecosystem processes.* A Multidisciplinary English Language Journal, 26: 578-583.

Spearman, C. (1904). *The proof and mesurements of association between two things.* American Journal of Psychology, 15: 72-101.

Sprintall, J. and Tomczak, M. (1992). *Evidence of the barrier layer in the surface layer of the tropics.* Journal of Geophysical Research. 97: 7305-7316.

Steffani, N. (2011). *Marine Benthic Specialist Study for a Proposed Development of Phosphate Deposits in the Sandpiper Phosphate Licence Area off the Coast of Central Namibia.* South Africa: Environmental Impact Assessment Report for the Marine Component, 31: 7305-7316.

Steinberg, D. K., Carlson, C. A., Bates, N. R., Goldthwait, S. A., Madin, L. P. and Michael, A. F. (2000). *Zooplankton vertical migration and the active transport of dissolved organic and inorganic carbon in the Sargasso Sea.* Deep-Sea Research I, 47(1): 137-158.

Steinberg, D. K., Van Mooy, B. A., Buesseler, K. P., Boyd, P. W., Kobari, T. and Karl, D. M. (2008). *Bacterial vs. zooplankton control of sinking particle flux in the ocean's twilight zone.* Limnology and Oceanography, 53: 1327-1338.

Stich, H. B. and Lampert, W. (1981). *Predator evasion as an explanation of diurnal vertical migration.* Nature, 293: 396-398.

Stramma, L. and England, M. (1999). *On the water masses and mean circulation of the South Atlantic Ocean.* Journal of Geophysical Research, 104: 20863-2883.

Suess, E. (1980). *Particulate organic carbon flux in the oceans-surface productivity and oxygen utilization.* Nature, 288: 260-263.

Summerhayes, C. P., Kroon, D., Rosell-Mellé, A., Jordan, R. W., Schrader , H.-J., Hearn, R. et al. (1995). *Variability in the Benguela Current upwelling system over the past 70000 years.* Progress in Oceanography, 35: 207-251.

Tenore, K. R. and Chesney, E. (1985). *The interaction of rate of food supply and population density upon the bioenergetics of the opportunistic polychaete, Capitella capitata (Type I).* Limnology and Oceanography, 30: 1188-1195.

Thiel, H. (1978). *Benthos in Upwelling regions.* Berlin. In: Boje, R. and Tomczak, M. (Eds.), Upwelling ecosystems. Springer Verlag, 124-138.

Timonin, A. G., Araschkevich, E. G., Drits, A. V. and Semenova, T. N. (1992). *Zooplankton dynamics in the northern Benguela ecosystem, with special reference to the copepod Calanoides carinatus.* South African Journal of Marine Science, 12: 545-560.

Tranter, D. J. (1962). *Zooplankton abundance in Australian waters.* Australian Journal of Marine and Freshwater Research, 13: 106-142.

Utne-Palm, A. C., Savanes, A. G., Bronwen, C., Stein, K., Nilsson, G. E., Braithwaits, V. A. et al. (2010). *Trophic Structure and Community Stability in an Overfished Ecosystem.* Science, 329: 333-336.

Venter, G. E. (1988). *Occurrence of jellyfish on the west coast off South West Africa / Namibia.* South African Science Program Report, 157: 56-61.

Veraart, A. J., de Klein, J. J. and Scheffer, M. (2011). *Warming can boost denitrification disproportionately due to altered oxygen dynamics.* PLoS ONE, 6(3): e18508. Verheye, H. M., Hutchings, L., Huggett, J. A. and Painting, S. J. (1992). *Mesozooplankton dynamics in the Benguela ecosystem, with emphasis on the herbivorous copepods.* South African Journal Marine Science, 12: 561-584.

Vinogradov, M. E. (1968). *Vertical distribution of the Oceanic zooplankton.* Academy of Science of the U.S.S.R., Institute of Oceanography.

Ward, B. B., Tuit, C. B., Jayakumar, A., Rich, J. J., Moffett, J. and Naqvi, S. W. (2008). *Organic carbon and not copper, controls denitrification in oxygen minimum zones of the ocean.* Deep-Sea Research I, 55: 1672-1683.

Wasmund, N., Lass, H. U. and Nausch, G. (2010). *Distribution of nutrients, chlorophyll and phytoplankton primary production in relation to hydrographic structures bordering the Benguela.* African Journal of Marine Science, 27: 177-190.

Weeks, S. J. and Shillington, F. A. (1995). *Phytoplankton pigment distribution and frontal structure in the subtropical convergence region south of Africa.* Deep-Sea Research I, 43(5): 739-768.

Wefer, G. and Fischer, G. (1993). *Seasonal patterns of vertical particle flux in equatorial and coastal upwelling areas of the eastern Atlantic.* Deep-Sea Research I, 40: 1613-1645.

Werner, J. (2012). *Untersuchungen zur Benthosbesiedlung auf dem Schelf und am Schelfhang im Auftriebsgebiet vor Namibia mit Hilfe eines ferngesteuerten Tauchfahrzeugs (Remotely Operated Vehicle, ROV).* Germany: Bachelor Thesis University of Hamburg.

Wiebe, P. H., Morton, A. M., Bradley, A. M., Backus, R. H., Craddock, J. E., Barber, V. et al. (1985). *New developments in the MOCNESS, an apparatus for sampling zooplankton and micronekton.* Marine Biology, 87: 313-323.

Zabel, M., Dahmke, A. and Schulz, H. D. (1998). *Regional distribution of diffusive phosphate and silicate fluxes through the sediment-water interface: the eastern South Atlantic.* Deep-Sea Research I, 45: 277-300.

Zettler, M. L., Bochert, R. and Pollehne, F. (2009). *Macrozoobenthos diversity in an oxygen minimum zone off northern Namibia.* Marine Biology, 156: 1949-1961.

7.1 Image sources

Shannon, L. V. and O'Toole, M. J. (2003). *Sustainability of the Benguela: ex africa semper aliquid novi.* Amsterdam. In: Hempel, G. and Sherman, K. (Eds.), Large Marine Ecosystems of the World: Trends in Exploitation. Protection and Research. Elsevier, 423pp.

NASA Earth Science EaSUREs DISCOVER Project (data source: http://oceancolor.gsfc.nasa.gov/) (lastrequest L. V. and O'Toole, M. J. (2003).(last visit 10.10.2013).

7 Appendix

Table 8: Raw data of each benthic megafauna, taxa captured by a Remotely Operated Vehicle (ROV) at the different stations. The red numbers are calculations of sub samples of the real number. (Type 16 is a fish at the Kunene slope which was not exactly specified see more Werner 2012)

Station	st. 277	st. 282	st.285	st.305	st.314	st.315
depth [m]	100	110	205	150	500	775
idealized route length (i.r.l.) [m]	119,22	279,01	343,26	421,89	596,07	335,28
transfer on i.r.l. [m]	119,22	284,12	351,12	430,39	607,51	339,82
Actiniaria		7	197	2	3	9
unidentified Actinopterygii	1		9	39	17	57
Medusa	242	60	6			5
Asteroidea		353	14			
Gastropoda		2	4	3132,41	27111,57	
Sufflogobius bibarbatus		60	35	8	2	0
Pennatulacea			26	10317,49	7766,35	30
other Crustacea					17	9
Shrimp				2	94	45
Merluccius paradoxus			1		9	
Helicolenus dactylopterus	1				7	0
Macrouridae					49	136
Callorhinchus braueri					46	29
Coelorinchus simorhynchus						2
Selachophidium guentheri					3	
Typ 16					3	
Coleoidea					1	
Bacterial mats [%]		50-79	20-49			

Table 9: Individual numbers per 100 m [ind. $100m^{-1}$] of each benthic megafauna taxa captured by a Remotely Operated Vehicle (ROV). at the different stations. The red numbers are calculation of sub samples on the real number. (Typ 16 is a fish at the Kunene slope which was not exactly specified see more Werner (2012))

Station	st. 277	st. 282	st. 285	st. 305	st. 314	st. 315
depth [m]	100	110	205	150	500	775
idealised route length (i.r.l.) [m]	119,22	279,01	343,26	421,89	596,07	335,28
transfer on i.r.l. [m]	119,22	284,12	351,12	430,39	607,51	339,82
Actiniaria		2,46	56,11	0,46	0,49	2,65
unidentified Actinopterygii	0,84		2,56	9,06	2,80	16,77
Medusa	202,99	21,12	1,71			1,47
Asteroidea		124,24	3,99			
Gastropoda		0,70	1,14	727,80	4462,72	
Sufflogobius bibarbatus		21,12	9,97	1,86	0,33	0,00
Pennatulacea			7,40	2397,22	1278,39	8,83
other Crustacea					2,80	2,65
Shrimp				0,46	15,64	13,24
Merluccius paradoxus			0,28		1,48	
Helicolenus dactylopterus	0,84				1,15	0,00
Macrouridae					8,07	40,02
Callorhinchus braueri					7,57	8,53
Coelorinchus simorhynchus						0,59
Selachophidium guentheri					0,49	
Typ 16					0,49	
Coleoidea					0,16	
Bacterial mats [%]		50-79	20-49			

Erklärung

Hiermit bestätige ich, Matthias Mertzen, dass die vorliegende Arbeit von mir selbständig verfasst wurde und ich keine anderen als die angegebenen Hilfsmittel – insbesondere keine im Quellenverzeichnis nicht benannten Internet–Quellen – benutzt habe und die Arbeit von mir vorher nicht einem anderen Prüfungsverfahren eingereicht wurde. Die eingereichte schriftliche Fassung entspricht der auf dem elektronischen Speichermedium.

Hamburg, den 07.11.2013

_____

(Matthias Mertzen)